

NEW POLYMER-SUPPORTED PHOTO-CATALYSTS FROM UNIMOLECULAR, PHOTO-
CATALYST INITIATOR SYSTEMS (UPCIS)

A Thesis

Presented to

The Faculty of the Department of Chemistry

Sam Houston State University

In Partial Fulfillment

of the Requirements for the Degree of

Master of Science

by

Matthew A. Peavy

August, 2020

NEW POLYMER-SUPPORTED PHOTO-CATALYSTS FROM UNIMOLECULAR, PHOTO-
CATALYST INITIATOR SYSTEMS (UPCIS)

by

Matthew A. Peavy

APPROVED:

Christopher E. Hobbs, PhD
Thesis Director

Dustin E. Gross, PhD
Committee Member

Benny E. Arney, PhD
Committee Member

John B. Pascarella, PhD
Dean, College of Science and Engineering
Technology

DEDICATION

This thesis is dedicated to my wife, Jessica Peavy, for all the support that was extended to me in this endeavor. Thank you for believing in me in this season of life.

Also, to the rest my family without who's support I would not have been able to complete this epic journey of knowledge, thank you.

ABSTRACT

Peavy, Matthew A., *New Polymer-Supported Photo-Catalysts from Unimolecular, Photo-Catalyst Initiator Systems (UPCIS)*. Master of Science (Chemistry), August, 2020, Sam Houston State University, Huntsville, Texas.

In today's environmentally conscious world, the development of greener catalysts is at the forefront of discovery. This is because many catalysts are, traditionally, based on environmentally toxic transition metals that are discarded as waste after only a single use. In this regard, the recovery and recycling of such catalysts is vital, in academia and industry. This is often achieved through the incorporation of a catalyst and/ or ligand into a polymer support to enable liquid/liquid or solid/liquid recovery. This incorporation is frequently accomplished through (i) polymerizing a monomer that has been pre-functionalized to contain a ligand/catalyst or (ii) using a post-polymerization modification strategy in which a ligand/catalyst is linked to a pre-made polymer. However, either method relies on the synthesis of a polymer that can require multiple species of its own (i.e. monomer, catalyst, ligand, and initiator). This problem can be averted with the rational design of a unimolecular, photo-catalyst initiator system (UPCIS) that can facilitate the synthesis of a polymer support that can subsequently be used, as a multi-functional catalyst, to carry out other reactions. These systems (in which the initiator, ligand, and/ or catalyst, are covalently linked to one another) can be used to facilitate atom transfer radical polymerizations (ATRP). Additionally, the implementation of a greener energy source can be achieved through the utilization of visible light to initiate these reactions. For the current research, reactions are initiated through irradiation with visible light sources, and the catalyst is easily recovered by solid/liquid separation and can be recycled up to five times without loss of activity.

KEY WORDS: Photocatalyst, Photo-redox, Polymer supported catalyst, Unimolecular, ATRP, Ruthenium, Bipyridine, Phenothiazine, Cycloaddition, Borylation

ACKNOWLEDGEMENTS

I would like to acknowledge my professional advisor, Dr. Christopher Hobbs, for all the support and knowledge that he has poured into me during this time. I would not have the knowledge and skills that I possess today without his investment in me.

I would also like to acknowledge my committee members, Dr. Dustin Gross and Dr. Benny Arney, without whom I would not have constructed as well written and in-depth a thesis. Without their time and energy and constant advisement, I cannot imagine finishing this task.

Lastly, I would like to acknowledge my fellow lab mates, for the help given to me along the way in conducting my research and keeping me on task.

All of you have made a forever impact upon my life and profession.

Thank you

TABLE OF CONTENTS

	Page
DEDICATION	iii
ABSTRACT	iv
ACKNOWLEDGEMENTS	vi
TABLE OF CONTENTS.....	vii
LIST OF TABLES	ix
LIST OF FIGURES	x
CHAPTER	
I INTRODUCTION	1
1.1 Green Catalytic Chemistry.....	1
1.2 Polymer Supported Catalyst (PSC).....	2
1.3 Photo Redox ATRP.....	3
1.4 Unimolecular Photo-Catalyst Initiator Systems.....	4
1.5 Multi-functional Catalytic Reactions	5
1.6 Catalytic Systems Investigated in this Work	5
1.7 Polymer Investigated	6
1.8 Objectives	6
II EXAMINATION OF RUTHENIUM BASED PSC.....	7
2.1 Background	7
2.2 Results.....	9
2.3 Discussion.....	14
2.4 Experimental.....	20

III EXAMINATION OF 10-PHENYLPHENOTHIAZINE BASED PSC.....	36
3.1 Background.....	36
3.2 Results.....	39
3.3 Discussion.....	42
3.4 Experimental.....	46
IV CONCLUSION.....	53
REFERENCES	56
APPENDIX.....	66
VITA.....	87

LIST OF TABLES

Table	Page
1 Polymerizations with UPCIS Ru1	10
2 UPCIS Ru2 polymerization results	13
3 RuPoly1 catalytic results from five cycles.....	14
4 PSC RuPoly1 metal retention.....	14
5 [2 + 2] Cycloaddition reaction reagent amounts.....	35
6 UPCIS PPH1 polymerization results.....	40
7 PPHPoly1 catalytic results from five cycles. Reaction 4 utilized a catalyst exposed to DCM during recovery from reaction 3.	42
8 Hawker et al. Polymerization Results.....	43
9 C-X Borylation reaction reagent amounts	52

LIST OF FIGURES

Figure	Page
1 Typical ATRP reaction.	3
2 Generic photo-redox polymerization mechanism.	4
3 Simplified ruthenium ^{II} polymerization mechanism.	7
4 UPCIS Ru1 and Ru2	8
5 Abbreviated [2 + 2] cycloaddition mechanism.	9
6 UPCIS Ru1 polymerization reaction scheme.	10
7 Ruthenium ^{II} concentration calibration curve.	11
8 PSC RuPoly UV-Vis absorbance curves.	12
9 UPCIS Ru2 polymerization scheme.	12
10 [2 + 2] cycloaddition of E1 scheme.	13
11 ATRP equilibrium diagrams.	16
12 Sacrificial electron donor mechanisms to form initiators.	17
13 Crystal field splitting energy differences.	17
14 Cycloaddition product C1 , isomers and byproduct.	19
15 Synthesis of 2 reaction scheme.	21
16 Synthesis of 3 reaction scheme.	22
17 Synthesis of 4 reaction scheme.	23
18 Synthesis of L1 reaction scheme.	24
19 Synthesis of 6 reaction scheme.	25
20 Synthesis of L2 reaction scheme.	26
21 Synthesis of UPCIS Ru1 reaction scheme.	27

22	Synthesis of UPCIS Ru3 reaction scheme.....	28
23	Synthesis of UPCIS Ru2 reaction scheme.....	29
24	Synthesis of PSC RuPoly1 reaction scheme.	30
25	Synthesis of PSC RuPoly2 reaction scheme.	31
26	Synthesis of 12	32
27	Synthesis of 13	33
28	Synthesis of E1 reaction scheme.	34
29	Synthesis of C1 by 2+2 cycloaddition reaction scheme.	34
30	10-Phenylphenothiazine polymerization mechanism.	37
31	UPCIS PPH1	37
32	10-Phenylphenothiazine borylation mechanism.	38
33	UPCIS PPH1 polymerization scheme.	39
34	UPCIS PPH1 calibration curve.	40
35	UV-Vis absorbance curve.	41
36	Borylation reaction scheme.....	42
37	Synthesis of 9	47
38	Synthesis of 10	48
39	Synthesis of PPH1	49
40	Synthesis of PPHPoly1 reaction scheme.	50
41	Borylation reaction scheme of B1	51

CHAPTER I

Introduction

1.1 Green Catalytic Chemistry

Green chemistry is defined by the Environmental Protection Agency (EPA) of the United States as “the design of chemical processes that reduce or eliminate the use or generation of hazardous substances. Green chemistry applies across the life cycle of a chemical product, including its design, manufacture, use, and ultimate disposal.”¹ This definition was pioneered by Paul Anastas.² Some of the twelve principles of green chemistry that Anastas presented will be called upon in this research to serve as a guide to ensure that the new system can be considered green.

One of the principles of green chemistry calls upon the necessity of catalysts due to their superiority over stoichiometric reagents.² But, while a catalyst is a molecular species that allows a reaction to proceed through a more energy efficient pathway by lowering the activation energy, many modern catalysts are based on expensive, toxic, and environmentally harmful transition metals. Further, in a typical laboratory setting, these species are used only once and discarded; this, in itself, represents a green chemistry issue.

By developing a unimolecular photo-catalyst initiator system, that can self-catalyze its own polymer supports, and then be recycled in multi-functional catalytic roles, the catalyst may be considered green. The polymer supported catalyst may meet many of the principles of green chemistry. The green chemistry principles of atom economy, energy efficiency, degradation, and pollution prevention will be achieved.

1.2 Polymer Supported Catalyst (PSC)

For a catalyst to be considered “green”, it must be easily recoverable in a form that is reusable, which serves to increase the catalyst’s life cycle. This can be achieved by attaching a catalyst to a polymer support, in which the catalyst is preserved and is easily recovered after a reaction by either a liquid/solid or liquid/liquid separation technique. The catalyst is then referred to as a polymer supported catalyst (PSC). Ever since the groundbreaking discovery of solid-phase synthesis using cross-linked polystyrene resins (“Merrifield resins”) by Merrifield and Letsinger (for which Merrifield won the Nobel Prize in 1984), many examples detailing the preparation and use of polymer supported catalysts have been reported.³⁻⁸ Polymer supports based on these species have been used to “heterogenize” what are typically homogeneous catalysts. Although these heterogeneous systems offer simple separation (gravity filtration) of catalyst from product, their insolubility can have detrimental effects on selectivity and reactivity. The first example of using soluble polymer supports were reported by Bayer and Schurig in 1975, who utilized functionalized, linear polystyrene (PS) and polyethylene glycol (PEG) oligomers.⁹ Since this discovery, a plethora of supports have been reported. Many of these supports are based on vinyl monomers, though protein, carbohydrate, and norbornene type monomers have been used.^{10,11} Each polymer contributes its unique physical and chemical properties to the polymer supported catalyst system. This allows for selectivity of solubility and other physical properties of the polymer supported catalyst to be tailored to its’ application. However, most of them are obtained by either (i) polymerizing a monomer that has been pre-functionalized with a ligand/catalyst or (ii) using a post-polymerization modification strategy in which a ligand/catalyst is linked to a

pre-made polymer, in a grafting to approach. This can be problematic as the polymer's own synthesis often requires four components (monomer, initiator, ligand, and transition metal catalyst) in which only two (monomer and initiator) are incorporated into the resulting macromolecular architecture. For instance, atom transfer radical polymerization (ATRP) requires an alkyl halide initiator, copper catalyst, and organic ligand to facilitate the polymerization of vinyl monomers as seen in Figure 1.¹² This reaction is dictated by a redox process between the alkyl halide initiator and the Cu(I) catalyst that results in an equilibrium between a “dormant” and an “active” state.¹³ ATRP has developed such that reactions are initiated not only thermally, but also electro-chemically, mechanically, from chemical redox methods, and photochemically.^{14–18}

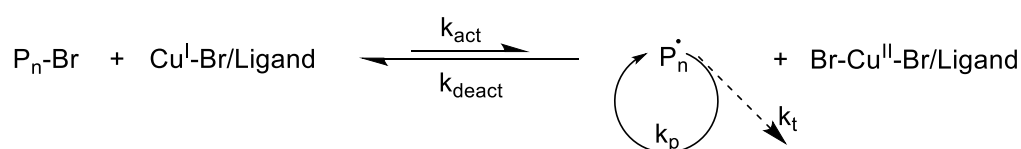


Figure 1. Typical ATRP reaction.

1.3 Photo Redox ATRP

Due to the low cost and near-nonexistent environmental impact, the use of light to facilitate chemical reactions (which has actually been known since the 19th century) has emerged as a strong alternative to traditional thermal reaction conditions. The excitation response from light in the visible region of elements such as Cr, Ti, Fe, Ru, and Ir has made them good candidates for photo-redox ATRP. In addition, organic catalysts have been used in the near ultra-violet (UV) region. These types of catalyst are known as photo-catalysts (PC). Photo-redox ATRP has utilized specific transition metals and organic dyes that are able to promote to an excited state, with long excitation lifetimes, to facilitate favorable redox potentials. Some photo-redox species also participate in

photochemical energy transfer.¹⁹ These processes trigger the generation of radical species that promote polymer propagation. A generic reaction mechanism for a photo redox polymerization is pictured in Figure 2. Photo-redox ATRP only solves a portion of the problem. While the energy source has become green the atom economy still hinders the “greenness” of the process.

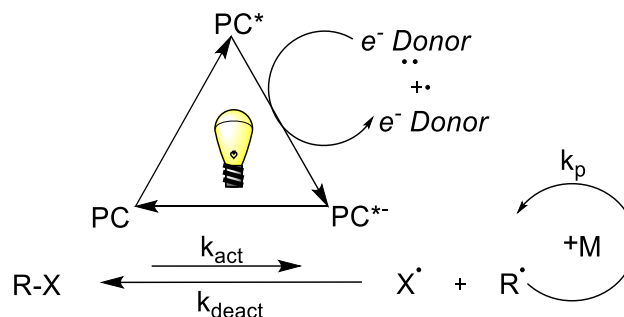


Figure 2. Generic photo-redox polymerization mechanism. Where R is the polymer chain and X is a halide.

1.4 Unimolecular Photo-Catalyst Initiator Systems

Our laboratory has reported on the use of ATRP for the preparation of new, polymer-supported salen catalysts.⁵ However, this system suffered in that the requisite transition metal complex used for the ATRP was not recovered or reused. An alternative approach that involves the incorporation of the ligand and metal complex into the polymer structure has been reported, but the potential for these unimolecular ligand initiator systems (ULISs) to act as recoverable catalysts has yet to be explored.²⁰ The previous research also failed to utilize a photocatalyst to enhance the “greenness”. Part of the research described in this thesis involves the synthesis of new, unimolecular photocatalyst initiator systems (UPCIS) in which the initiator, ligand and metal center or organic catalyst, are linked covalently. This allows for easy catalyst recovery for recycling in polymerization and other multi-functional catalytic reactions.

1.5 Multi-functional Catalytic Reactions

Multi-functional catalytic reactions are loosely defined by many as the ability of a catalyst to carry out multiple catalytic functions (not necessarily in a single pot).²¹ By having a catalyst with the capability of producing multiple compounds the green aspect of the catalyst in question is enhanced in that the use of the catalyst is affected through this ability. In the current research, the catalysts are able to initiate both polymerization, and post-polymerization synthetic reactions.

1.6 Catalytic Systems Investigated in this Work

1.6.1 Tris-bipyridine Ruthenium^{II} based

Two types of green catalyst were studied, the first is a tris-bipyridine ruthenium^{II} dihexafluorophosphate based catalyst and the second is an organic phenyl-phenothiazine based catalyst. The first green catalyst contains a visible light responsive Ru^{II} metal center and modified bipyridine (bpy) ligands. Ru^{II}(bpy)₃ catalysts are well studied and their long lived photo-excitation properties (≈ 600 ns) are well understood.^{22,23} Ru^{II}(bpy)₃ has been effectively employed as a catalyst for several polymerizations, and cycloaddition reactions in the past.²⁴⁻²⁶ Cycloadditions are useful tools for the synthesis of cyclic structures. Adding to the “greenness” of this catalyst is its capacity as a multi-functional catalyst.

1.6.2 10-Phenylphenothiazine Based

The second green catalyst investigated is based upon a modified phenyl-phenothiazine, a known photo-responsive catalyst.²⁷ The 10-phenylphenothiazine (PhPTZ) catalyst is well studied due to the shared characteristics with its parent compound, phenothiazine (PTZ). PhPTZ has also shown the ability to facilitate

polymerization and borylation reactions utilizing light from the near UV and visible region.^{28,29} Adding to the greenness of this catalyst is the fact that it is completely organic, thus does not contain any harmful or environmentally toxic metals.

1.7 Polymer Investigated

Poly(methyl methacrylate) (PMMA) is utilized in this research as the polymer support. PMMA has proven to be a viable polymer capable of being polymerized through photo redox ATRP.¹⁸ This is due to the fact that PPMA has a heat of polymerization reported to be between 13 and 13.6 kcal/mol of monomer by isothermal calorimetry.³⁰ PMMA also has intrinsic properties that make it an ideal photocatalyst support. PMMAs are highly UV and light resistant and provide excellent light transmission. PMMA is also insoluble in methanol providing a readily available solvent for the liquid/ solid separation. Furthermore, PMMAs are 100% recyclable, which may add an additional green component to this research.

1.8 Objectives

To our knowledge, the full functionality of recoverable polymer supported catalysts, having an integrated initiator to pseudo self-catalyze the polymer supports itself and subsequently used for multiple photo-activated reactions, has not been developed. It is the goal of this research to discover and synthesize such a catalyst and verify its effectiveness through multi-functional reactions as a green solution to conventional catalysts.

CHAPTER II

Examination of Ruthenium Based PSC

2.1 Background

Polymerizations facilitated by ruthenium^{II} catalysts have been studied since being first reported in 1995 with a $\text{RuCl}_2(\text{PPh}_3)_3$ complex.³¹ Ruthenium^{II} has been employed for ATRP reactions, as well as ionic polymerizations. However, the use of $\text{Ru}^{\text{II}}(\text{bpy})_3$ in photo-induced polymerizations was not realized until 2011.¹³ The proposed mechanism, as seen in Figure 3, starts through excitation by visible light of the Ru^{II} metal center to the excited state $\text{Ru}^{\text{II}*}$, which has a reduction potential of 0.78V vs a saturated calomel electrode (SCE) in acetonitrile.³² The metal is then reduced through the transfer of an electron from the sacrificial electron donor, *N,N*-diisopropylethylamine (DIPEA or Hünig's base). Here the electron can be transferred to the initiator to cause a reversible pseudo halogen transfer of the bromine, allowing the radical initiator to react with a monomer unit of methyl methacrylate. The propagation step continues until the radical end is deactivated by combining with another radical polymer end or through coordination with the aforementioned bromine and the electron is eliminated through reduction of the DIPEA back to a neutral species.

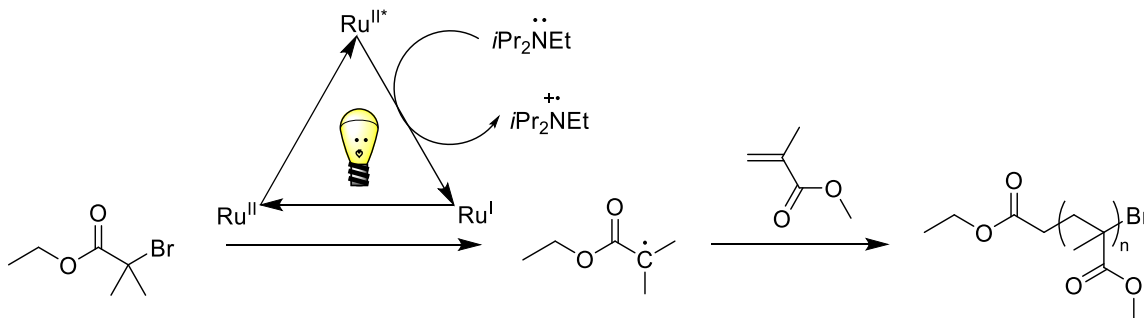


Figure 3. Simplified ruthenium^{II} polymerization mechanism

In contrast to $\text{Ru}^{\text{II}}(\text{bpy})_3$ polymerizations, UPCIS **Ru1** and **Ru2** have the initiator integrated into its framework as seen in Figure 4. This addition is expected to not interfere with the electronics of the catalyst and its ability to catalyze the reaction. The reaction mechanism is much the same as that seen in Figure 3, except the initiator is covalently attached to the bpy ligand. This serves to allow the catalyst to undergo a pseudo “self-catalyzed” process when forming the polymer supports. The integrated initiator becomes the point of propagation during the polymerization, and the need for an additional catalyst to facilitate the polymerization is eliminated.

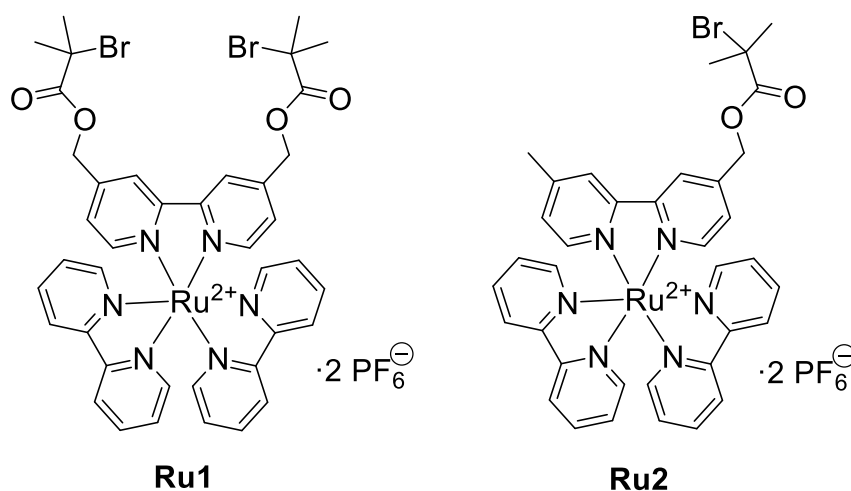


Figure 4. UPCIS **Ru1** and **Ru2**.

Not only has $\text{Ru}^{\text{II}}(\text{bpy})_3$ acted as an effective polymerization catalyst, but it has also proven itself in its ability to facilitate [2 + 2] intra and intermolecular cycloadditions. These reactions have been studied since 2008.²⁵ The proposed mechanism, as seen in Figure 5, involves the excitation of the Ru^{II} metal center to an excited state through visible light absorption. In this state the metal center is reduced to Ru^{I} through abstraction of an electron from a sacrificial electron donor to the metal center. The electron is then transferred to the enone, which can then undergo a step-wise [2 + 2] cycloaddition and

allow the Ru^{I} to be oxidized back to a Ru^{II} state.³³ The mechanism for the intermolecular [2 + 2] cycloaddition is the same, except that only one molecule is reduced to the radical form to facilitate the step-wise [2 + 2] cycloaddition with another neutral molecule.

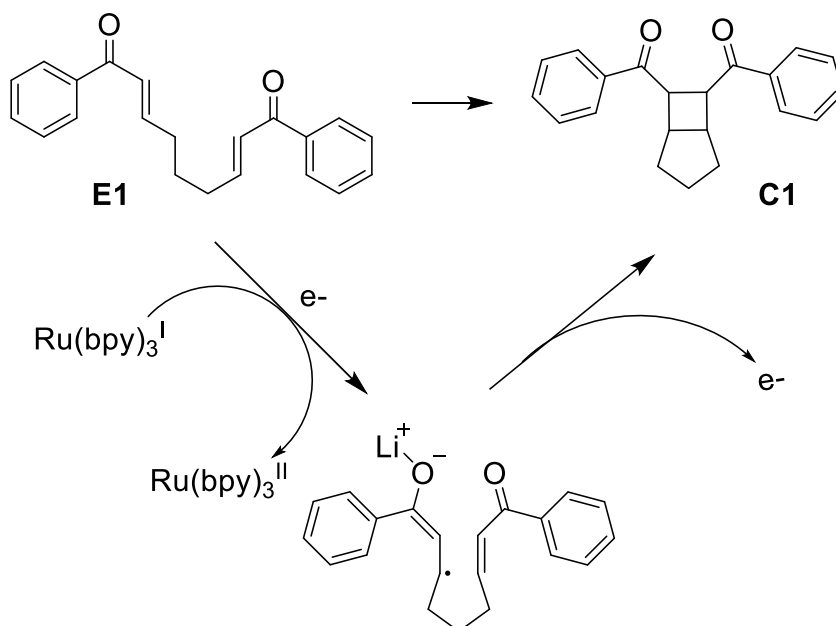


Figure 5. Abbreviated [2 + 2] cycloaddition mechanism.

2.2 Results

2.2.1 Polymer Supports Results

The synthesis of UPCIS **Ru1** is detailed in Section 2.4. Polymerizations of methyl methacrylate utilizing UPCIS **Ru1** were carried out in anhydrous solvent, under a nitrogen atmosphere. The monomer to initiator ratio was varied from 100:1 to 125:1. The UPCIS **RuPoly1** were initiated through irradiation with a 30-watt incandescent lamp for 20 hours. DIPEA was utilized as a sacrificial electron donor in *N,N*-dimethylformamide (DMF), as seen in Figure 6.

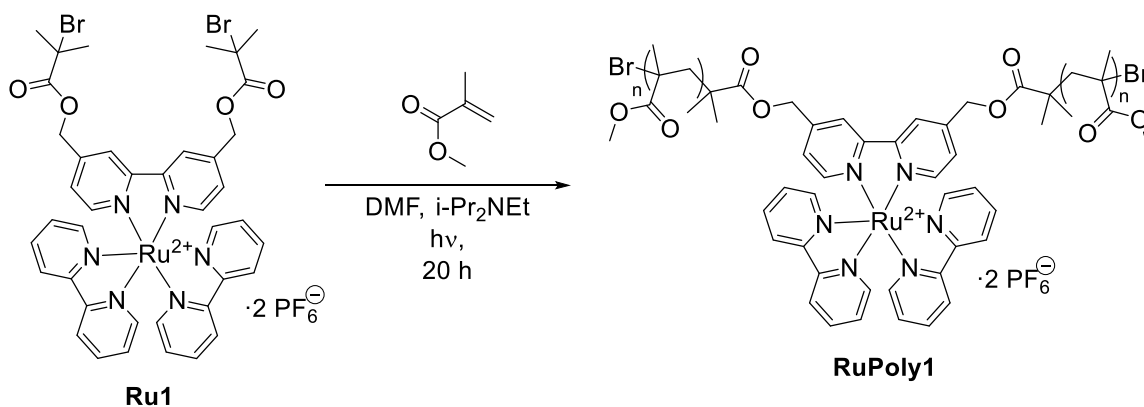


Figure 6. UPCIS **Ru1** polymerization reaction scheme.

Four polymerizations were carried out, as listed in Table 1, for the PSC **RuPoly1**. In addition, two control experiments were carried out in which Control 1 was kept in the dark for the 20 hours, and Control 2 was allowed to react without the addition of initiator utilizing $\text{Ru}^{\text{II}}(\text{bpy})_3$ as the catalyst. Table 1 also includes a rewash of the product from polymerization reaction 4 with ethanol to remove the lower molecular weight polymer chains.

Table 1
Polymerizations with UPCIS **Ru1**

Polymerization Reaction	M:I Ratio	% Yield	% Conv.	M_n via UV-Vis (g/mol)	M_n via GPC (g/mol)	\bar{D}
1	100	48	85	56700	26800	2.20
2	100	21	80	73900	31700	2.29
3	100	15	96	57800	-	-
4	125	49	68	43400	15200	2.39
Control 1	125	0	0	-	-	-
Control 2	-	10	98	-	-	-
4-Rewash	125	--	--	50700	20400	2.20

The PSCs were subjected to ^1H and ^{13}C NMR to verify successful polymerizations. The PSCs were then analyzed via UV-vis spectroscopy at 454 nm in acetonitrile for determination of average molecular weight per Ru^{II} metal center as

compared to a four-sample standard curve of $\text{Ru}^{\text{II}}(\text{bpy})_3\text{Cl}_2$ in acetonitrile at 451 nm. A plot of the calibration standards is seen in Figure 7.

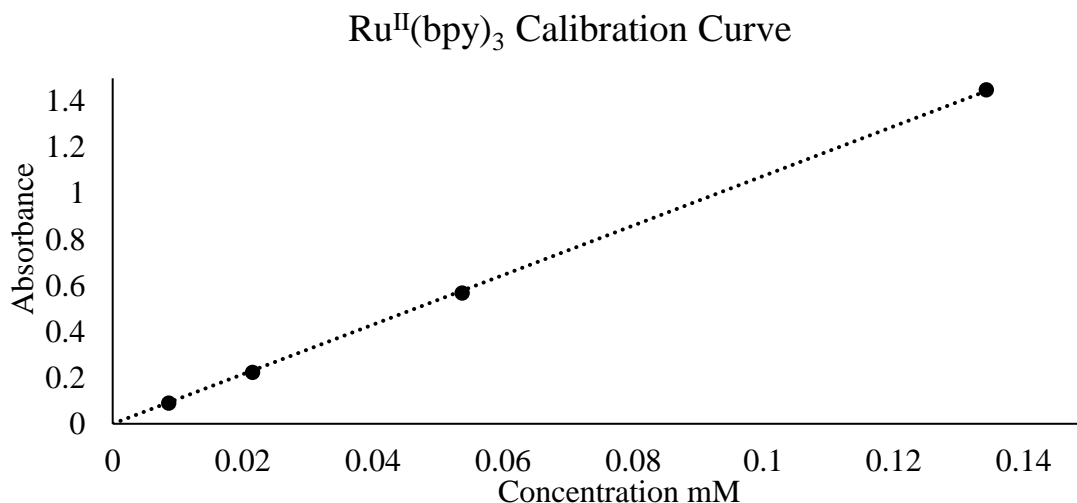


Figure 7. Ruthenium^{II} concentration calibration curve.

A regression with a zero intercept was performed on the calibration standards to calculate the calibration equation for determination of concentration as seen in Eq. 01. The calibration equation produced a R^2 value of 0.99. The ruthenium concentration was then used to determine the average molecular weight of the PSC sample per ruthenium metal center.

$$Y = 10.76X \quad \text{Eq01}$$

The UV-vis absorption revealed a bathochromic shift of 3 nm for the PSC **RuPoly1** in the absorption maxima for the metal to ligand charge transfer band (MLCT). This shift is visible in Figure 8, with the absorbance of PSC **RuPoly1** from 600 to 350 nm. As a secondary check of the molecular weights, gel permeation chromatography with refractive index (GPC) detection was used to determine the number average molecular weight. The GPC also served to reveal the poly-dispersity index values (M_w/M_n or \mathcal{D}) of the polymer supported catalysts as a measure of the polymerization control.

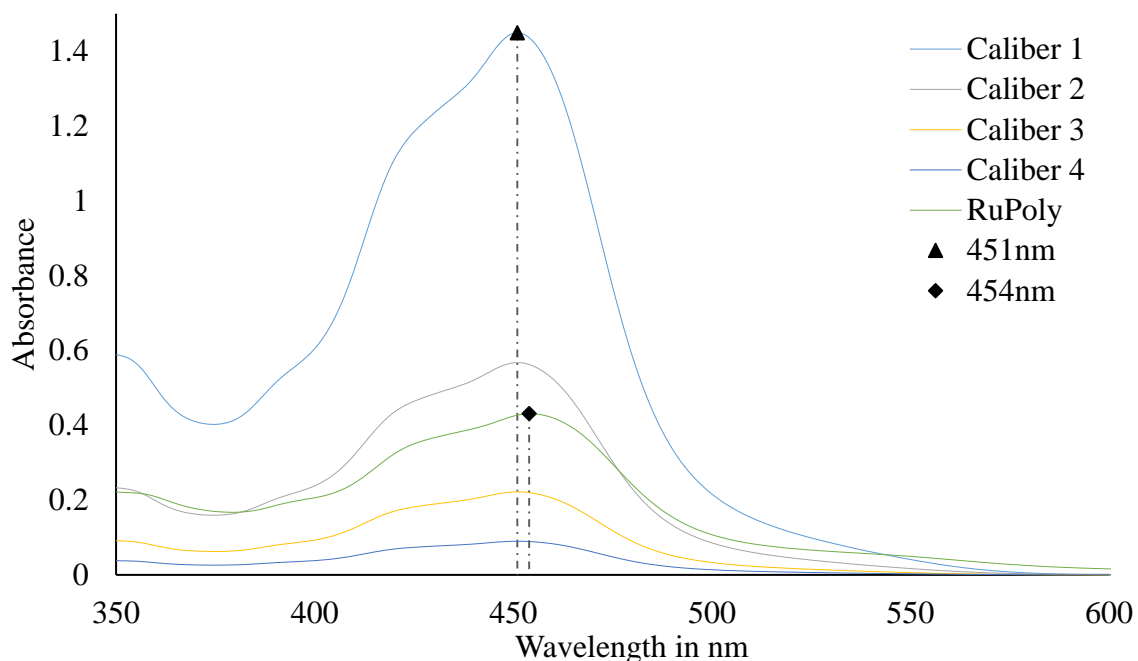


Figure 8. PSC **RuPoly** UV-Vis absorbance curves. The 3 nm shift is visible between the dashed vertical lines.

Similarly, UPCIS **Ru2** was also used to facilitate synthesis of PSC **RuPoly2** through the same conditions as UPCIS **RuPoly1** as seen in Figure 9. The detailed synthesis of UPCIS **Ru2** is available in Section 2.4.

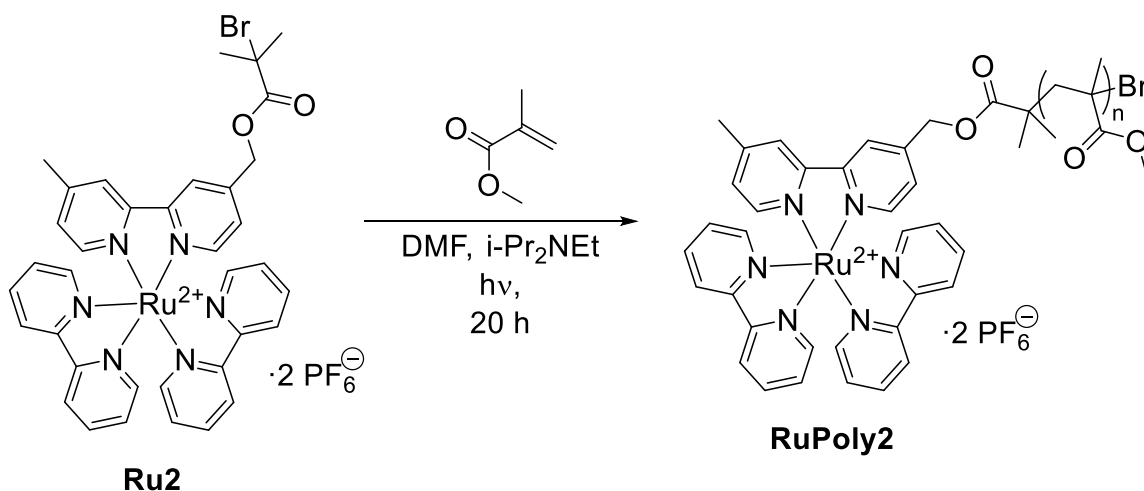


Figure 9. UPCIS **Ru2** polymerization scheme.

The polymerization experiment results are listed in Table 2, with the UV-vis and GPC determined number average molecular weights and D values. The same calibration

curve was used for PSC **RuPoly2** as was utilized for PSC **RuPoly1** to determine the ruthenium concentration and then the average molecular weights. The absorbance maxima for the MLCT band was also found to be at 454 nm revealing a 3 nm red shift as compared to the standard $\text{Ru}^{\text{II}}(\text{bpy})_3\text{Cl}_2$.

Table 2
UPCIS Ru2 polymerization results

Polymerization Reaction	M:I Ratio	% Yield	% Conv.	M_n UV-Vis (g/mol)	M_n via GPC (g/mol)	D
1	250	6	96	66369	-	-
2	250	18	25	59904	14500	2.54

2.2.2 [2 + 2] Cycloaddition Reactions

The PSC **RuPoly1** was then used in a 2.5 mol%, based upon the average molecular weight calculated based upon the UV-vis absorbance, equivalent to the catalyze [2 + 2] cycloaddition reactions of 1,9-diphenyl-(*E,E*)-2,7-nonadiene-1,9-dione (**E1**) as seen in Figure 10. The reaction was again initiated through irradiation of PSC **RuPoly1** with a 30-watt incandescent lamp for 5 hours. Lithium tetrafluoroborate (LiBF_4) was used as a stabilizing counter ion and DIPEA was utilized as the sacrificial electron donor in methylene chloride.

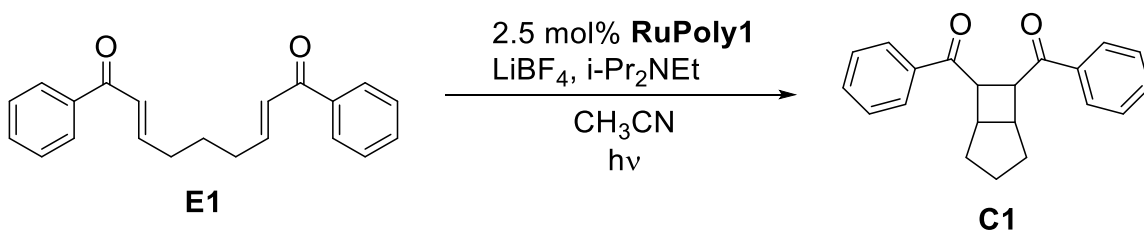


Figure 10. [2 + 2] cycloaddition of **E1** scheme.

The reaction was executed five times with the same catalyst being recycled from the first reaction through the last. The results are listed in Table 3. The reaction products were analyzed by ^1H NMR for determination of isomeric, as well as byproduct, ratios

after removal of the PSC. It should be noted that the PSC was separated through precipitation in methanol after each reaction with an average recovery of 89%. A small amount of cycloaddition product, **C1** was discovered by ^1H NMR to carryover with the PSC in each of the precipitations.

Table 3
RuPoly1 catalytic results from five cycles.

Reaction	reactant (mmol)	product (mmol)	% yield	Isomeric + byp ratio P/I+byprd
1	0.35	0.11	32	0.72
2	0.38	0.15	40	0.85
3	0.28	0.14	51	0.77
4	0.20	0.15	76	1.14
5	0.07	0.04	64	1.11

2.2.3 Metal Retention Results

To evaluate the retention of the metal center within the PSCs it was necessary to conduct additional UV-vis absorption and GPC measurements after utilization in five cycloaddition reactions. The previous calibration equation was then used to determine the ruthenium concentration and thereafter the average molecular weights. The results are listed in Table 4 below.

Table 4
PSC RuPoly1 metal retention

Polymerization Reaction	Initial M_n via UV-Vis (g/mol)	Initial M_n via GPC (g/mol)	New M_n via UV-Vis (g/mol)	New M_n via GPC (g/mol)	% change UV-Vis	% change GPC
1	56700	26800	113000	43400	199%	162%
4	43400	15200	78400	51500	181%	339%

2.3 Discussion

While UPCIS **RuPoly1** was able to facilitate photo-redox polymerizations, there was no control over the polymerization. The control of the polymerization is indicated by

the D value. This value is a ratio of the weight average molecular weight (M_w) over the number average molecular weight (M_n). The weight average molecular weight is determined by the sum the polymer chains times their respective molecular weights squared divided by the sum of the polymer chains times their respective molecular weights. This value is then divided by the sum of the polymer chains times their respective molecular weights divided by the total number of polymer chains. The M_w is always larger than the M_n . The D values ranged from 2.19 to 2.39 for these polymerizations as seen in Table 1. These results indicate that the catalyst is acting as it has in previous polymerization experiments where D values were found to be 2.1.¹³ The differences in yield, as compared to literature, may be attributed to the metal to initiator ratio. In the current research the metal to initiator ratio is 1:2 for UPCIS **Ru1**. This is supported in literature, where Park, *et al.* found a correlation between the percent yield and the metal to initiator ratio.¹³ It was discovered that with a ratio of 1:50 there was a 23% yield, but when the ratio was 1:250 there was a 31% yield for a four hour reaction time. This may also be the case for the decreased yields present in Table 2 for the UPCIS **Ru2** polymerization reactions where the ratio of metal to initiator is 1:1. By increasing the initiator ratio, the reaction equilibrium will rest predominantly in the dormant state, where there are no radicals formed.³⁴ That is the equilibrium will lie to the left in Figure 2. This is necessary for well controlled polymerizations as Matyjaszewski *et al.* reported early on in the development of controlled polymerizations.³⁴ The ratio of k_{act}/k_{deact} should be much less than one for well controlled polymerizations. Control of polymerization is dictated by the number of reactive sites available in solution at one time.³⁵ For well controlled polymer chains it is necessary for an active site to only react with monomer in

solution as seen in the top example of Figure 11. The bottom example results in polymer chains with widely varying chain lengths that may be terminated in a fashion that will not allow for reactivation for propagation. For the current research, the number of metal centers that can provide active initiators producing active radicals is a 1:2 ratio for UPCIS **Ru1** and 1:1 for UPCIS **Ru2**. These ratios suggest that the bottom example in Figure 11 is a more likely equilibrium and the ratio of k_{act}/k_{deact} is close to or larger than unity. This ultimately results in uncontrolled polymerizations with low yields and large D values.

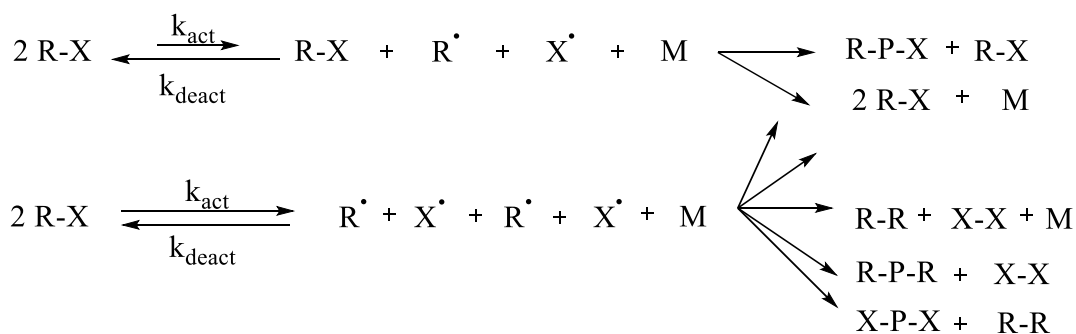


Figure 11. ATRP equilibrium diagrams. Where R-X is the initiator and M is a monomer unit and P is the polymer.

The polymerization control experiments offered some surprising insight to this reaction. The light free experiment resulted in no polymer formation in the reaction vessel as is expected. However, the initiator-free reaction resulted in a large amount of polymer formation. This is attributed to the sacrificial electron donor after loss of an electron generating an initiator through C-C cleavage or hydrogen abstraction on the carbon alpha to the nitrogen, as seen in Figure 12.³⁶ Both proposed mechanisms provide a radical species that can initiate polymerization of the monomer or terminate propagation. The propagation step of the polymerization is terminated when the active ends of the polymers either react with another active polymer chain end or another sacrificial electron donor generated radical. With the excess of sacrificial electron donor, DIPEA,

availability to this source of initiation and termination would result in higher D values.

The terminations of active polymer chains by the DIPEA formed radicals would also result in loss of reactivation and a dead polymer chain.

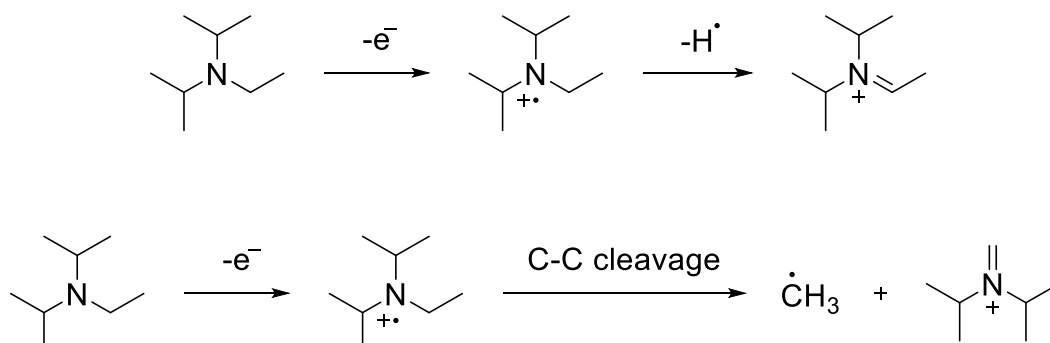


Figure 12. Sacrificial electron donor mechanisms to form initiators.

Also, of interest was the 3 nm shift in the UV-vis spectrum of the PSC as compared to $\text{Ru}^{\text{II}}(\text{bpy})_3$. This red shift is indicative of electron donation from the substituents in the 4 and 4' positions on the bipyridine rings. These same types of shifts were observed in monodentate pyridine ligands when electron donating substituents were placed in the 4 position.³⁷ This electron donation into the metal center caused a destabilization of the $4d\pi$ orbitals in $\text{Ru}^{\text{II}}(\text{bpy})_3$.³⁸ This shift also denotes a destabilization of the metal to ligand bond allowing for easy ligand substitution. By adding additional electron density into the bipyridine ligand, the crystal field splitting energy (Δ_o) is reduced, as seen when comparing the left and center crystal field splitting diagrams in Figure 13.

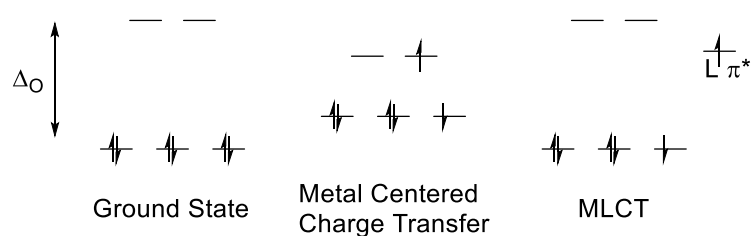


Figure 13. Crystal field splitting energy differences.

The electron donation may result in the energy spacing between the triplet excited state MLCT energy level and the triplet metal centered (MC) excited energy level decreasing as noticed when comparing the center and right crystal field splitting diagrams in Figure 13. This would allow the radiationless decay of the excited state Ru^{II} to more easily pass through this energy level in an internal conversion event prior to decaying to the ground state.³⁹ While in the triplet MC excited energy level an electron may populate the metal σ^* orbital. This will promote bond dissociation of the ligand with the metal center resulting in a five-coordinate species. This is especially true in the presence of coordinating ions like bromide and in a low polarity solvent.³²

Comparing the current PSC to $\text{Ru}^{\text{II}}(\text{bpy})_3$ in previous research, the bpy ligand that is no longer bidentate to the metal can completely dissociate leaving a neutral $\text{Ru}(\text{bpy})_2\text{X}_2$ where X is a coordinated anion from the solution. The current polymerization reactions were conducted in acetonitrile, considered a high polarity solvent that would limit this effect, but also given the fact that the bromide ion is free in solution this effect may be of larger impact than initially suspected. This may eventually allow the ruthenium metal to completely dissociate from the polymer bound bipyridine and be found simply within the polymer matrix and not covalently linked as part of the polymer itself. This could then cause the catalyst concentration to diminish as subsequent multifunctional catalytic reactions were carried out, causing unexpected results in the reactions as seen in the [2 + 2] cycloaddition reactions.

The results from the [2 + 2] cycloaddition did not show good agreement with previous literature results when $\text{Ru}^{\text{II}}(\text{bpy})_3$ was used as the PC.³³ The previous research by Yoon *et al.* did indicate that the isomers, **I1** and **I2**, and byproduct (**byprd**), seen in

Figure 14, are products of the reaction but were reported in much lower ratios than seen in the present research. The isomers and byproduct were found initially in electrochemically promoted [2 + 2] cycloaddition reactions of **E1** by Krische *et al.*⁴⁰ Yoon *et al.* was able to reproduce the isomers and byproducts by subjecting diastereomerically-pure **C1** to prolonged exposure to the PC Ru^{II}(bpy)₃. It was deduced that through prolonged contact with the catalyst the stereo specific **C1** molecule will erode to the isomers and byproduct.⁴¹ Utilizing the previous research results, it may be considered that the polymer matrix within the solution may act as a type of cage or barrier causing some of the catalyzed product to be overly exposed to the catalyst. This phenomenon may be exacerbated if the PSC metal is at a lower concentration than is expected in the polymer.

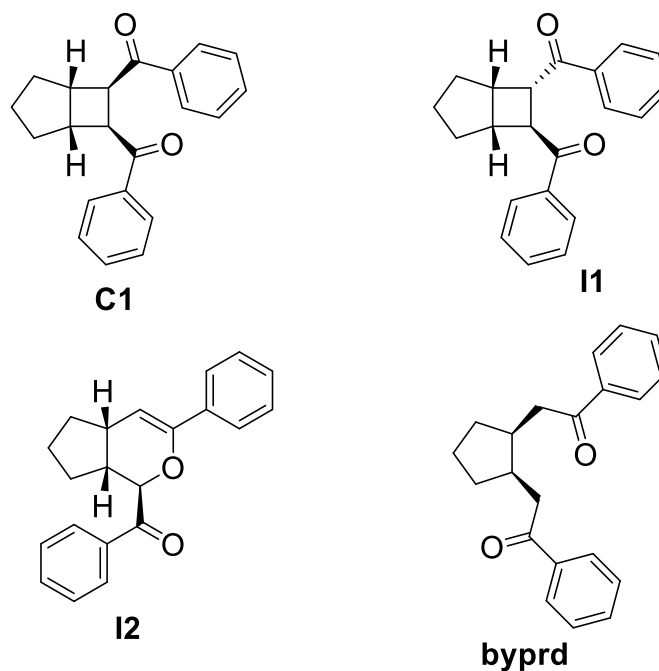


Figure 14. Cycloaddition product **C1**, isomers and byproduct.

The metal retention experiments were necessary to determine if the concentration of the metal of the PSC was lost over the course of the cycloaddition reactions. By the

results presented in Table 4, it is well observed that the metal center concentration is severely diminished after five recycles. This may indicate that the polymer supported ligand of bipyridine may be dissociating from the Ru^{II} metal center. Research by Sauvage *et al.* has shown that a sterically bulky ligand that has electron donating substituents will selectively undergo photochemical labilization.⁴² The bidentate bpy ligands that were lost were readily replaced with solvent molecules of acetonitrile in that research.⁴² This leads to the possibility that if the metal center is still incorporated into the polymer backbone during the time that the cycloaddition reactions are taking place that there may exist a high probability of polymer supported ligand dissociation and coordination of acetonitrile or some other anionic species from the reaction. This would result in the possibility of a Ru^{II}(bpy)₂(CH₃CN)₂ catalyst simply being trapped in the polymer matrix, and subsequently transferred to the next reaction or lost during the PSC recovery step.

2.4 Experimental

All air or moisture sensitive reactions were carried out under a nitrogen atmosphere utilizing standard Schlenk techniques. The glassware was flame dried to ensure the absence of moisture from the reaction. Purification through column chromatography was accomplished with 60 Å silica gel. The elution was verified through visualization on silica gel coated glass thin layer chromatography (TLC) plates, using a 254 nm ultra-violet (UV) handheld light source for illumination. All starting materials were purchased from commercial sources (Alfa Aesar, Sigma Aldrich, and TCM Chemicals), and used without further purification unless specifically mentioned. Products were verified through ¹H and ¹³C NMR spectroscopy with a JEOL Eclipse 300 MHz spectrometer. Chemical shifts are reported in δ (ppm) relative to the ¹H and ¹³C signal of

the deuterated solvent used ($\{CDCl_3: 7.26 \text{ } ^1H, 77.16 \text{ } ^{13}C\}$, $\{d_6\text{-DMSO}: 2.49 \text{ } ^1H, 39.52 \text{ } ^{13}C\}$). Further characterization of indicated products was accomplished through UV-vis spectroscopy and gel permeation chromatography (GPC). UV-vis absorbance measurements were generated using a Jasco V-750 equipped with dual light sources of deuterium and tungsten lamps. The instrument was set to scan from 800 to 220 nm in 0.2 nm steps at 400 nm/min. GPC analysis was conducted using a Viscotek VE 1122 solvent delivery system and VE 3580 RI detector with LT4000L mixed column and molecular weight data were calculated relative to polystyrene standards.

(4'-{[(2-bromo-2-methylpropanoyl)oxy]methyl}-[2,2'-bipyridin]-4-yl)methyl-2-bromo-2-methylpropanoate (L1)

Synthesis of 2

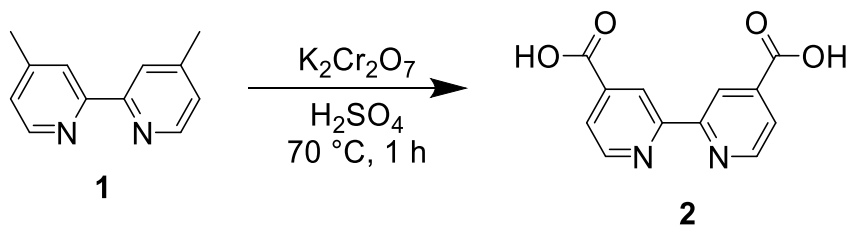


Figure 15. Synthesis of **2** reaction scheme.

The synthesis procedure was modified from literature.⁴³ A 250 mL round bottom flask equipped with a stir bar was charged with **1** (2.11 g, 11.5 mmol) and concentrated sulfuric acid (53 mL, 987 mmol) and heated to 70 °C with stirring. Potassium dichromate (10.1 g, 34.4 mmol) was slowly added to the solution while maintaining stirring. The solution was maintained with stirring at 70 °C for one hour. The hot solution was then poured over 300 g ice and allowed to stir for one hour (observed fine yellow precipitate). The solution was then vacuum filtered and rinsed with water. The filtered solid was then suspended in 70 mL 50% aqueous nitric acid in a round bottom flask. The solution was

then heated to 120 °C with stirring for four hours. The solution was then allowed to cool to room temperature and poured over 300 g ice without stirring. The suspension was left overnight (observed a white precipitate). The resulting precipitate was vacuum filtered and rinsed with water. The product was allowed to dry under vacuum yielding **2** as a fine white powder in 93% yield (2.92 g). Spectral data matched literature values.⁴⁴ ¹H-NMR (300 MHz, DMSO-*d*₆) δ 8.91 (d, *J* = 4.9 Hz, 2H, Ar-H), 8.83 (s, 2H, Ar-H), 7.91 (dd, *J* = 4.9, 1.5 Hz, 2H, Ar-H)

Synthesis of **3**

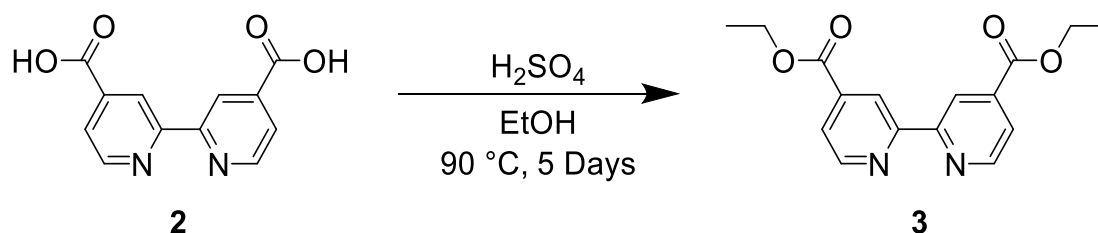


Figure 16. Synthesis of **3** reaction scheme.

The synthesis procedure was modified from literature.⁴³ A 250 mL round bottom flask equipped with a stir bar was charged with **2** (2.62 g, 10.7 mmol) and 150 mL ethanol. The suspension was stirred for 1 minute, then concentrated sulfuric acid (2.29 mL, 43.0 mmol) was slowly added. While stirring, the mixture was refluxed for 5 days at 90 °C. The solution was then allowed to cool to room temperature and transferred to a 500 mL round bottom flask. Then 160 mL of water was added and allowed to mix for 10 minutes. The ethanol was then evaporated via rotary evaporator. The solution was then neutralized with 10% potassium hydroxide solution (observed a white precipitate). The suspension was then vacuum filtered and rinsed with water. The solid was allowed to dry on the vacuum to reveal **3** as a fine white powder in 93% yield (2.98 g). Spectral data matched literature values.⁴⁵ ¹H-NMR (300 MHz, DMSO-*d*₆) δ 8.95 (d, *J* = 4.9 Hz, 2H,

Ar-H), 8.84 (s, 2H, Ar-H), 7.93 (dd, $J = 4.9, 1.5$ Hz, 2H, Ar-H), 4.41 (q, $J = 7.1$ Hz, 4H, OCH_2CH_3), 1.37 (t, $J = 7.1$ Hz, 6H, CH_2CH_3)

Synthesis of 4

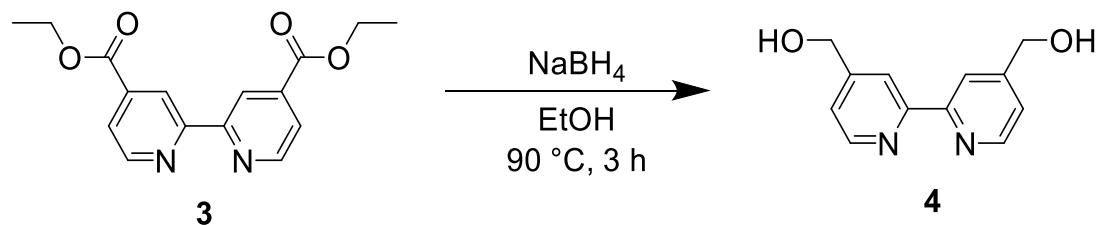


Figure 17. Synthesis of **4** reaction scheme.

The synthesis procedure was modified from literature.⁴³ A 250 mL round bottom flask equipped with a stir bar was charged with **3** (2.98 g 9.93 mmol) and 191 mL ethanol. The suspension was allowed to mix for 10 minutes then sodium borohydride (8.26 g, 218 mmol) was slowly added. The mixture was then allowed to stir under reflux for three hours at 90 °C. The solution was then allowed to cool to room temperature and ammonium chloride (100 mL, aq., sat.) was slowly added to the solution. The ethanol was then evaporated via rotary evaporator. Water was then added to the round bottom flask until no white precipitate was present. The organic layer was then extracted with ethyl acetate (4 X 50 mL). The organic layers were then combined and dried over anhydrous sodium sulfate. Finally, the solvent was evaporated via rotary evaporator to reveal **4** as a white powder in 34% yield (0.73 g). Spectral data matched literature values.⁴⁶ ¹H-NMR (300 MHz, DMSO-*d*₆) δ 8.59 (d, $J = 4.9$ Hz, 2H, Ar-H), 8.38 (s, 2H, Ar-H), 7.36 (d, $J = 4.2$ Hz, 2H, Ar-H), 5.51 (s, 2H, -OH), 4.62 (s, 4H, Ar- CH_2OH)

Synthesis of L1

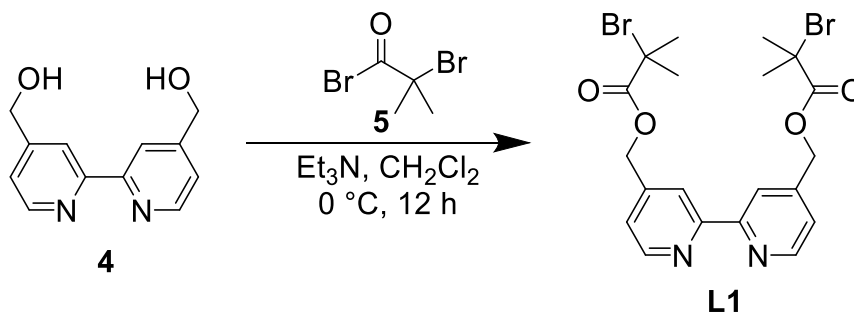


Figure 18. Synthesis of **L1** reaction scheme.

A two necked, round bottom flask, equipped with a magnetic stir bar, was submerged in an ice/water bath and charged with **4** (1.23 g, 5.94 mmol) and methylene chloride (125 mL) while stirring under a nitrogen atmosphere. Triethylamine (1.66 mL, 11.9 mmol) was then added via syringe and this mixture was allowed to stir for ten minutes. Via syringe, α -bromoisobutyryl bromide **5** (2.20 mL, 17.8 mmol) was slowly added, and the reaction mixture was allowed to stir overnight while warming to room temperature. At this point, the reaction mixture was washed with 3 portions of water and the organic layer was isolated and dried over anhydrous sodium sulfate. This solution was then filtered, and excess solvent was removed via rotary evaporator. **L1** was purified via silica gel column chromatography (methylene chloride:acetone, 100:7). Removal of excess solvent produced **L1** as light-yellow crystals in 62% yield (1.89 g). $^1\text{H-NMR}$ (300 MHz, $\text{DMSO-}d_6$) δ 8.78 (d, $J = 5.1$ Hz, 2H, Ar-H), 8.48 (s, 2H, Ar-H), 7.62 (d, $J = 4.1$ Hz, 2H, Ar-H), 5.42 (s, 4H, Ar- CH_2), 1.97 (s, 12H, $\text{CBr}(\text{CH}_3)_2$). $^{13}\text{C-NMR}$ (76 MHz, $\text{DMSO-}d_6$) δ 154.91 (s, 2C), 153.17 (s, 2C), 148.37 (s, 4C), 122.11 (s, 4C), 117.99 (s, 4C), 61.55 (s, 4C)

[2-(4-methylpyridin-2-yl)pyridine-4-yl]methyl-2-bromo-2-methylpropanoate (L2)

Synthesis of 6

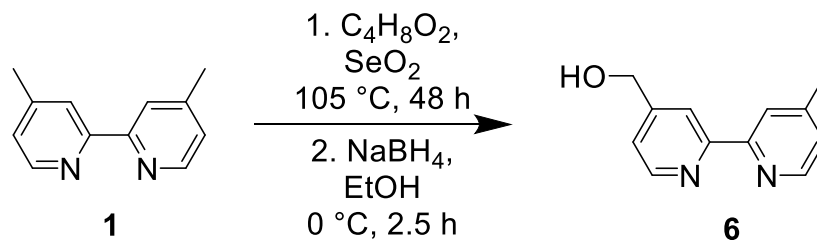


Figure 19. Synthesis of **6** reaction scheme.

The synthesis procedure was modified from literature.⁴⁷ A round bottom flask, equipped with a magnetic stir bar was charged with **1** (2.00 g, 10.9 mmol), 1,4-dioxane (100 mL, 1170 mmol), and selenium dioxide (2 g, 18.0 mmol). The mixture was allowed to stir for 48 hours at 105 °C under a nitrogen atmosphere. The mixture was then cooled to room temperature and filtered. The solvent was removed via rotary evaporator. The solid was then dissolved in methylene chloride and filtered to remove the selenium byproducts. The dissolution and filter procedure were repeated three times. The solvent was then removed via rotary evaporation. The solid was suspended in 25 mL methanol. The temperature of the solution was then reduced to 0 °C and 0.30 g sodium borohydride in 0.20 g sodium hydroxide in 2.50 mL water was added dropwise to the solution while stirring. The solution was allowed to move to room temperature and stirring was continued for 2.5 hours. The organic layer was extracted with methylene chloride (3 X 25 mL) and washed with water. The organic layers were then concentrated via rotary evaporator and purified via column chromatography (methylene chloride:methanol:ammonium chloride (aq. sat.), 94.7:5.8:0.5). to reveal **6** as a white solid in 41% yield (0.90 g). Spectral data matched literature values.⁴⁸ ¹H-NMR (300 MHz, CDCl₃) δ 8.58 (d, *J* = 4.8 Hz, 1H), 8.50 (d, *J* = 4.8 Hz, 1H), 8.31 (s, 1H), 8.19 (s,

1H), 7.29 (d, $J = 4.5$ Hz, 1H), 7.15 (d, $J = 4.5$ Hz, 1H), 4.77 (s, 2H), 3.64 (s, 1H), 2.43 (s, 3H)

Synthesis of L2

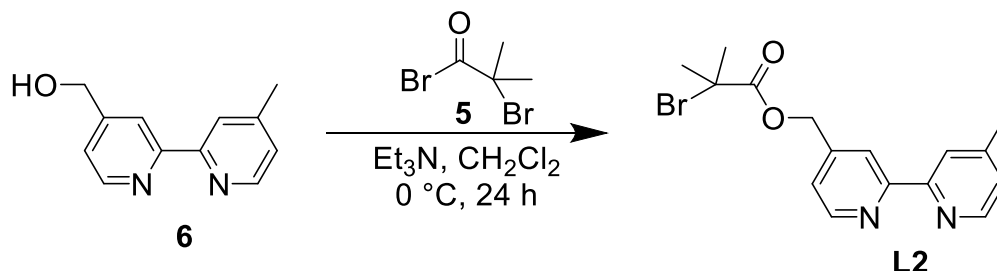


Figure 20. Synthesis of **L2** reaction scheme.

A two necked 250 mL round bottom flask, equipped with a magnetic stir bar under a nitrogen atmosphere, was charged with **6** (0.90 g, 4.50 mmol) and 116 mL methylene chloride and placed in an ice bath at $0\text{ }^\circ\text{C}$. After stirring was started 2.50 mL triethylamine was added via syringe. The solution was allowed to mix for ten minutes, then **5** (5.50 mL, 35.6 mmol) was slowly added via syringe to the solution. The solution was stirred overnight allowing the solution to move to room temperature. The reaction mixture was then washed with water and the organic layer separated. The organic layer was then dried over anhydrous sodium sulfate and the solvent was evaporated via rotary evaporator. The crude product **L2** was purified via silica gel column chromatography (methylene chloride:acetone= 100:7). The solvent was evaporated to yield **L2** as a dark brown oil in 50% yield (0.79 g). $^1\text{H-NMR}$ (300 MHz, CDCl_3) δ 8.68 (d, $J = 5.2$ Hz, 1H), 8.53 (d, $J = 4.8$ Hz, 1H), 8.37 (s, 1H), 8.23 (s, 1H), 7.34 (d, $J = 4.8$ Hz, 1H), 7.15 (d, $J = 4.1$ Hz, 1H), 5.30 (s, 2H), 2.44 (s, 3H), 1.99 (s, 6H). $^{13}\text{C-NMR}$ (76 MHz, CDCl_3) δ 170.73 (s, 1C), 155.93 (s, 1C), 154.77 (s, 1C), 149.10 (s, 1C), 148.46 (s, 1C), 147.99 (s, 1C), 145.16 (s, 1C), 124.64 (s, 1C), 121.72 (s, 1C), 121.16 (s, 1C), 118.86 (s, 1C), 65.30 (s, 1C), 55.02 (s, 1C), 30.38 (s, 2C), 20.87 (s, 1C)

Ruthenium ligand coordination

Ru1

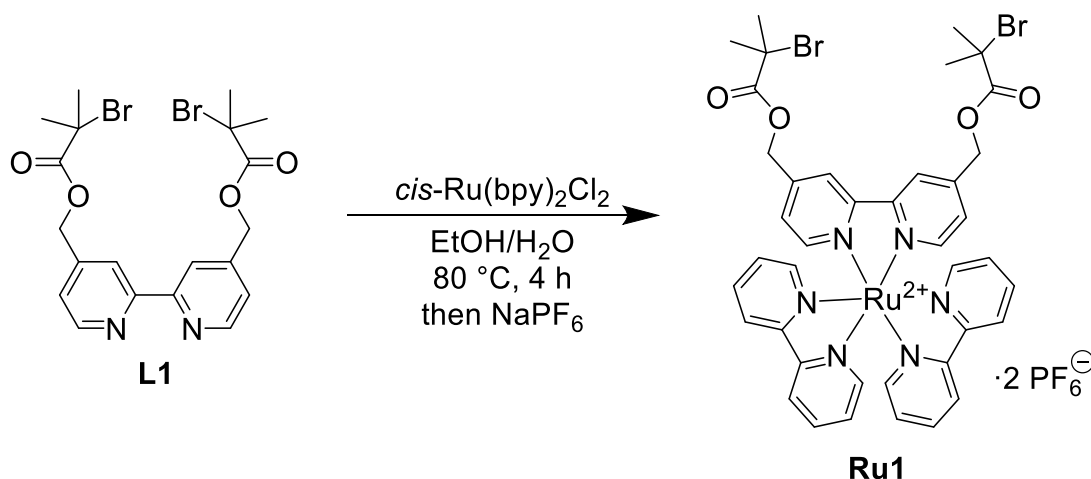


Figure 21. Synthesis of UPCIS **Ru1** reaction scheme.

The synthesis procedure was modified from literature.³⁷ A round-bottomed flask, equipped with a magnetic stir bar and a water-jacketed reflux condenser, was charged with **L1** (0.21 g, 0.41 mmol), a 1:1 ethanol:water mixture (9.19 mL), followed by *cis*-Ru(bpy)₂Cl₂ (0.20 g, 0.41 mmol). This dark red mixture was placed on an oil bath regulated at 80 °C and allowed to stir at reflux for 4 hours in the dark. At this time, the mixture was subjected to a hot filtration and the excess solvent was removed via rotary evaporator while maintaining a dark environment. To this crude mixture was added water (20.0 mL) followed by potassium hexafluorophosphate (0.75 g, 4.07 mmol). The precipitate was allowed to settle overnight and was subsequently isolated via vacuum filtration to provide **Ru1** as a red solid in 54% yield (0.33 g). ¹H-NMR (300 MHz, DMSO- *d*₆) δ 8.83 (d, *J* = 8.3 Hz, 4H), 8.71 (s, 2H), 8.16 (t, *J* = 7.4 Hz, 4H), 7.80-7.69 (m, 6H), 7.52 (t, *J* = 6.0 Hz, 6H), 5.46 (s, 4H), 1.95 (s, 12H).

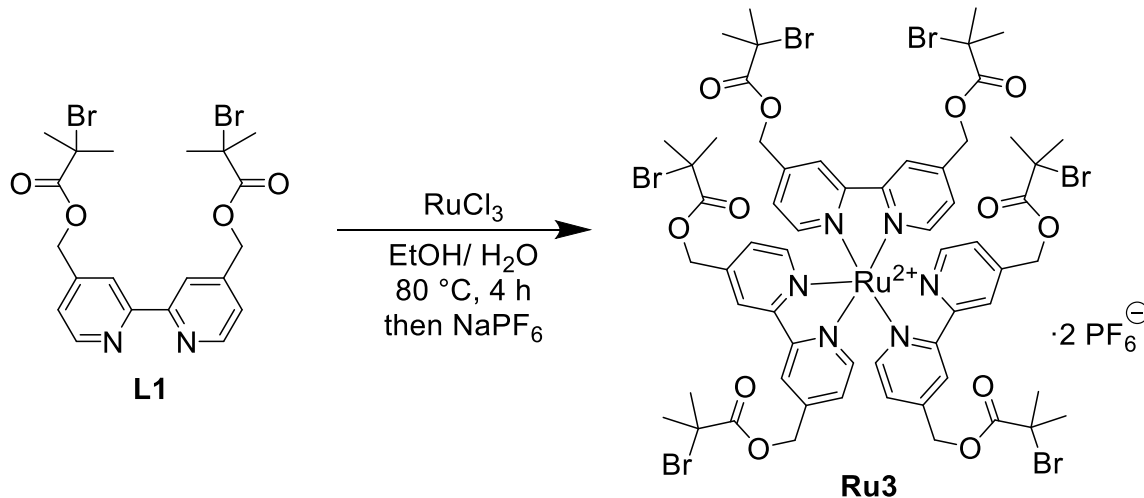
Ru3

Figure 22. Synthesis of UPCIS **Ru3** reaction scheme.

The synthesis procedure was modified from literature.³⁷ A round-bottomed flask, equipped with a magnetic stir bar and a water-jacketed reflux condenser, was charged with **L1** (0.62 g, 1.20 mmol), a 1:1 ethanol:water mixture (9.19 mL), followed by $\text{Ru}^{\text{III}}\text{Cl}_3$ (0.08 g, 0.40 mmol). This dark red mixture was placed on an oil bath regulated at $80\text{ }^\circ\text{C}$ and allowed to stir at reflux for 10 hours in the dark. At this time, the mixture was subjected to a hot filtration and the excess solvent was removed via rotary evaporator while maintaining a dark environment. To this crude mixture was added water (20 mL) followed by potassium hexafluorophosphate (0.75 g, 4.07 mmol). The precipitate was allowed to settle overnight and was subsequently isolated via vacuum filtration to provide **Ru3** as a dark red solid in 23% yield (0.18 g). $^1\text{H-NMR}$ (300 MHz, $\text{DMSO-}d_6$) δ 10.02-7.42 (m, 22H), 5.57-5.36 (m, 12H), 2.25-2.00 (m, 36H).

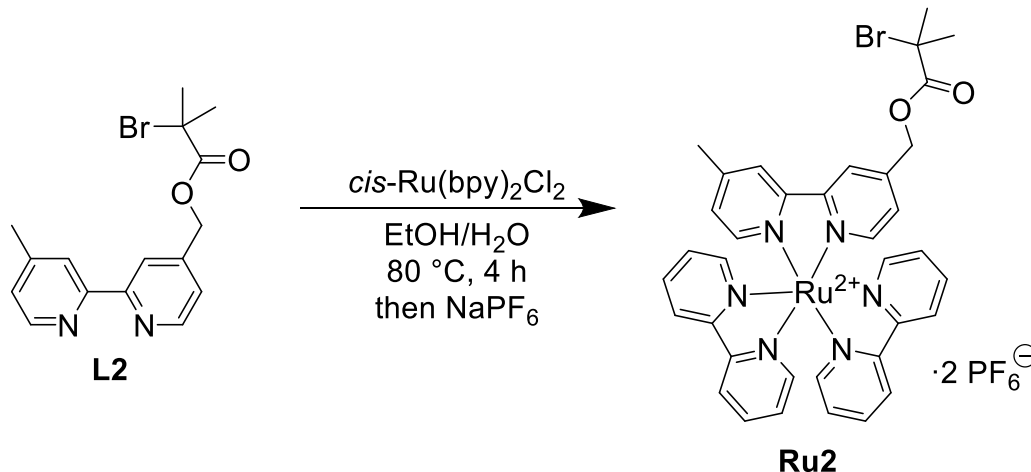
Ru2

Figure 23. Synthesis of UPCIS **Ru2** reaction scheme.

The synthesis procedure was modified from literature.³⁷ A round-bottomed flask, equipped with a magnetic stir bar and a water-jacketed reflux condenser, was charged with **L2** (0.14 g, 0.41 mmol), a 1:1 ethanol:water mixture (9.19 mL), followed by *cis*-Ru(bpy)₂Cl₂ (0.20 g, 0.41 mmol). This dark red mixture was placed on an oil bath regulated at 80 °C and allowed to stir at reflux for 4 hours in the dark. At this time, the mixture was subjected to a hot filtration and the excess solvent was removed via rotary evaporator while maintaining a dark environment. To this crude mixture was added water (20.0 mL) followed by potassium hexafluorophosphate (0.75 g, 4.07 mmol). The precipitate was allowed to settle overnight and was subsequently isolated via vacuum filtration to provide **Ru2** as a red solid in 59% yield (0.26 g). ¹H-NMR (300 MHz, DMSO-*d*₆) δ 8.82 (d, *J* = 8.3 Hz, 5H), 8.63 (s, 1H), 8.15 (t, *J* = 7.6 Hz, 4H), 7.77-7.69 (m, 5H), 7.56-7.47 (m, 6H), 7.38 (d, *J* = 5.5 Hz, 1H), 5.44 (s, 2H), 2.51 (s, 3H), 1.95 (s, 6H).

Ruthenium catalyst polymerization

Polymerizations utilized methyl methacrylate that was passed through a column of basic alumina four times to remove radical scavenger stabilizers. ^1H NMR analysis of the polymer supported catalyst was used to determine successful polymer formation.

RuPoly1

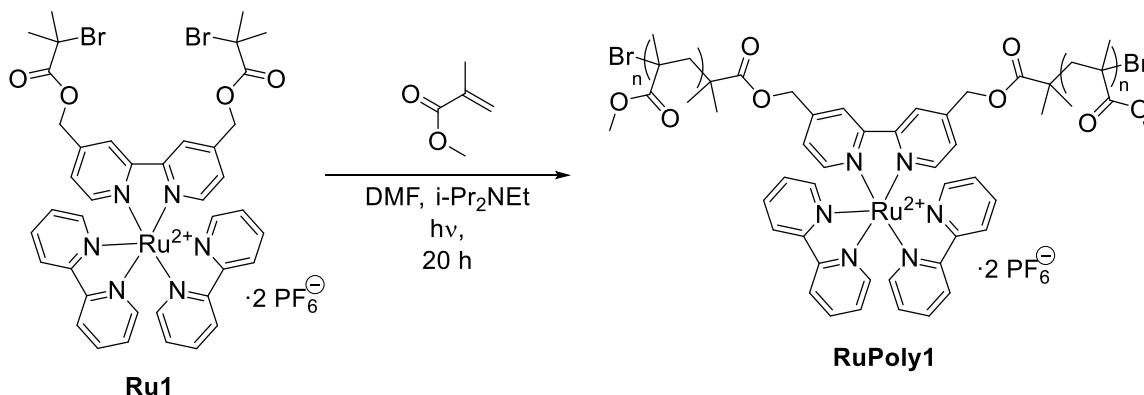


Figure 24. Synthesis of PSC **RuPoly1** reaction scheme.

The synthesis procedure was modified from literature.¹³ A flame dried, Schlenk flask, equipped with a magnetic stir bar, was charged with DMF (6.78 mL), methyl methacrylate (6.78 mL, 63.8 mmol), and DIPEA (2.67 ml, 15.3 mmol). This mixture was placed under a nitrogen atmosphere and frozen in a bath of liquid nitrogen. To this solid mixture was added **Ru1** (0.31 g, 0.26 mmol) and the mixture was subjected to 3 freeze-pump-thaw cycles in the dark. Once thawed, a 30-watt frosted incandescent lamp was placed approx. 15 cm away from the reaction flask, which was allowed to stir for 20 hours. At this point, **RuPoly1** was isolated via solvent precipitation into methanol followed by vacuum filtration. **RuPoly1** was further purified by dissolving in a minimal amount of acetonitrile followed by precipitating into methanol to provide **RuPoly1** as a red/orange solid in 35% yield (2.34 g). ^1H -NMR (300 MHz, CDCl_3) δ 3.59 (s, 3H), 1.81-2.07 (m, 2H), 0.63-1.21 (m, 3H)

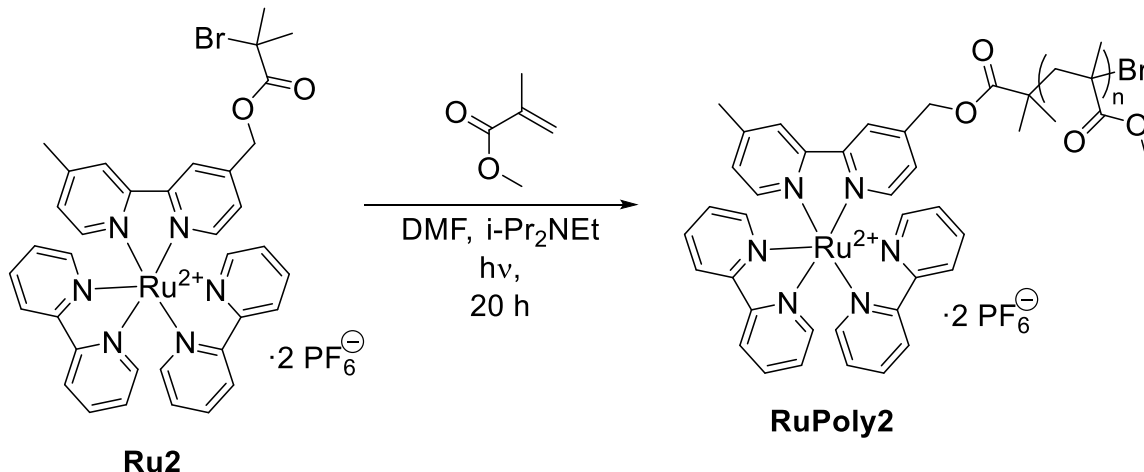
RuPoly2

Figure 25. Synthesis of PSC **RuPoly2** reaction scheme.

A flame dried, Schlenk flask, equipped with a magnetic stir bar, was charged with DMF (4.00 mL), methyl methacrylate (4.00 mL, 37.6 mmol), and DIPEA (1.57 ml, 9.01 mmol). This mixture was placed under a nitrogen atmosphere and frozen in a bath of liquid nitrogen. To this solid mixture was added **Ru2** (0.16 g, 0.15 mmol) and the mixture was subjected to 3 freeze-pump-thaw cycles in the dark. Once thawed, a 30-watt frosted incandescent lamp was placed approx. 15 cm away from the reaction flask, which was allowed to stir for 20 hours. At this point, **RuPoly2** was isolated via solvent precipitation into methanol followed by vacuum filtration to provide **RuPoly2** as a red/orange solid in 5% yield (0.22 g). ¹H-NMR (300 MHz, CDCl₃) δ 3.60 (s, 3H), 1.81-2.17 (m, 2H), 0.84-1.27 (m, 3H)

Polymerization Control Experiment #1 (PCE1)

A flame dried, Schlenk flask, equipped with a magnetic stir bar, was charged with DMF (6.78 mL), methyl methacrylate (6.78 mL, 63.8 mmol), and DIPEA (2.67 ml, 15.3 mmol). This mixture was placed under a nitrogen atmosphere and frozen in a bath of liquid nitrogen. To this solid mixture was added **Ru1** (0.31 g, 0.26 mmol) and the

mixture was subjected to 3 freeze-pump-thaw cycles in the dark. Once thawed, the solution was allowed to stir for 20 hours in the dark. At this point, **RuPoly1** was isolated via solvent precipitation into methanol followed by vacuum filtration to provide no precipitate.

Polymerization Control Experiment #2 (PCE2)

A flame dried, Schlenk flask, equipped with a magnetic stir bar, was charged with DMF (6.78 mL), methyl methacrylate (6.78 mL, 63.8 mmol), and DIPEA (2.67 ml, 15.3 mmol). The contents of the flask were frozen and Ru(bpy)₃Cl₂ (0.08 g 0.12 mmol) was added. This mixture was then placed under a nitrogen atmosphere and subjected to 3 freeze-pump-thaw cycles in the dark. Once thawed, a 30-watt frosted incandescent lamp was placed approx. 15 cm away from the reaction flask, which was allowed to stir for 20 hours. At this point, any polymer was isolated via solvent precipitation into methanol followed by vacuum filtration to provide **PMMA** as a white solid in 10% yield (0.64 g). Characterized by ¹H NMR.

Cycloaddition reaction

Phenacyltriphenylphosphonium bromide (12)

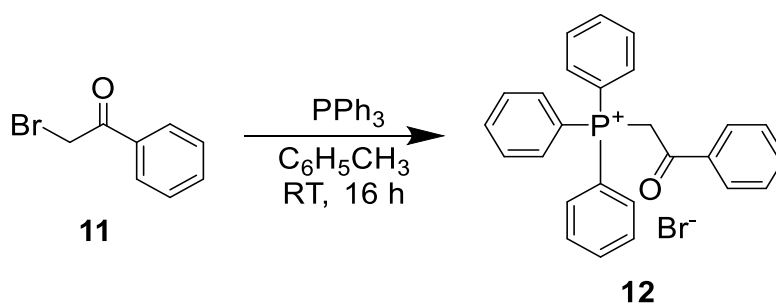


Figure 26. Synthesis of **12**.

The synthesis procedure was modified from literature.⁴⁹ A 150 mL round bottom flask, equipped with a magnetic stir bar, was charged with **11** (5.00 g, 25.1 mmol)

dissolved in 40 mL toluene. While stirring triphenyl-phosphine (6.60 g, 25.1 mmol) was added dropwise after being dissolved in 20 mL toluene. The solution was allowed to stir at room temperature for 16 hours. The solution was then vacuum filtered, and the precipitate was rinsed with ethanol. The excess solvent was removed under vacuum to reveal **12** as a white salt in 85% yield (9.85 g). Spectral data matched literature values.⁵⁰

1-Phenyl-2-(triphenylphosphoranylidene)ethenone (13)

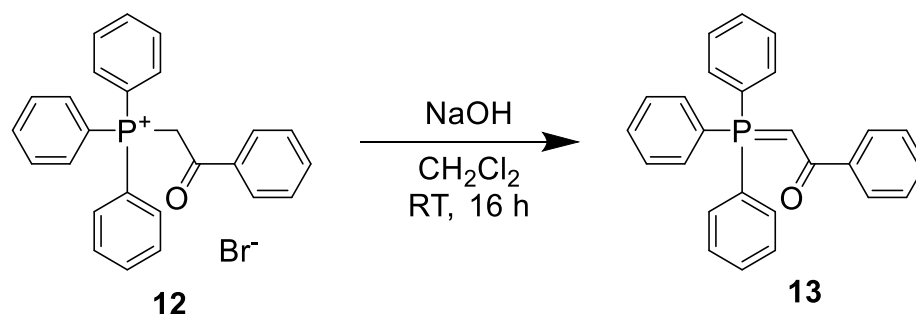


Figure 27. Synthesis of **13**

The synthesis procedure was modified from literature.⁴⁹ A 50 mL round bottom flask, equipped with a magnetic stir bar was charged with **12** (10.0 g, 21.7 mmol) and 22.0 mL of methylene chloride. While stirring 10.8 mL of 2M sodium hydroxide was added. The mixture was then allowed to stir at room temperature for 16 hours. After the allotted time the phases were separated, and the aqueous phase was washed with methylene chloride (3 X 10 mL). The organic extracts were then combined and dried over anhydrous sodium sulfate. The solvent was then evaporated via rotary evaporator to reveal **13** as a white solid in 99% yield (8.246 g). Spectral data matched literature values.⁵⁰

1,9-diphenyl-(E,E)- 2,7-nonadiene-1,9-dione (E1)

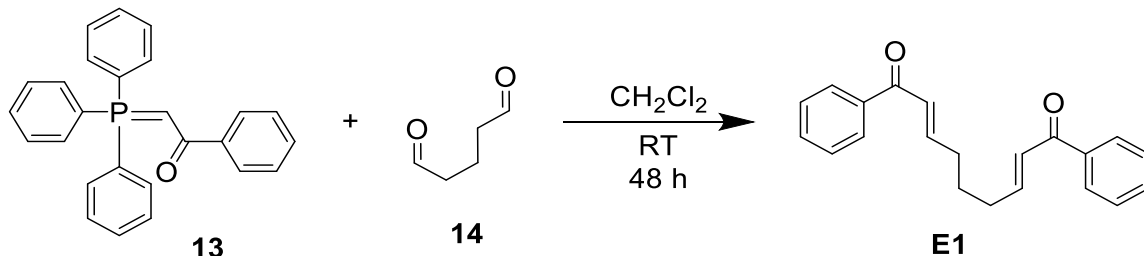


Figure 28. Synthesis of **E1** reaction scheme.

The synthesis procedure was modified from literature.⁵¹ A 50 mL round bottom flask, equipped with a magnetic stir bar was charged with **13** (9.51g, 25.0 mmol), **14** (1.80 mL, 10.0 mmol) and 20.0 mL methylene chloride. The solution was allowed to stir at room temperature for 48 hours. After the allowed time, the solvent was evaporated via rotary evaporator to reveal crude **E1** as a yellow residue. The crude **E1** was then purified by flash chromatography eluting with methylene chloride:ethyl acetate (100:1). The solvent was then removed via rotary evaporator to reveal **E1** in 36% yield (1.10 g) as a light-yellow oil. Spectral data matched literature protocols. Spectral data matched literature values. Spectral data matched literature values.⁵¹ ¹H-NMR (300 MHz, CDCl₃) δ 7.93 (d, J = 7.2 Hz, 4H), 7.55 (t, J = 7.4 Hz, 2H), 7.46 (t, J = 7.2 Hz, 4H), 6.89-7.11 (m, 4H), 2.39 (q, J = 7.0 Hz, 4H), 1.72-1.82 (m, 2H)

[2 + 2] cycloaddition reaction (C1)

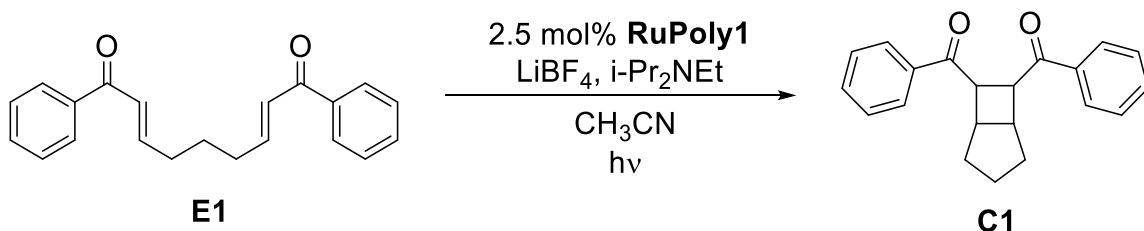


Figure 29. Synthesis of **C1** by 2+2 cycloaddition reaction scheme.

The synthesis procedure was modified from literature.²⁵ The reagent amounts were dependent upon the amount of RuPoly1 recovered from each reaction, refer to Table

5 for specific reagent amounts. A flame dried round bottom flask, equipped with a magnetic stir bar, was charged with **E1** (1 equivalent), lithium tetrafluoroborate (2 equivalents), diisopropylethylamine (2 equivalents), and minimal acetonitrile. The round bottom was then covered with foil and frozen with liquid nitrogen, then PSC **RuPoly1** (2.5 mol%, based upon average molecular weight calculated from UV-vis measurement) was added. Three freeze, pump, thaw cycles were done under nitrogen. The round bottom flask was then irradiated with a 30-watt incandescent household lamp set 10cm away for 5 hours with a strong flow of air to maintain room temperature. The round bottom flask was then covered with foil and the solvent evaporated to a minimal amount. The solution was then precipitated into methanol and left to settle for 15 minutes. The mixture was then vacuum filtered to recover the PSC **RuPoly1**. The filtrate was then evaporated via rotary evaporator and purified via column chromatography (hexanes:ethylacetate 5:1) to reveal **C1** with a mixture of isomers and byproduct as a white solid with an average yield of 53% after five reactions where the catalyst was reused in each reaction. Spectral values were compared to literature for determination of product, isomers, and byproduct ratios.⁴⁰

Table 5
[2 + 2] Cycloaddition reaction reagent amounts

Reagent	rxn1	rxn 2	rxn 3	rxn 4	rxn 5
E1 (mmol)	0.34	0.29	0.23	0.19	0.17
RuPoly1 (mmol)	0.0084	0.0072	0.0056	0.0048	0.0041
LiBF ₄ (mmol)	0.77	0.68	0.53	0.44	0.39
i-PrNEt ₃ (mmol)	0.77	0.68	0.53	0.44	0.39

CHAPTER III

Examination of 10-Phenylphenothiazine Based PSC

3.1 Background

10-phenylphenothiazine (PhPTZ) has recently proven itself as a viable organic catalyst for controlled living polymerization reactions. The catalyst was utilized in polymerization reactions in 2014 by Hawker *et al.* to polymerize methyl methacrylate using an ethyl bromophenylacetate initiator.⁵² Hawker's group was also able to polymerize 2-(dimethyl-amino)ethyl methacrylate (DMAEMA) with this PC. The PC was shown to be capable of well-controlled living polymerization with D values as low as 1.18. PhPTZ was also used by Hawker's group to synthesis a macroinitiator to facilitate block co-polymerizations using CuBr catalyst and styrene with a D value of 1.06.¹⁸ These results indicated that PhPTZ not only produced a well-controlled polymerization, but also had a high fidelity of chain ends, representative of living polymerizations.

The mechanism is similar to a metal catalyzed reaction in that the catalyst is set into an excited state through photon absorption in the visible region of the spectrum. It then differs in that the PC is easily oxidized and will undergo electron transfer to the initiator in the solution, as seen in Figure 30, without the need of a sacrificial electron donor. The initiator then forms a radical, through loss of the halide ion, that enables polymerization of vinyl monomers. The halide is coordinated to the PC to form a radical cation salt. This is very similar to the reaction of phenothiazine with halomethanes investigated by Petrushenko, *et al.*⁵³

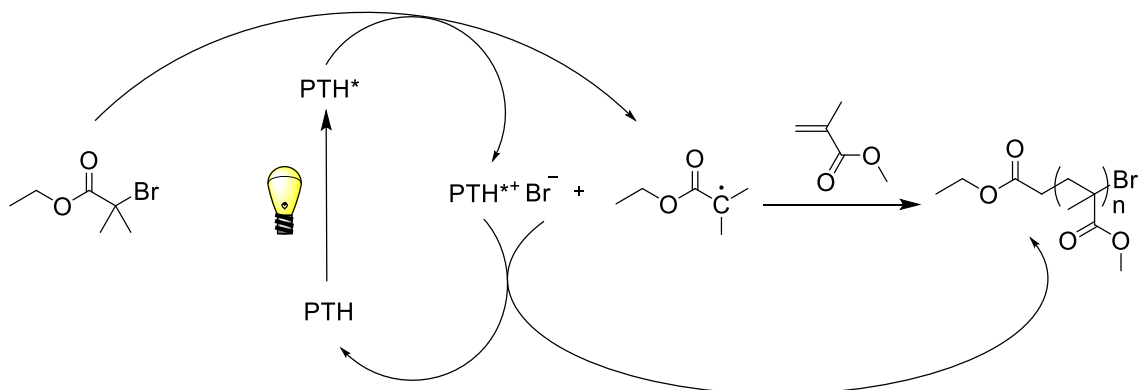


Figure 30. 10-Phenylphenothiazine polymerization mechanism.

For the current research the initiator is incorporated onto the PC through covalent bonds resulting in the organic UPCIS **PPH1** as seen in Figure 31. The covalently bonded initiator is not believed to initiate through intramolecular interactions but through intermolecular interactions with additional UPCIS in solution. While not facilitating a reduction in the entropy of the reaction, it does increase the atom economy. That is, by incorporating the initiator into the catalyst and, this UPCIS then incorporated into the polymer network, the number of atoms in the product is equal to the number of atoms used in totality in theory. This lends credence to the idea of its green character.

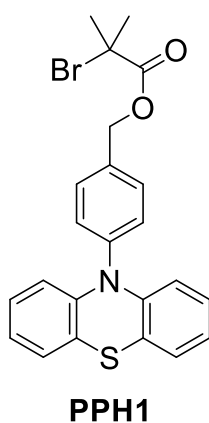


Figure 31. UPCIS **PPH1**.

10-Phenylphenothiazine has not only acted as an efficient PC for polymerization reactions, but has also been used for borylation reactions, though with limited success.²⁸ The simplified mechanism by which this reaction takes place, as seen in Figure 32, is very similar to the polymerization mechanism. 10-Phenylphenothiazine has an excited state reduction potential of -2.9 to -2.51 V vs SCE, allowing the electron transfer to take place between the PC* and the 4-iodotoluene, which has a reduction potential of -2.39V.^{28,54} The intermediate excited state PC forms a radical cationic salt with the iodide ion. The radical toluene then reacts with the bis(pinacolato)-diboron (B_2pin_2) forming the desired borylation product.

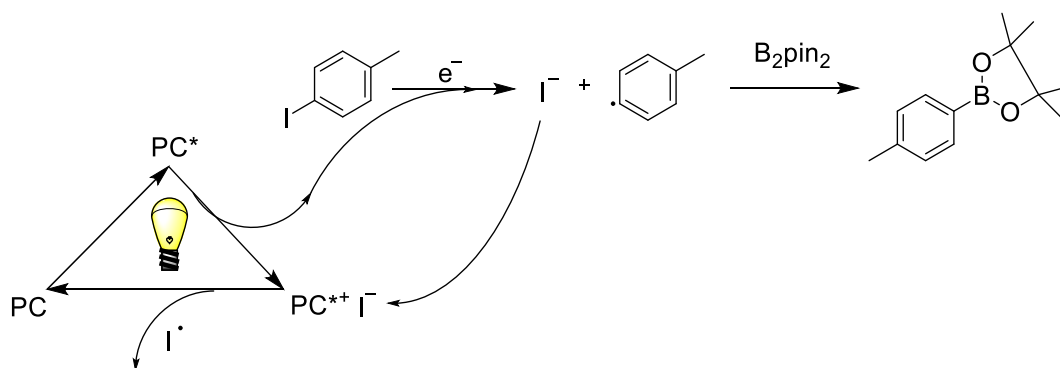


Figure 32. 10-Phenylphenothiazine borylation mechanism.

The addition of polymer supports to the PC, in the current research, aids in the separation of the catalyst through a liquid/solid extraction technique. The PSC will readily precipitate in methanol. This allows the same PC to be reused multiple times and in a multifunctional catalytic role. While helping to recover the catalyst, the polymer supports should not cause adverse effects to the electronics of the catalyst, thereby affecting the catalytic activity.

3.2 Results

3.2.1 Polymer Supports Results

UPCIS **PPH1** was synthesized by first reacting phenothiazine with p-bromo benzaldehyde in a palladium catalyzed cross coupling.⁵⁵ The benzaldehyde functionalized phenothiazine was then reduced to the alcohol through established synthetic techniques. Lastly, α -bromoisobutyryl bromide was utilized in an esterification reaction to produce UPCIS **PPH1**. The detailed reactions can be found in Section 3.4. UPCIS **PPH1** was then utilized in three polymerization experiments utilizing methyl methacrylate as the monomer in *N,N*-dimethylacetamide (DMA). The reaction was modified from literature.⁵² The UPCIS **PPH1** was initiated through irradiation with a common 23-watt compact fluorescent lamp and allowed to react for 24 hours.

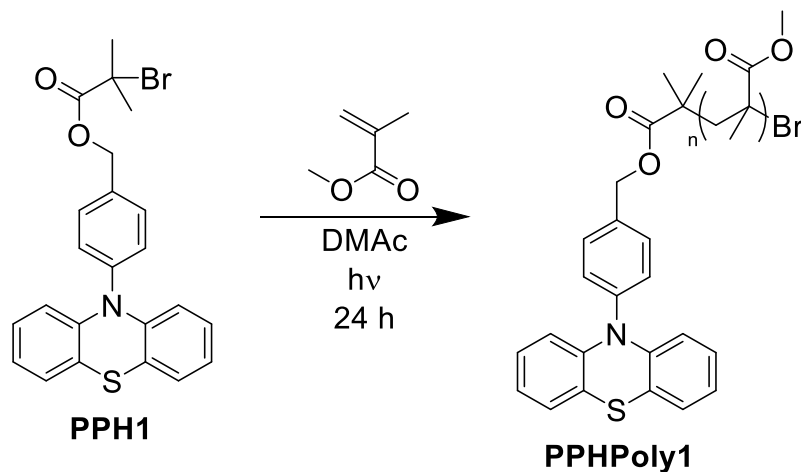


Figure 33. UPCIS **PPH1** polymerization scheme.

The results of each polymerization are recorded below in Table 6. The PSCs were subjected to ^1H and ^{13}C NMR analysis to verify successful polymerizations.

Table 6
UPCIS PPH1 polymerization results

Polymerization Reaction	M:I Ratio	% Yield	% Conv.	M_n via UV-Vis (g/mol)	M_n via GPC (g/mol)	\bar{D}
1	127	9	22	6670	8000	2.29
2	127	38	67	13900	12000	1.55
3	127	33	50	11200	11700	1.42

The PSCs were then analyzed via UV-vis spectroscopy at 301 nm in acetonitrile for determination of the PhPTZ concentration that was then used to calculate the average molecular weights as compared to a four-sample standard curve of UPCIS **PPH1** in acetonitrile at 313 nm. A plot of the calibration standards is seen in Figure 34.

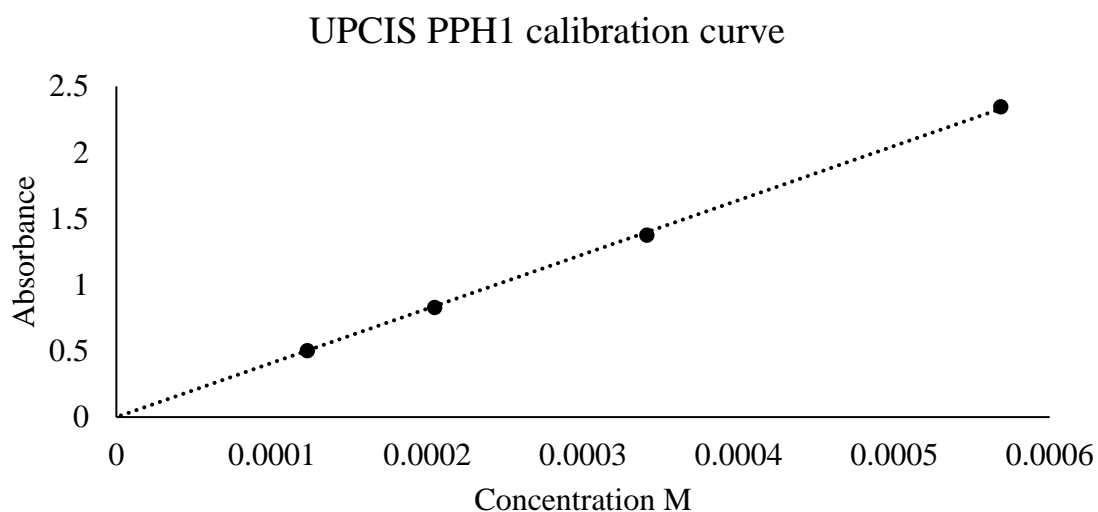


Figure 34. UPCIS **PPH1** calibration curve.

A regression with a zero intercept was performed on the calibration standards to calculate the calibration equation for determination of concentration as seen in Eq. 02.

$$Y = 4098.76X \quad 02$$

The calibration equation produced a R^2 value of 1.00. The calibration equation was used to determine the average molecular weight per PhPTZ subunit. The UV-vis absorption revealed a hypsochromic shift of 12 nm for the PSC **PPHPoly1** and a change in the

absorbance chromatogram shape. This shift and change is evident in Figure 35, with the absorbance of PSC **PPHPoly1** and the standard calibers from 400 to 250 nm.

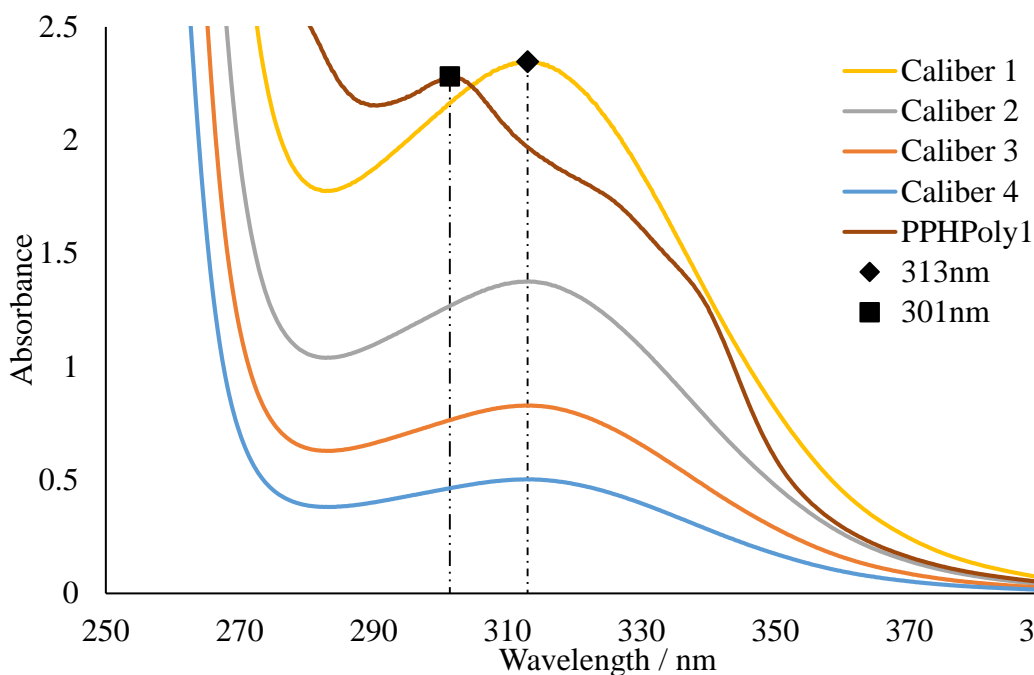


Figure 35. UV-Vis absorbance curve. The 12nm blue shift is visible between the dashed vertical lines.

As a secondary check of the average molecular weights, GPC was used. The GPC also served to determine the D values of the PSCs to ascertain if the polymerizations were controlled.

3.2.2 C-X Borylation Reactions

The PSC **PPHPoly1** was then used to catalyze a C-X borylation reaction at 0.5 mol%, based upon the average molecular weight calculated from the UV-vis absorbance of the PhPTZ subunit, utilizing a 23-watt compact fluorescent lamp as the initiation source, as seen in Figure 36, with cesium carbonate in acetonitrile.

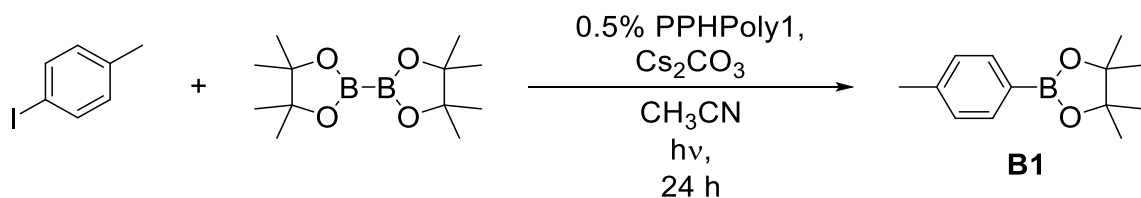


Figure 36. Borylation reaction scheme.

The results of the C-X borylation reactions are listed in Table 7. Each reaction was run for 24 hours before being stopped by removing the light source and covering the reaction vessel. The reaction was analyzed by ¹H NMR for determination of success and calculation of percent conversion. It should be noted that the PSC was recovered after each reaction through precipitation in methanol, with an average recovery of 73%. No borylation reaction products or reactants were found to carry over with the PSC by ¹H NMR analysis of the precipitate.

Table 7

PPHPoly1 catalytic results from five cycles. Reaction 4 utilized a catalyst exposed to DCM during recovery from reaction 3.

Cycle	% Conversion
1	82
2	99
2	99
4	58
5	98

3.3 Discussion

The success of the pseudo “self-catalyzed” polymerization reactions with UPCIS **PPH1** were determined by comparing the yields and conversion to those from the lab of Hawker *et al.*, who utilized an ethyl α-bromophenylacetate and an ethyl α-bromo isobutyrate as initiators and a 380 nm light source.⁵² The previous research had yields between 6 and 30% with conversions of 14 to 36%, as seen in Table 8.⁵² The reaction times were significantly less with the maximum being only 7.5 hours compared to the

current experiments 24 hour reaction time. The data suggest that the UPCIS **PPH1** may be an adequate catalyst for photo-redox pseudo self-polymerization reactions.

Table 8
Hawker et al. Polymerization Results

Polymerization Reaction	M:I Ratio	% Yield	% Conv.	M_n (g/mol)	\bar{D}	reaction time h
3A	50	6	25	1400	1.08	7.5
3C	100	9	14	2600	1.33	2.5
4	100	30	36	5100	1.12	5.5
P2	100	25	25	3600	1.19	5
S4	100	12	19	5300	1.30	5

By comparing the \bar{D} values from the current research with those of Hawker *et al.* the degree of control may be evaluated. The PSC **PPHPoly1** had \bar{D} values between 2.29 and 1.42 according to Table 6. The polymerization reaction resulting in a 2.29 \bar{D} value was the result of experimental errors on the first polymerization reaction. The errors were corrected in the following reactions and the \bar{D} values have a smaller variance. The last two values indicate that there is some degree of control in the polymerization reactions. While the degree of control is larger than the previously reported literature values, this may be due to the prolonged reaction time and larger conversions of monomer.⁵²

The catalyst to initiator ratio did not appear to greatly affect the control of polymerization. The equilibrium of the ATRP reaction is expected to be close to one with a 1:1 catalyst to initiator ratio. As with other polymerization reactions reported in literature the degree of control is greatly affected by this ratio. For reference purposes, Hawker *et al.* reported a 10:1 initiator to catalyst ratio.⁵² This fact may be partially responsible for the better control noticed in literature.

Catalytic activity for the polymerization reactions may be evaluated by looking more closely at the UV-vis absorbance results obtained for UPCIS **PPH1** and comparing them to previous studies. For reference, it is important to state that N-phenyl-phenothiazine (PhPTZ), the parent catalytic compound, has an absorption max at 320 nm.⁵⁶ When comparing the UPCIS **PPH1** to PhPTZ, it can be seen that there is a 7 nm hypsochromic shift. This shift may indicate that the covalently linked initiator acts as an electron donating substituent into the *N*-phenyl ring. This is based upon research by the labs of Grampp *et al.* and Wagenknecht *et al.*^{56,57} Wagenknecht *et al.* also detailed how electron donor substituents would induce flattening of the central ring, containing the nitrogen and sulfur atoms, allowing more aromatic character and lowering the reduction potential.⁵⁶ This effect should help in the effort to reduce the initiator moiety on the UPCIS **PPH1** providing an advantage in the polymerization reactions. Not only are the UV-vis absorbances useful for the polymerization reaction, but they are also of importance to the borylation reaction.

The PSC **PPHPoly1** appeared to have a possible hypsochromic shift of 19 nm as compared to PhPTZ. The shift had to be referred to as possible due to the irregular shape of the chromatogram as compared to PhPTZ. This shift may still indicate that the electron donating nature of the polymer chain is greater than that of the integrated initiator. This may be attributed to the polymer chain sharing electron density with the PhPTZ core. Through the ability of the polymer chain to donate electron density to the core, the aromatic character should increase according to Wagenknecht *et al.* thereby reducing the reduction potential to a greater extent.⁵⁶ This additional benefit may be the reason for the high yields in the C-X borylation reaction.

The use of a PhPTZ catalyst by Larionov *et al.* for the borylation reaction was reported as having “a substantial decrease in the catalytic activity.”²⁸ The decrease was such that no record of the borylation results using PhPTZ were included. With that in mind, it may be that with the added reductive potential extended the PhPTZ catalytic subunit of PSC **PPHPoly1**, that the reaction is now more feasible and may render more adequate results. With an average conversion of 87%, when compared to a 92% yield with PTZ, it does show that the catalyst was able to facilitate the reaction reasonably well. It is also important that the percent conversion remained fairly consistent, except in Reaction 4 as is explained later, from the first reaction through the last using the same catalyst each time.

Of final consideration when using the PSC **PPHPoly1** are the temporary adverse effects upon exposure to methylene chloride. This was noticed in Reaction 4 in Table 7, where the PSC from Reaction 3 was double precipitated, and concentrated in methylene chloride. Upon exposure to the methylene chloride the solution color became green. Upon evaporation of the methylene chloride the PSC was the expected white solid. But, when added into the experiment for Reaction 4 the initial color was green, in contrast to the standard red color noticed in previous experiments. After some time, the reaction returned to the normal red color. These color changes were noticed in previous literature when PhPTZ was double oxidized.²⁷ In literature the color also changed back to red upon exposure to light in a solution of acetonitrile. It is hypothesized that during the time needed to return to the red color the catalyst was not active in the solution, accounting for the lower conversion of Reaction 4 within the same time as previous reactions.

3.4 Experimental

All air or moisture sensitive reactions were carried out under a nitrogen atmosphere utilizing standard Schlenk techniques. The glassware was flame dried to ensure the absence of moisture from the reaction. Purification through column chromatography was accomplished with 60 Å silica gel. The elution was verified through visualization on silica gel coated glass thin layer chromatography (TLC) plates, using a 254 nm ultra-violet (UV) handheld light source for illumination. All starting materials were purchased from commercial sources (Alfa Aesar, Sigma Aldrich, and TCM Chemicals), and used without further purification unless specifically mentioned. Products were verified through ^1H and ^{13}C NMR spectroscopy with a JEOL Eclipse 300 MHz spectrometer. Chemical shifts are reported in δ (ppm) relative to the ^1H and ^{13}C signal of the deuterated solvent used ($\{\text{CDCl}_3: 7.26 \text{ } ^1\text{H}, 77.16 \text{ } ^{13}\text{C}\}$, $\{d_6\text{-DMSO}: 2.49 \text{ } ^1\text{H}, 39.52 \text{ } ^{13}\text{C}\}$). Further characterization of indicated products was accomplished through UV-vis spectroscopy and gel permeation chromatography (GPC). UV-vis absorbance measurements were generated using a Jasco V-750 equipped with dual light sources of deuterium and tungsten lamps. The instrument was set to scan from 800 to 220 nm in 0.2 nm steps at 400 nm/min. GPC analysis was conducted using a Viscotek VE 1122 solvent delivery system and VE 3580 RI detector with LT4000L mixed column and molecular weight data were calculated relative to polystyrene standards.

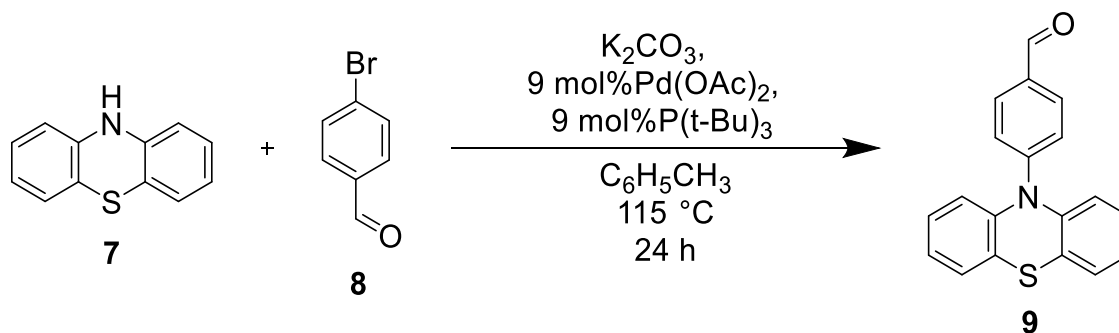
4-(10H-phenothiazin-10-yl) benzaldehyde (9)

Figure 37. Synthesis of **9**.

The synthesis procedure was modified from literature.⁵⁸ Inside a glove box, a flame dried 250mL Schlenk flask, equipped with a magnetic stir bar, was charged with **7** (4.00 g, 20.1 mmol), **8** (4.07 g, 22.0 mmol), potassium carbonate (8.30 g, 60.1 mmol), palladium acetate (0.40 g, 1.78 mmol), tri-tertbutyl-phosphene (0.41 g, 2.03 mmol), and degassed toluene (100 mL). At this point the Schlenk flask was sealed with a rubber septum and removed from the glove box. Then under a strong flow of nitrogen the septum was replaced with a water jacketed reflux condenser and allowed to reflux under nitrogen for 24 hours at $115\text{ }^\circ C$. The flask was then allowed to cool to room temperature and the mixture was vacuum filtered. The filtrate was then evaporated via rotary evaporator to provide the crude product **9** as a yellow oil. The crude product was purified via column chromatography (hexane:ethyl acetate= 10:1). The product was the last fractions to elute from the column. The solvent was then evaporated to reveal purified **9** as a yellow powder in 60.27% yield (3.67g). Spectral data matched literature values.⁵⁹

1H -NMR (300 MHz, $CDCl_3$) δ 9.83 (s, 1H), 7.73 (d, $J = 9.0$ Hz, 2H), 7.41 (d, $J = 8.3$ Hz, 2H), 7.24-7.28 (m, 4H), 7.12-7.19 (m, 4H) ^{13}C -NMR (76 MHz, $CDCl_3$) δ 190.70 (s, 1C), 150.38 (s, 1C), 141.28 (s, 2C), 132.69 (s, 2C), 131.78 (s, 2C), 130.48 (s, 1C), 128.86 (s, 2C), 127.42 (s, 2C), 126.08 (s, 2C), 125.65 (s, 2C), 116.93 (s, 2C)

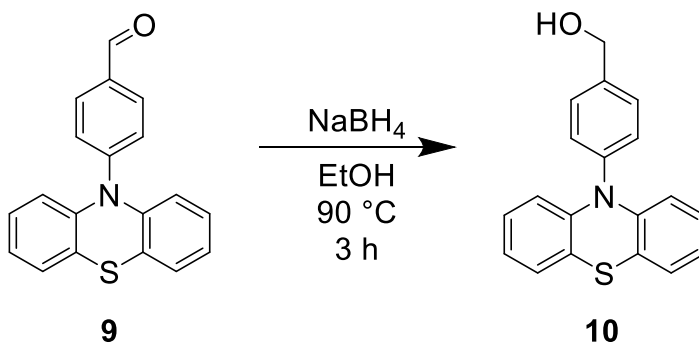
(4-(10H-phenothiazin-10-yl) phenyl)methanol (10)

Figure 38. Synthesis of **10**.

A flame dried 100 mL, round-bottomed flask, equipped with a magnetic stir-bar and a water-jacketed reflux condenser was charged with **9** (0.50 g, 1.65 mmol) and ethanol (30.0 mL). Sodium borohydride (0.62 g, 16.5 mmol) was then slowly added to the solution while stirring. The reaction mixture was then placed on an oil bath regulated at 90° C and allowed to stir at reflux three hours. At this point, the reaction solution was allowed to cool to room temperature, followed by the addition of saturated aqueous ammonium chloride (15 mL). The excess ethanol was removed under vacuo followed by the addition of water until all white precipitate was dissolved. This solution was then extracted with ethyl acetate (4 X 20mL). The organic layer was isolated and dried with anhydrous sodium sulfate. Filtration and removal of excess solvent by rotary evaporation provided **10** as purple crystals in 73% yield (0.40 g). ¹H-NMR (301 MHz, CDCl₃) δ 7.62-7.56 (m, 2H), 7.40-7.35 (m, 2H), 7.02 (dd, *J* = 6.7, 2.6 Hz, 2H), 6.85-6.78 (m, 4H), 6.24-6.20 (m, 2H), 5.19-4.82 (m, 2H). ¹³C-NMR (76 MHz, CDCl₃) δ 144.32 (s, 1C), 141.04 (s, 1C), 140.29 (s, 1C), 130.93 (s, 2C), 129.60 (s, 2C), 126.95 (s, 3C), 126.87 (s, 2C), 122.63 (s, 3C), 120.35 (s, 1C), 116.21 (s, 2C), 64.49 (s, 1C)

4-(10H-phenothiazin-10-yl) benzyl 2-bromo-2-methylpropanoate (PPH1)

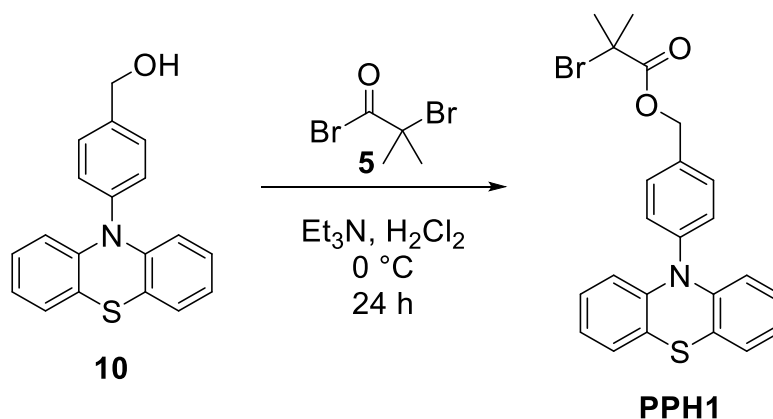


Figure 39. Synthesis of **PPH1**.

A flame-dried, two-necked, 25mL round-bottomed flask, equipped with a magnetic stir-bar was charged with **10** (0.10 g, 0.33 mmol) and methylene chloride (8.90 mL). This solution was allowed to stir under a nitrogen atmosphere for several minutes. This solution was then placed in an ice/water bath and allowed to reach 0° C with stirring. Triethylamine (0.23 mL, 1.64 mmol) was subsequently added via syringe and the reaction mixture was allowed to stir for one minute. At this point, **5** (0.05 mL, 0.39 mmol) was slowly added via syringe. This reaction mixture was allowed to stir overnight while warming to room temperature. Methanol (8 mL) was then added to quench the reaction, which was allowed to stir for 10 minutes more. The excess solvent was then removed via rotary evaporation followed by the addition of methylene chloride (10 mL). This solution was washed with four, 20 mL portions of water. The organic layer was isolated, dried over anhydrous sodium sulfate and filtered. The excess solvent was removed via rotary evaporation to provide **PPH1** as an off-white solid. This crude material was purified via column chromatography (silica gel, methylene chloride:acetone, 100:7) to provide pure **PPH1** as an off-white solid in 69% yield (0.1 g). ¹H-NMR (300

MHz, CDCl₃) δ 7.59 (d, $J = 8.3$ Hz, 2H), 7.39 (d, $J = 8.3$ Hz, 2H), 7.04 (dd, $J = 7.1, 1.9$ Hz, 2H), 6.91-6.80 (m, 4H), 6.26 (dd, $J = 7.7, 1.5$ Hz, 2H), 5.31 (s, 2H), 2.01 (s, 6H) ¹³C-NMR (76 MHz, CDCl₃) δ 171.59 (s, 1C), 144.29 (s, 1C), 141.49 (s, 1C), 134.94 (s, 1C), 130.40 (s, 2C), 130.01 (s, 2C), 126.97 (s, 4C), 122.84 (s, 2C), 121.06 (s, 1C), 116.69 (s, 2C), 66.99 (s, 1C), 55.70 (s, 1C), 30.88 (s, 2C), 1.14 (s, 1C)

Polymerization of organic catalyst (PPHPoly1)

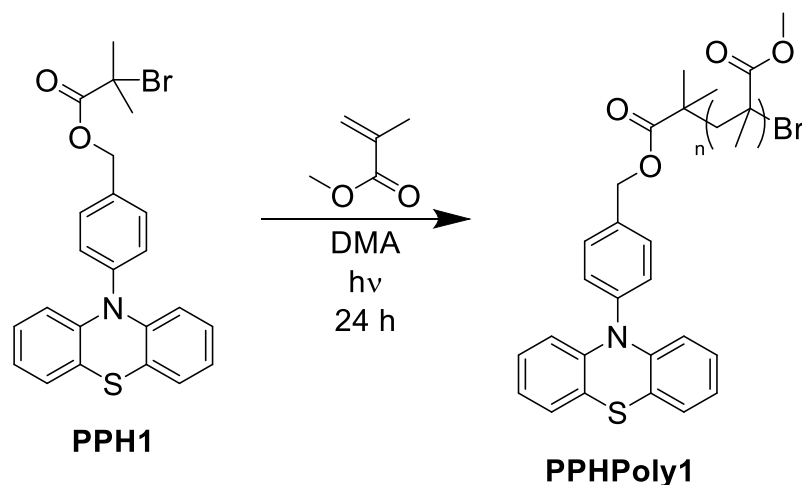


Figure 40. Synthesis of **PPHPoly1** reaction scheme.

The reaction involved a modified literature procedure.⁵² A flame-dried, 50 mL, round-bottomed flask, equipped with a magnetic stir-bar and covered with aluminum foil was charged with methyl methacrylate (1.80 mL, 16.9 mmol) and DMA (2.40 mL, 25.6 mmol). This mixture was placed under a nitrogen atmosphere and frozen in a bath of liquid nitrogen. While frozen, **PPH1** (58.0 mg, 0.13 mmol) was added. This mixture was then subjected to three freeze-pump-thaw cycles. Upon warming to room temperature, the aluminum foil was removed, and the reaction mixture was subjected to irradiation with a 23-watt compact fluorescent bulb (placed 0.1 cm away) for 24 hours. **PPHPoly1** was isolated via solvent precipitation into methanol followed by vacuum filtration. This

product was further purified by suspension in diethyl-ether followed by vacuum filtration to provide **PPHPoly1** as a white solid in 38% yield (0.68 g). $^1\text{H-NMR}$ (300 MHz, CDCl_3) δ 7.51-7.60 (m, 2H), 7.34 (d, $J = 8.3$ Hz, 2H), 7.00 (d, $J = 7.6$ Hz, 2H), 6.77-6.91 (m, 4H), 6.21 (t, $J = 6.0$ Hz, 2H), 5.13 (s, 2H), 3.56 (s, 1585H), 1.40-2.05 (m, 1053H), 0.80-1.17 (m, 1576H).

Borylation reaction forming 4,4,5,5-tetramethyl-2-(p-tolyl)-1,3,2-dioxaborolane (B1)

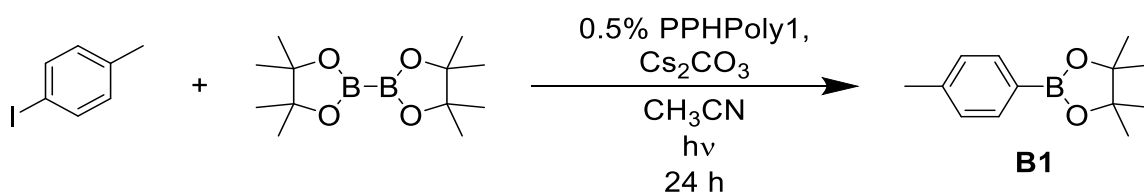


Figure 41. Borylation reaction scheme of **B1**.

The synthesis procedure was modified from literature.²⁸ The reagent amounts were dependent upon the amount of RuPoly1 recovered from each reaction, refer to Table 9. A flame-dried, 50 mL, two necked, round-bottomed flask, equipped with a magnetic stir-bar was placed under a nitrogen atmosphere and charged with 100 equivalents acetonitrile, 1 equivalent 4-iodo-toluene, 2 equivalents B₂Pin₂, and 2 equivalents cesium carbonate. This mixture was then frozen in a bath of liquid nitrogen followed by the addition of 0.5 mol% **PPHPoly1**. This mixture was then subjected to three cycles of freeze-pump-thaw and allowed to warm to room temperature while stirring. At this point, the mixture was irradiated with a 23-watt compact fluorescent bulb (placed 0.1 cm from the flask) for 24 hours. Then the majority of the solvent was removed via rotary evaporation in the dark. **PPHPoly1** was then isolated by solvent precipitation into methanol followed by vacuum filtration. Percent conversion was determined by $^1\text{H NMR}$ prior to separation of the PSC. The filtrate (containing product **B1**) was suspended in

water (20 mL) and extracted with ethyl acetate (3 x 20 mL). This organic phase was then isolated and dried over anhydrous sodium sulfate and filtered. Average conversion was determined to be 87% over 5 cycles where **PPHPoly1** was reused in each reaction.

Spectral data matched literature protocols.²⁸

Table 9

C-X Borylation reaction reagent amounts

Reagent	rxn 1	rxn 2	rxn 3	rxn 4	rxn 5
4-iodo toluene (mmol)	2.44	1.73	1.16	0.9	0.6
B2pin2 (mmol)	5.98	3.32	2.23	1.69	1.14
Cs ₂ CO ₃ (mmol)	6.44	3.37	2.16	1.69	1.21
PPHPoly1 (mmol)	0.013	0.008	0.006	0.004	0.003
CH ₃ CN (mmol)	287	287	211	163	115

CHAPTER IV

Conclusion

The objective of this work was to development of an effective green PSC within the parameters of some of the principles of green chemistry. The primary criterion was, first and foremost, the ability to recover and reuse the catalyst while retaining catalytic activity. To this extent, the PSC **RuPoly1** and **RuPoly2** were not effective catalysts. The confirmation that the metal center is retained in the polymer backbone was uncertain. Therefore, it does not merit additional evaluation against the principles of green chemistry and is not a viable solution as it was designed.

Through modification of the ligands of a ruthenium based UPCIS, the ability to maintain reactivity and restrict ligand lability may be controlled. Modifications such as coordination to a tridentate or tetradentate ligand and acetonitrile co-ligands could possibly eliminate the problems associated with this ligand substitution. Although the problems associated with the need for a sacrificial electron donor still pose problems within the synthesis of polymer supports for this catalyst. The use of a transition metal catalyst that could facilitate direct electron transfer without the need of sacrificial electron donors and has no labile ligands may be the only means to incorporate a transition metal catalyst into a polymer back bone through pseudo self-catalysis method.

PPHPoly1, on the other hand, has shown promise as a capable PSC. The use of **PPHPoly1** follows many of the principles of green chemistry. The principle of prevention is met through the absence of a possibly toxic or hazardous transition metal and its ability to be easily separated from the reaction, and recycled in multiple successive reactions, extending the life cycle of the chemical product.

Additionally, the principle of atom economy is observed when utilizing the UPCIS **PPH1** in the pseudo self-catalyzing polymerization reaction. Through incorporation of the initiator onto the catalyst the product then contains the initiator, polymer, and catalyst. The waste is then reduced to the unreacted monomer and solvent, when applicable. This utilization of the UPCIS reduces the waste of a typically five component ATRP reaction to only two components of waste.

The third principle incorporated into the green solution for catalysis is the energy efficiency. By stepping away from conventional thermal activation energy is conserved, this becomes especially important on large scale processes. While electricity being used to generate most photo-chemical reactions is still not efficient, the ability to initiate both the UPCIS **PPH1** and PSC **PPHPoly1** through visible light may change this. The Sun is the most readily available source of visible light. With the integration of solar light into the reaction parameters the use of UPCIS **PPH1** and PSC **PPHPoly1** may become more energy efficient.

Lastly, the principle of degradation is to be considered. While this principle is difficult to address, PSC **PPHPoly1** has the capacity to have its polymer chain recycled in up to 98% purity. It is also important to consider the low toxicity of PhPTZ (LD50 of 178 mg/kg in mice intravenously).⁶⁰ While it does produce carbon oxides, nitrogen oxides (NO_x), and sulphur oxides when exposed to fire, it has no hazards associated with its natural degradation.

Moving forward additional characterization must be done on PSC **PPHPoly1** to fully understand its capabilities as a polymer supported photo-catalyst. The redox potential of this catalyst should be fully investigated along with a detailed look at its

fluorescent emission maxima. The PSC must also be used in other reactions to confirm its ability as a multi-functional PSC catalyst. Upon completion of this thorough investigation and positive results associated with its use as a multi-functional PSC catalyst, then PSC **PPHPoly1** may be one of the solutions to the problem of catalysis as it concerns green chemistry.

REFERENCES

- (1) Basics of Green Chemistry | Green Chemistry | US EPA
<https://www.epa.gov/greenchemistry/basics-green-chemistry> (accessed Apr 20, 2020).
- (2) Anastas, P.; Eghbali, N. Green Chemistry: Principles and Practice. *Chem. Soc. Rev.* **2010**, *39* (1), 301–312. <https://doi.org/10.1039/b918763b>.
- (3) Khamatnurova, T. V; Johnson, M.; Santana, D.; Bazzi, H. S.; Bergbreiter, D. E. Designing Phase Selectively Soluble Polymer-Supports for Dimethylaminopyridine and Phosphine-Ligated Pd(0) Catalysts. *Top. Catal.* **2014**, No. 57, 1438–1444. <https://doi.org/10.1007/s11244-014-0315-3>.
- (4) Lu, J.; Toy, P. H. Organic Polymer Supports for Synthesis and for Reagent and Catalyst Immobilization. *Chem. Rev.* **2009**, No. 109, 815–838. <https://doi.org/10.1021/cr8004444>.
- (5) Liu, Y.; Hobbs, C. E. Corrigendum to Phase-Selectively Soluble, Polymer-Supported Salen Catalyst Prepared Using Atom Transfer Radical Polymerization (ATRP). *Polym. (United Kingdom)* **2018**, *135*, 25–29. <https://doi.org/10.1016/j.polymer.2018.02.037>.
- (6) Lin, B.; Lawler, D.; McGovern, G. P.; Bradley, C. A.; Hobbs, C. E. Terminal Functionalization of Atactic Polypropylene: A New Soluble Polymer Support. *Tetrahedron Lett.* **2013**, *54* (8), 970–974. <https://doi.org/10.1016/j.tetlet.2012.12.046>.
- (7) Merrifield, R. B. Solid Phase Peptide Synthesis. I. The Synthesis of a Tetrapeptide. *J. Am. Chem. Soc.* **1963**, *85* (14), 2149–2154. <https://doi.org/10.1021/ja00897a025>.

- (8) Letsinger, R. L.; Kornet, M. J. Popcorn Polymer as a Support in Multistep Syntheses. *J. Am. Chem. Soc.* **1963**, *85* (19), 3045–3046.
<https://doi.org/10.1021/ja00902a054>.
- (9) Bayer, E.; Schurig, V. Soluble Metal Complexes of Polymers for Catalysis. *Angew. Chem. Int. Ed. Engl.* **1975**, *14* (7), 493–494.
<https://doi.org/10.1002/anie.197504932>.
- (10) Bergbreiter, D. E.; Tian, J.; Hongfa, C. Using Soluble Polymer Supports to Facilitate Homogeneous Catalysis. *Chem. Rev.* **2009**, *109* (2), 530–582.
<https://doi.org/10.1021/cr8004235>.
- (11) Bergbreiter, D. E. Using Soluble Polymers To Recover Catalysts and Ligands. **2002**. <https://doi.org/10.1021/cr010343v>.
- (12) Mishra, V.; Kumar, R. Living Radical Polymerization-A Review. *J. Sci. Res.* **2012**, *56*, 141–176. <https://doi.org/10.1016/j.mtcomm.2018.10.021>.
- (13) Zhang, G.; Young Song, I.; Han Ahn, K.; Park, T.; Choi, W. Free Radical Polymerization Initiated and Controlled by Visible Light Photocatalysis at Ambient Temperature. *Macromolecules* **2011**, *44*, 7594–7599.
<https://doi.org/10.1021/ma201546c>.
- (14) Xia, J.; Matyjaszewski, K. Controlled/"Living" Radical Polymerization. Atom Transfer Radical Polymerization Catalyzed by Copper(I) and Picolyamine Complexes. *Macromolecules* **1999**, *32* (8), 2434–2437.
<https://doi.org/10.1021/ma981694n>.
- (15) Li, B.; Yu, B.; Huck, W. T. S.; Zhou, F.; Liu, W. Electrochemically Induced Surface-Initiated Atom-Transfer Radical Polymerization. *Angew. Chem. Int. Ed.*

- 2012**, *51* (21), 5092–5095. <https://doi.org/10.1002/anie.201201533>.
- (16) Wang, Z.; Pan, X.; Li, L.; Fantin, M.; Yan, J.; Wang, Z.; Wang, Z.; Xia, H.; Matyjaszewski, K. Enhancing Mechanically Induced ATRP by Promoting Interfacial Electron Transfer from Piezoelectric Nanoparticles to Cu Catalysts. *Macromolecules* **2017**, *50*, 45. <https://doi.org/10.1021/acs.macromol.7b01597>.
- (17) Dadashi-Silab, S.; Lorandi, F.; Fantin, M.; Matyjaszewski, K. Redox-Switchable Atom Transfer Radical Polymerization. *Chem. Commun.* **2019**, *55* (5), 612–615. <https://doi.org/10.1039/C8CC09209E>.
- (18) Fors, B. P.; Hawker, C. J. Control of a Living Radical Polymerization of Methacrylates by Light. *Angew. Chem. Int. Ed.* **2012**, *51* (35), 8850–8853. <https://doi.org/10.1002/anie.201203639>.
- (19) Chen, M.; Zhong, M.; Johnson, J. A. Light-Controlled Radical Polymerization: Mechanisms, Methods, and Applications. *Chem. Rev.* **2016**, *116* (Photochemistry in Organic Synthesis), 10167–10211. <https://doi.org/10.1021/acs.chemrev.5b00671>.
- (20) Jana, S.; Parthiban, A.; Choo, F. M. Unimolecular Ligand-Initiator Dual Functional Systems (ULIS) for Low Copper ATRP of Vinyl Monomers Including Acrylic/Methacrylic Acids. *Chem. Commun.* **2012**, *48* (35), 4256–4258. <https://doi.org/10.1039/c2cc16663a>.
- (21) Fogg, D. E.; Dos Santos, E. N. Tandem Catalysis: A Taxonomy and Illustrative Review. *Coord. Chem. Rev.* **2004**, *248*, 2365–2379. <https://doi.org/10.1016/j.ccr.2004.05.012>.
- (22) Xia, H.; Zhu, Y.; Lu, D.; Li, M.; Zhang, C.; Yang, B.; Ma, Y. Ruthenium(II)

- Complexes with the Mixed Ligands 2,2'-Bipyridine and 4,4'-Dialkyl Ester-2,2'-Bipyridine as Pure Red Dopants for a Single-Layer Electrophosphorescent Device. *J. Phys. Chem.* **2006**, *B* (110), 18718–18723. <https://doi.org/10.1021/jp0615149>.
- (23) Xiao, P.; Zhang, J.; Dumur, F.; Tehfe, M. A.; Morlet-Savary, F.; Graff, B.; Gigmes, D.; Fouassier, J. P.; Lalevée, J. Visible Light Sensitive Photoinitiating Systems: Recent Progress in Cationic and Radical Photopolymerization Reactions under Soft Conditions. *Prog. Polym. Sci.* **2015**, *41*, 32–66. <https://doi.org/10.1016/J.PROGPOLYMSCI.2014.09.001>.
- (24) Magenau, A. J. D.; Kwak, Y.; Schrö, K.; Matyjaszewski, K. Highly Active Bipyridine-Based Ligands for Atom Transfer Radical Polymerization Scheme 1. Dormant-Active Equilibrium in ATRP. *ACS Macro Lett.* **2012**, *1* (4), 508–512. <https://doi.org/10.1021/mz3000489>.
- (25) Ischay, M. A.; Anzovino, M. E.; Du, J.; Yoon, T. P. Efficient Visible Light Photocatalysis of [2+2] Enone Cycloadditions. *J. Am. Chem. Soc.* **2008**, *130* (39), 12886–12887. <https://doi.org/10.1021/ja805387f>.
- (26) Rueping, M.; Vila, C.; Koenigs, R. M.; Poscharny, K.; Fabry, D. C. Dual Catalysis: Combining Photoredox and Lewis Base Catalysis for Direct Mannich Reactions. *Chem. Commun.* **2011**, *47* (8), 2360–2362. <https://doi.org/10.1039/C0CC04539J>.
- (27) Yasukouchi, K.; Taniguchi, I.; Yamaguchi, H.; Ayukawa, J.; Ohtsuka, K.; Tsuruta, Y. Kinetics and Mechanism of the Reaction of 10-Phenylphenothiazine Dication with Water in Acetonitrile. *J. Org. Chem.* **1981**, *46* (8), 1679–1683. <https://doi.org/10.1021/jo00321a031>.

- (28) Jin, S.; Dang, H. T.; Haug, G. C.; He, R.; Nguyen, V. D.; Nguyen, V. T.; Arman, H. D.; Schanze, K. S.; Larionov, O. V. Visible Light-Induced Borylation of C-O, C-N, and C-X Bonds. *J. Am. Chem. Soc.* **2020**, *142*, 1603–1613.
<https://doi.org/10.1021/jacs.9b12519>.
- (29) Pan, X.; Fang, C.; Fantin, M.; Malhotra, N.; So, W. Y.; Peteanu, L. A.; Isse, A. A.; Gennaro, A.; Liu, P.; Matyjaszewski, K. Mechanism of Photoinduced Metal-Free Atom Transfer Radical Polymerization: Experimental and Computational Studies. *J. Am. Chem. Soc.* **2016**, *138* (7), 2411–2425.
<https://doi.org/10.1021/jacs.5b13455>.
- (30) Roberts, D. E. Heats of Polymerization. A Summary of Published Values and Their Relation to Structure. *J. Res. Natl. Bur. Stand. (1934)*. **1950**, *44*, 221–232.
- (31) Kato, M.; Kamigaito, M.; Sawamoto, M.; Higashimura, T. Polymerization of Methyl Methacrylate with the Carbon Tetrachloride/Dichlorotris-(Triphenylphosphine)Ruthenium(II)/ Methylaluminum Bis(2,6-Di-Tert-Butylphenoxide) Initiating System: Possibility of Living Radical Polymerization. *Macromolecules* **1995**, *28* (5), 1721–1723. <https://doi.org/10.1021/ma00109a056>.
- (32) Juris, A.; Balzani, V.; Barigelletti, F.; Campagna, S.; Belser, P.; von Zelewsky, A. Ru(II) Polypyridine Complexes: Photophysics, Photochemistry, Electrochemistry, and Chemiluminescence. *Coord. Chem. Rev.* **1988**, *84* (C), 85–277.
[https://doi.org/10.1016/0010-8545\(88\)80032-8](https://doi.org/10.1016/0010-8545(88)80032-8).
- (33) Yoon, T. P. Visible Light Photocatalysis: The Development of Photocatalytic Radical Ion Cycloadditions. *ACS Catal.* **2013**, No. 3, 895–902.
<https://doi.org/10.1021/cs400088e>.

- (34) Matyjaszewski, K.; Gaynor, S. G.; Greszta, D.; Mardare, D.; Shigemoto, T.; Wang, J.-S. Unimolecular and Bimolecular Exchange Reaction in Controlled Radical Polymerization. *Macromol. Symp.* **1995**, *95* (1), 217–231.
- (35) Fantin, M.; Isse, A. A.; Gennaro, A.; Matyjaszewski, K. Understanding the Fundamentals of Aqueous ATRP and Defining Conditions for Better Control. *Macromolecules* **2015**. <https://doi.org/10.1021/acs.macromol.5b01454>.
- (36) Hu, J.; Wang, J.; Nguyen, T. H.; Zheng, N. The Chemistry of Amine Radical Cations Produced by Visible Light Photoredox Catalysis. *Beilstein J. Org. Chem.* October 1, 2013, pp 1977–2001. <https://doi.org/10.3762/bjoc.9.234>.
- (37) Zhou, Q. X.; Yang, F.; Lei, W. H.; Chen, J. R.; Li, C.; Hou, Y. J.; Ai, X. C.; Zhang, J. P.; Wang, X. S.; Zhang, B. W. Ruthenium(II) Terpyridyl Complexes Exhibiting DNA Photocleavage: The Role of the Substituent on Monodentate Ligand. *J. Phys. Chem. B* **2009**, *113* (33), 11521–11526. <https://doi.org/10.1021/jp905506w>.
- (38) Vu, A. T.; Santos, D. A.; Hale, J. G.; Garner, R. N. Tuning the Excited State Properties of Ruthenium(II) Complexes with a 4-Substituted Pyridine Ligand. *Inorganica Chim. Acta* **2016**, *450*, 23–29. <https://doi.org/10.1016/j.ica.2016.05.007>.
- (39) Caspar, J. V.; Sullivan, B. P.; Kober, E. M.; Meyer, T. J. Application of the Energy Gap Law to the Decay of Charge Transfer Excited States, Solvent Effects. *Chem. Phys. Lett.* **1982**, *91* (2), 91–95. [https://doi.org/10.1016/0009-2614\(82\)80114-0](https://doi.org/10.1016/0009-2614(82)80114-0).
- (40) Bauld, N. L. Anion Radical Chain Cycloaddition of Tethered Enones: Intramolecular Cyclobutanation and Diels–Alder Cycloaddition. *Org. Lett.* **2002**, *4*

- (4), 611–613. <https://doi.org/10.1021/ol0172065>.
- (41) Hurlley, A. E.; Cismesia, M. A.; Ischay, M. A.; Yoon, T. P. Visible Light Photocatalysis of Radical Anion Hetero-Diels-Alder Cycloadditions. *Tetrahedron* **2011**, *67*, 4442–4448. <https://doi.org/10.1016/j.tet.2011.02.066>.
- (42) Laemmel, A.-C.; Collin, J.-P.; Sauvage, J.-P. Efficient and Selective Photochemical Labilization of a Given Bidentate Ligand in Mixed Ruthenium(II) Complexes of the Ru(Phen)₂L₂⁺ and Ru(Bipy)₂L₂⁺ Family (L = Sterically Hindering Chelate). *Eur. J. Inorg. Chem.* **1999**, *1999* (3), 383–386. [https://doi.org/10.1002/\(sici\)1099-0682\(199903\)1999:3<383::aid-ejic383>3.3.co;2-0](https://doi.org/10.1002/(sici)1099-0682(199903)1999:3<383::aid-ejic383>3.3.co;2-0).
- (43) Kopecky, A.; Liu, G.; Agushi, A.; Agrios, A. G.; Galoppini, E. Synthesis of Bifunctional Ru Complexes with 1,2-Dithiolane and Carboxylate-Substituted Ligands. *Tetrahedron* **2014**, *70* (36), 6271–6275. <https://doi.org/10.1016/j.tet.2014.04.042>.
- (44) Paridala, K.; Lu, S. M.; Wang, M. M.; Li, C. Tandem One-Pot CO₂ Reduction by PMHS and Silyloxycarbonylation of Aryl/Vinyl Halides to Access Carboxylic Acids. *Chem. Commun.* **2018**, *54* (82), 11574–11577. <https://doi.org/10.1039/c8cc06820h>.
- (45) Herrero, C.; Quaranta, A.; Fallahpour, R. A.; Leibl, W.; Aukauloo, A. Identification of the Different Mechanisms of Activation of a [Ru II(Tpy)(Bpy)(OH₂)₂]²⁺ Catalyst by Modified Ruthenium Sensitizers in Supramolecular Complexes. *J. Phys. Chem. C* **2013**, *117* (19), 9605–9612. <https://doi.org/10.1021/jp4025816>.

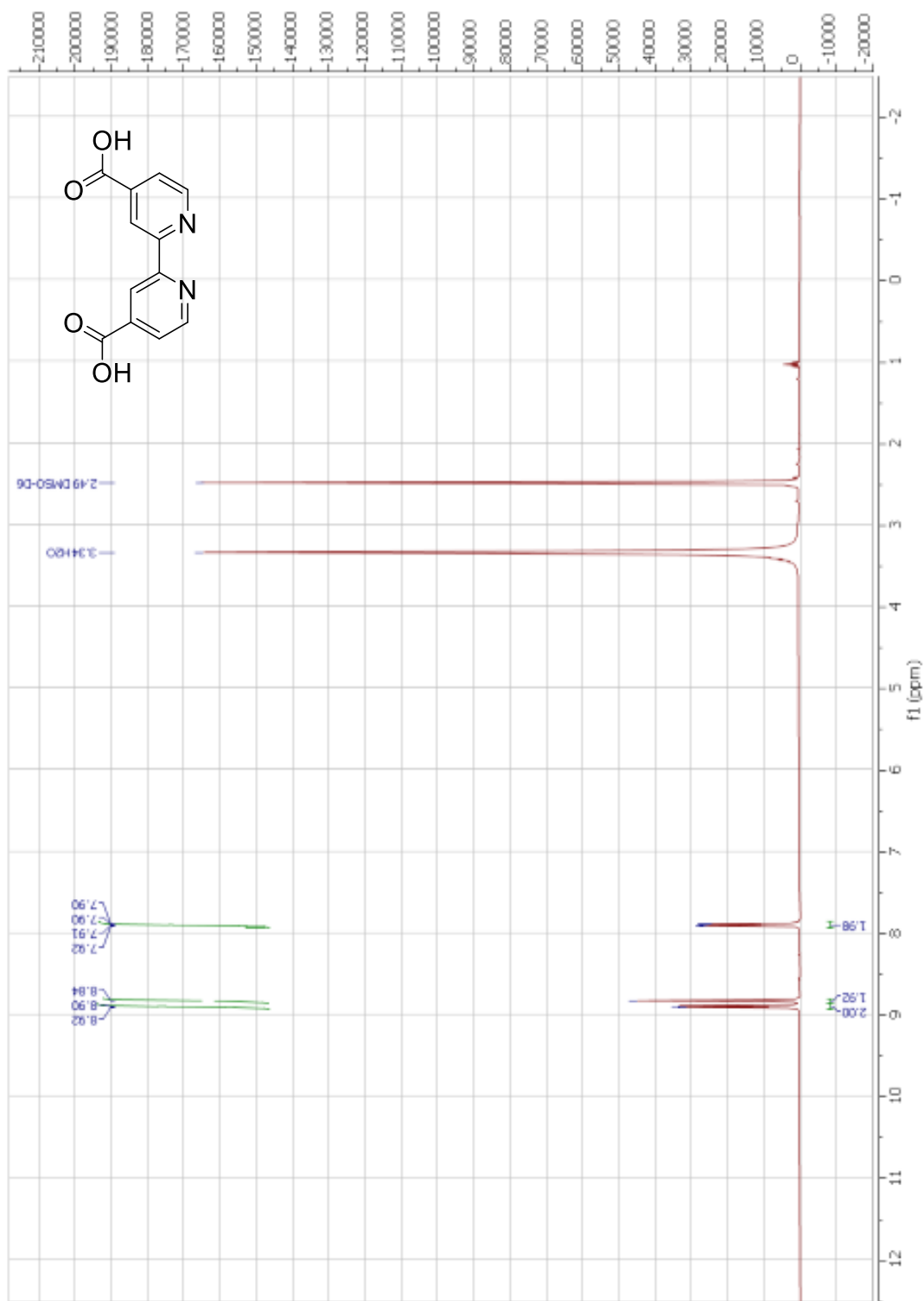
- (46) Prakasam, T.; Lusi, M.; Elhabiri, M.; Platas-Iglesias, C.; Olsen, J. C.; Asfari, Z.; Cianféroni-Sanglier, S.; Debaene, F.; Charbonnière, L. J.; Trabolsi, A. Simultaneous Self-Assembly of a [2]Catenane, a Trefoil Knot, and a Solomon Link from a Simple Pair of Ligands. *Angew. Chem. Int. Ed.* **2013**, *52* (38), 9956–9960. <https://doi.org/10.1002/anie.201302425>.
- (47) Berg, K.; Tran, A.; Raymond, M.; Abrahamsson, M.; Wolny, J.; Redon, S.; Andersson, M.; Sun, L.; Styring, S.; Hammarström, L.; et al. Covalently Linked Ruthenium(II)–Manganese(II) Complexes: Distance Dependence of Quenching and Electron Transfer. *Eur. J. Inorg. Chem.* **2002**, *2001* (4), 1019–1029. [https://doi.org/10.1002/1099-0682\(200104\)2001:4<1019::aid-ejic1019>3.3.co;2-y](https://doi.org/10.1002/1099-0682(200104)2001:4<1019::aid-ejic1019>3.3.co;2-y).
- (48) Zhou, H.; Chen, D.; Bai, J. K.; Sun, X. L.; Li, C.; Qiao, R. Z. Effect of Ligand Sequence-Specific Modification on DNA Hybrid Catalysis. *Org. Biomol. Chem.* **2017**, *15* (32), 6738–6745. <https://doi.org/10.1039/c7ob01249g>.
- (49) Yang, J.; Felton, G. A. N.; Bauld, N. L.; Krische, M. J. Chemically Induced Anion Radical Cycloadditions: Intramolecular Cyclobutanation of Bis(Enones) via Homogeneous Electron Transfer. *J. Am. Chem. Soc.* **2004**, *126* (6), 1634–1635. <https://doi.org/10.1021/ja030543j>.
- (50) Hodgson, G. K.; Scaiano, J. C. Heterogeneous Dual Photoredox-Lewis Acid Catalysis Using a Single Bifunctional Nanomaterial. *ACS Catal.* **2018**, *8* (4), 2914–2922. <https://doi.org/10.1021/acscatal.7b04032>.
- (51) Gong, J. J.; Li, T. Z.; Pan, K.; Wu, X. Y. Enantioselective Intramolecular Rauhut–Currier Reaction Catalyzed by Chiral Phosphinothiourea. *Chem. Commun.* **2011**, *47* (5), 1491–1493. <https://doi.org/10.1039/c0cc04412a>.

- (52) Treat, N. J.; Sprafke, H.; Kramer, J. W.; Clark, P. G.; Barton, B. E.; Read De Alaniz, J.; Fors, B. P.; Hawker, C. J. Metal-Free Atom Transfer Radical Polymerization. *J. Am. Chem. Soc.* **2014**, *136* (45), 16096–16101. <https://doi.org/10.1021/ja510389m>.
- (53) Petrusenko, K. B.; Klyba, L. V.; Smirnov, V. I.; Shevchenko, S. G. Electron Transfer in the Photochemical Reactions of Phenothiazine with Halomethanes. *Russ. Chem. Bull.* **2001**, *50* (5), 798–804. <https://doi.org/10.1023/A:1011338605283>.
- (54) Christensen, J. A.; Phelan, B. T.; Chaudhuri, S.; Acharya, A.; Batista, V. S.; Wasielewski, M. R. Phenothiazine Radical Cation Excited States as Super-Oxidants for Energy-Demanding Reactions. *J. Am. Chem. Soc.* **2018**, *140* (15), 5290–5299. <https://doi.org/10.1021/jacs.8b01778>.
- (55) Jiang, R.; Liu, M.; Huang, H.; Huang, L.; Huang, Q.; Wen, Y.; Cao, Q.; Tian, J.; Zhang, X.; Wei, Y. A Novel Self-Catalyzed PhotoATRP Strategy for Preparation of Fluorescent Hydroxyapatite Nanoparticles and Their Biological Imaging. *Appl. Surf. Sci.* **2018**, *434*, 1129–1136. <https://doi.org/10.1016/J.APSUSC.2017.11.039>.
- (56) Speck, F.; Rombach, D.; Wagenknecht, H.-A. *N*-Arylphenothiazines as Strong Donors for Photoredox Catalysis – Pushing the Frontiers of Nucleophilic Addition of Alcohols to Alkenes. *Beilstein J. Org. Chem.* **2019**, *15* (1), 52–59. <https://doi.org/10.3762/bjoc.15.5>.
- (57) Borowicz, P.; Herbich, J.; Kapturkiewicz, A.; Anulewicz-Ostrowska, R.; Nowacki, J.; Grampp, G. Nature of the Lowest Triplet States of 4'-Substituted *N*-Phenylphenothiazine Derivatives. *Phys. Chem. Chem. Phys.* **2000**, *2* (19), 4275–

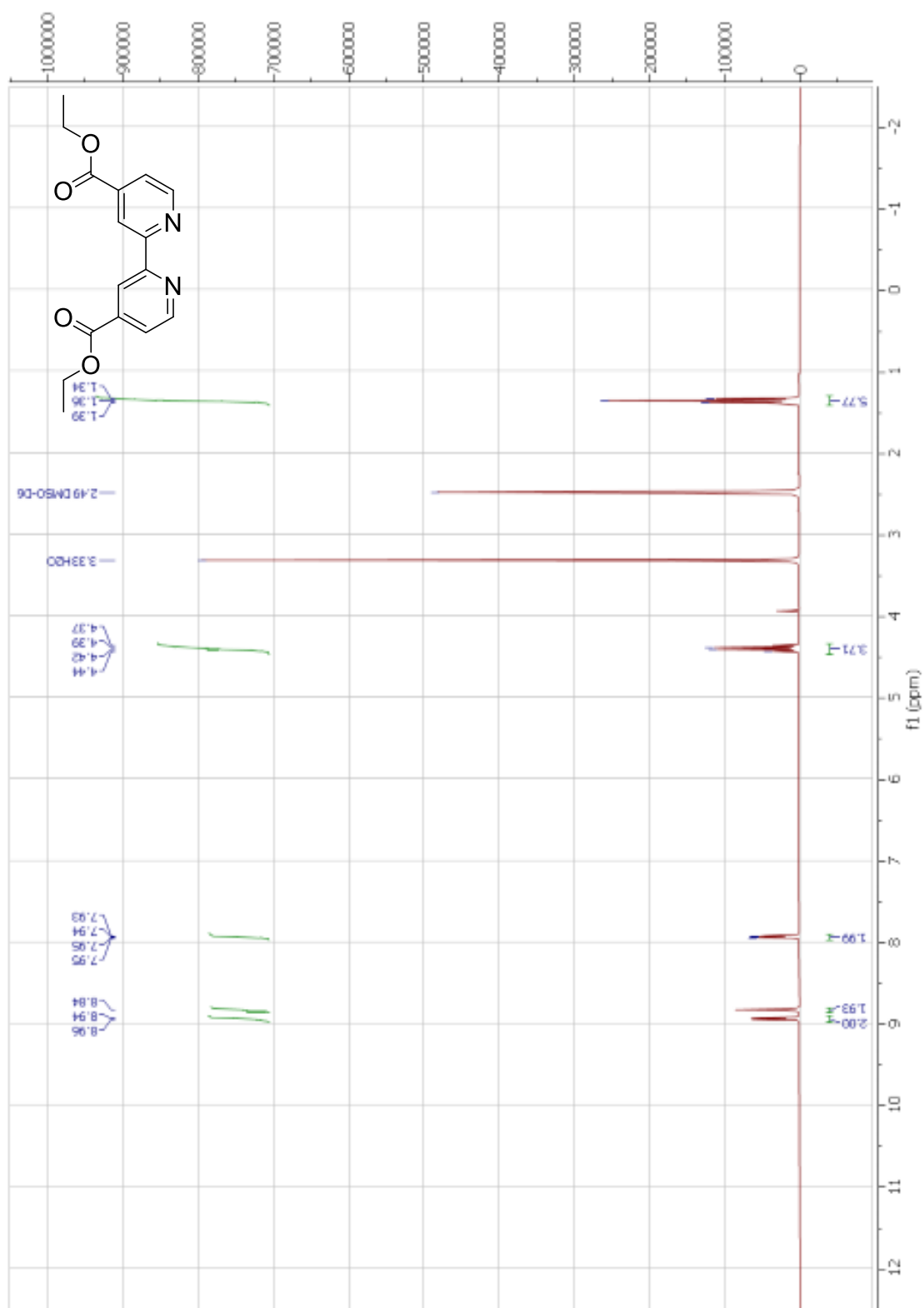
4280. <https://doi.org/10.1039/b005058j>.

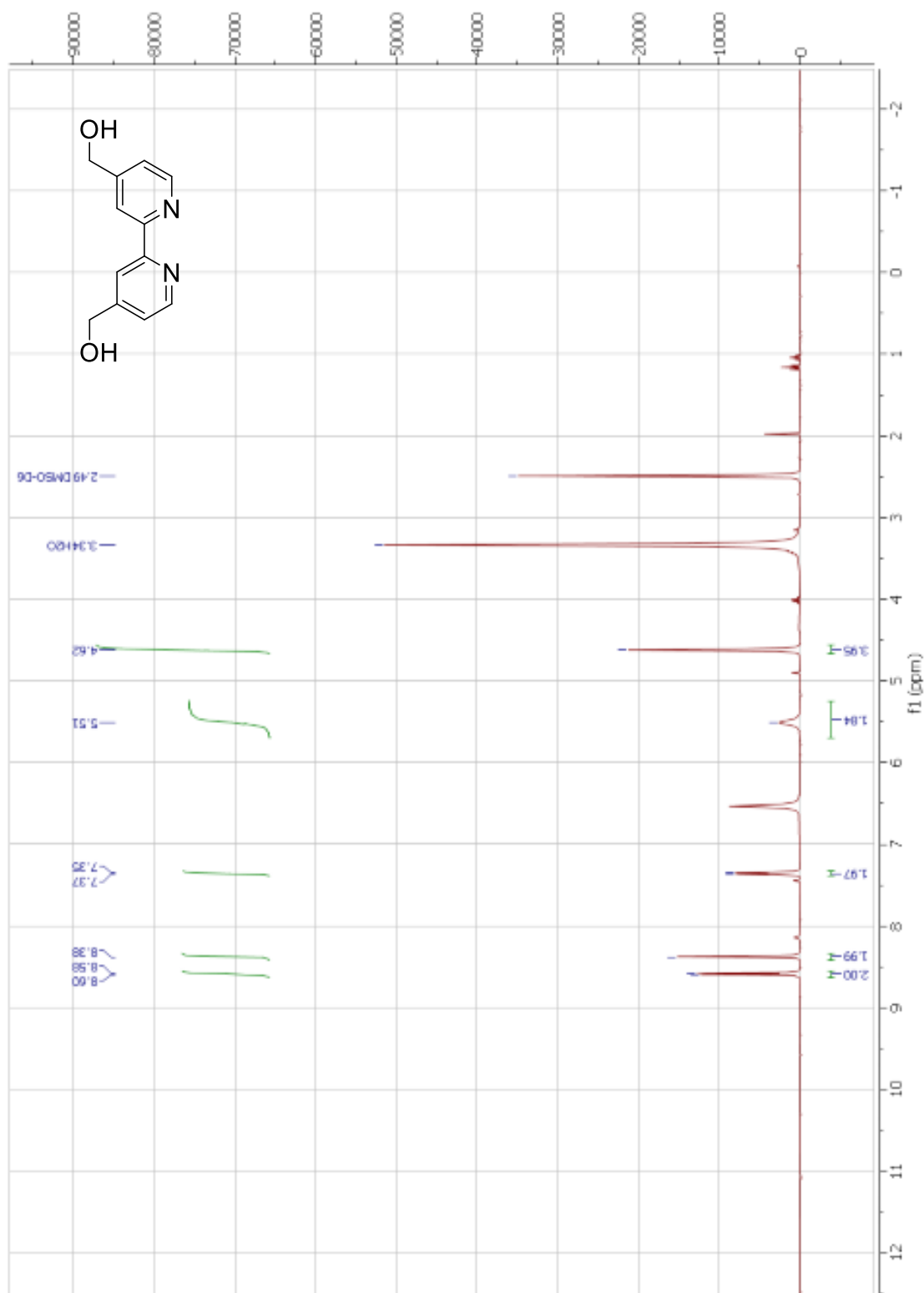
- (58) Jiang, R.; Liu, M.; Huang, H.; Huang, L.; Huang, Q.; Wen, Y.; Cao, Q. yong; Tian, J.; Zhang, X.; Wei, Y. A Novel Self-Catalyzed PhotoATRP Strategy for Preparation of Fluorescent Hydroxyapatite Nanoparticles and Their Biological Imaging. *Appl. Surf. Sci.* **2018**, *434*, 1129–1136.
<https://doi.org/10.1016/j.apsusc.2017.11.039>.
- (59) Mondal, B.; Mukherjee, P. S. Cage Encapsulated Gold Nanoparticles as Heterogeneous Photocatalyst for Facile and Selective Reduction of Nitroarenes to Azo Compounds. *J. Am. Chem. Soc.* **2018**, *140* (39), 12592–12601.
<https://doi.org/10.1021/jacs.8b07767>.
- (60) National Center for Biotechnology Information. PubChem Database. 10-Phenylphenothiazine, CID=95203,
<https://pubchem.ncbi.nlm.nih.gov/compound/10-Phenylphenothiazine> (accessed Jun 10, 2020).

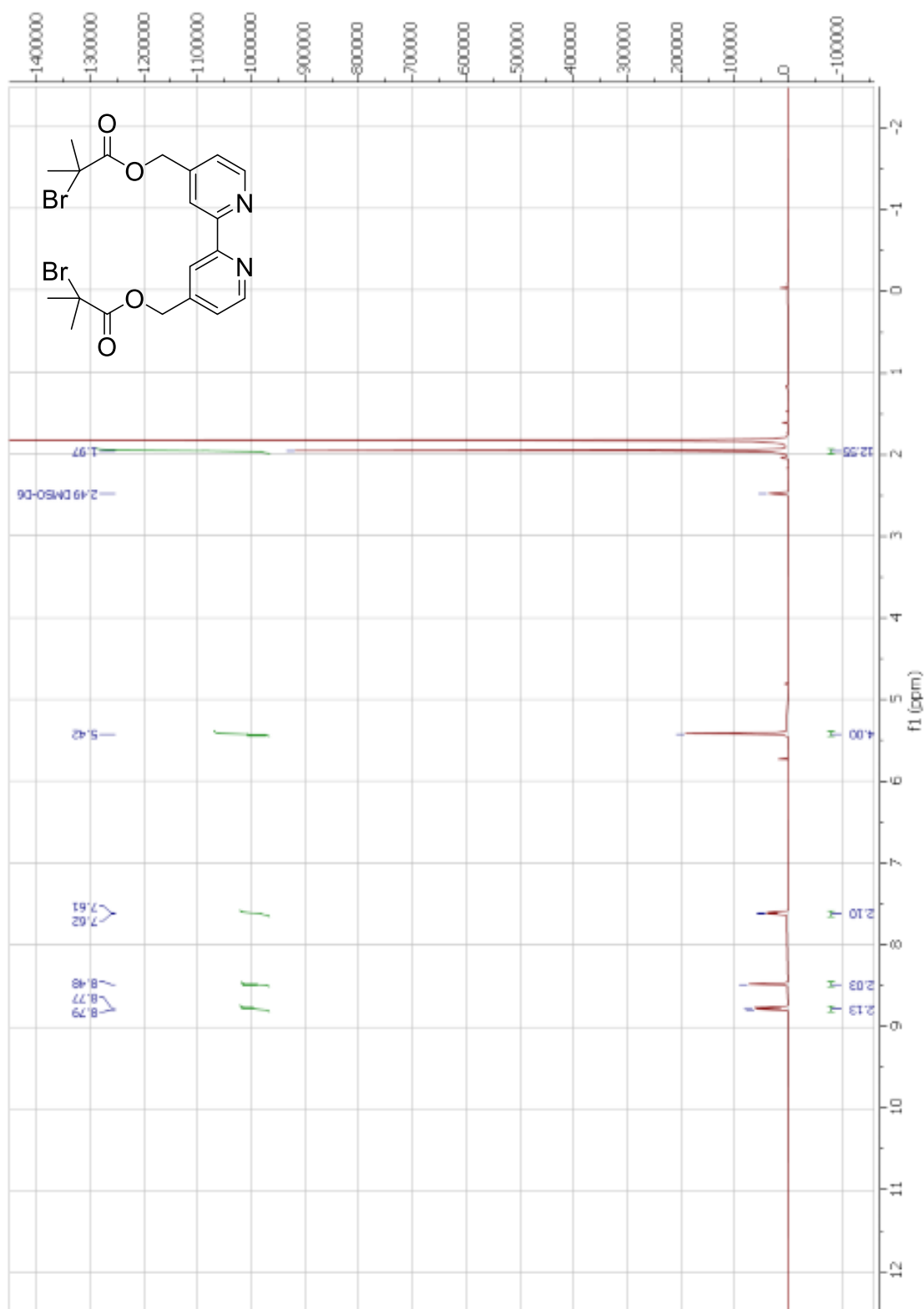
APPENDIX
NMR spectra for the synthesized compounds

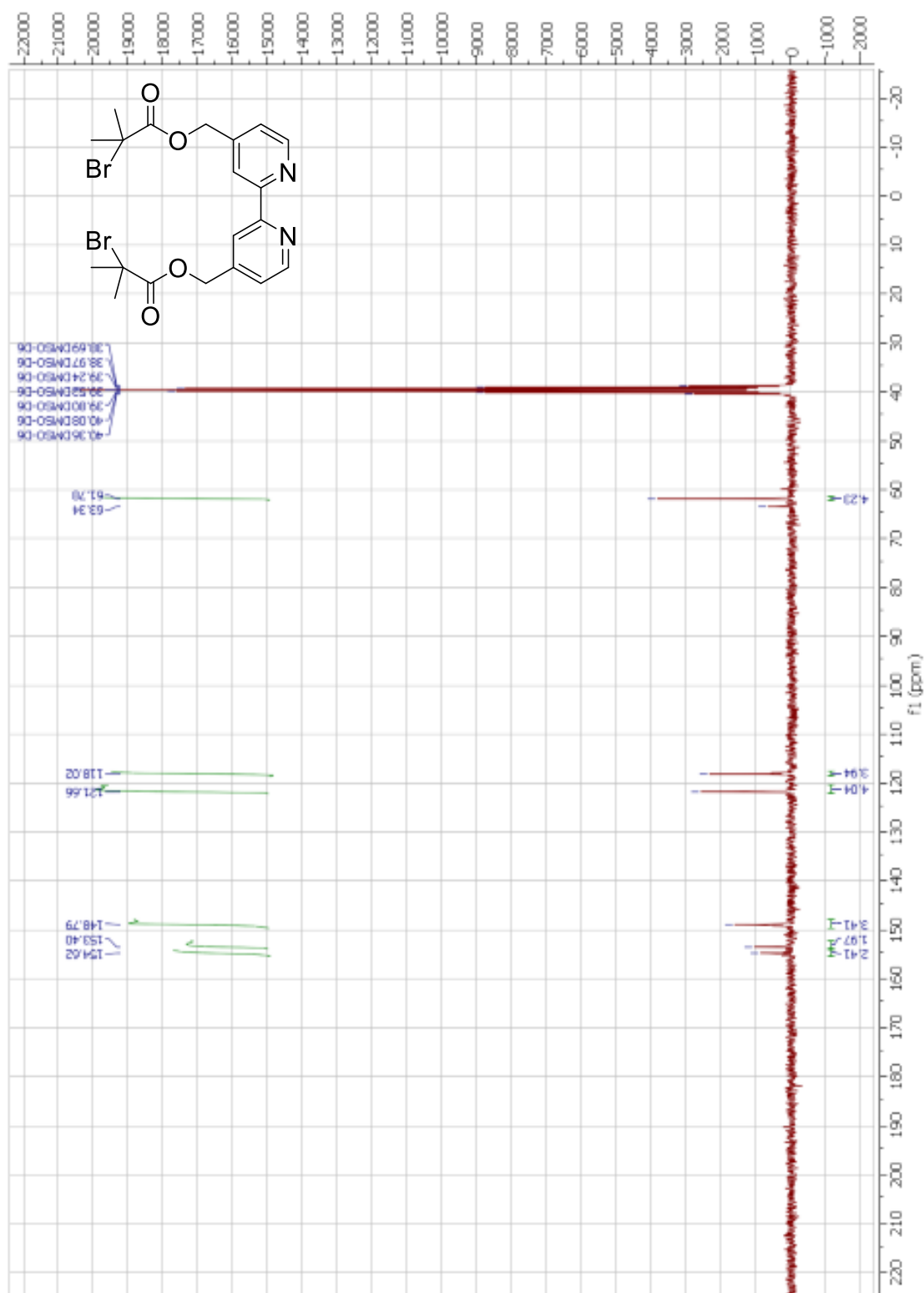


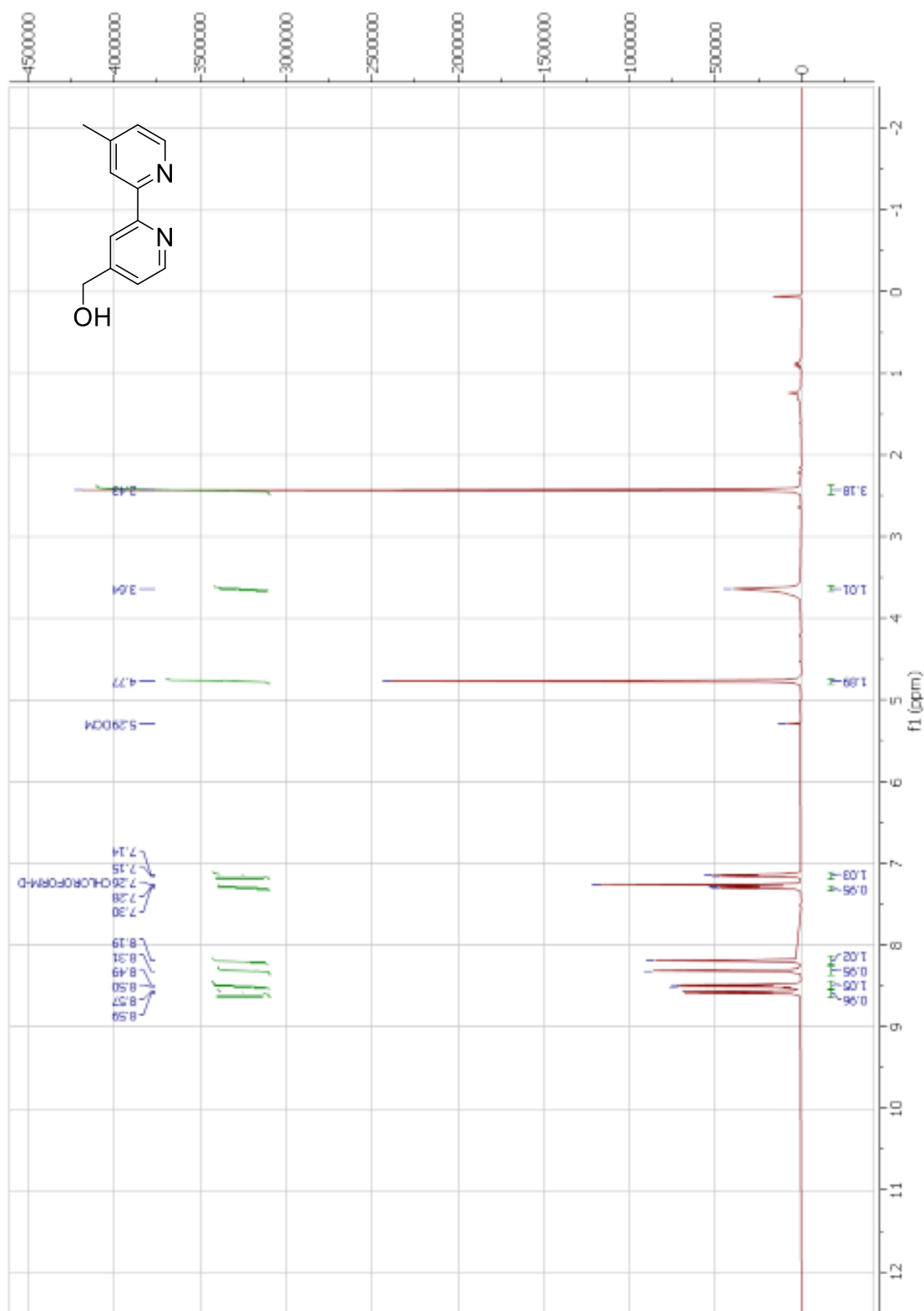
^1H NMR spectrum of 2

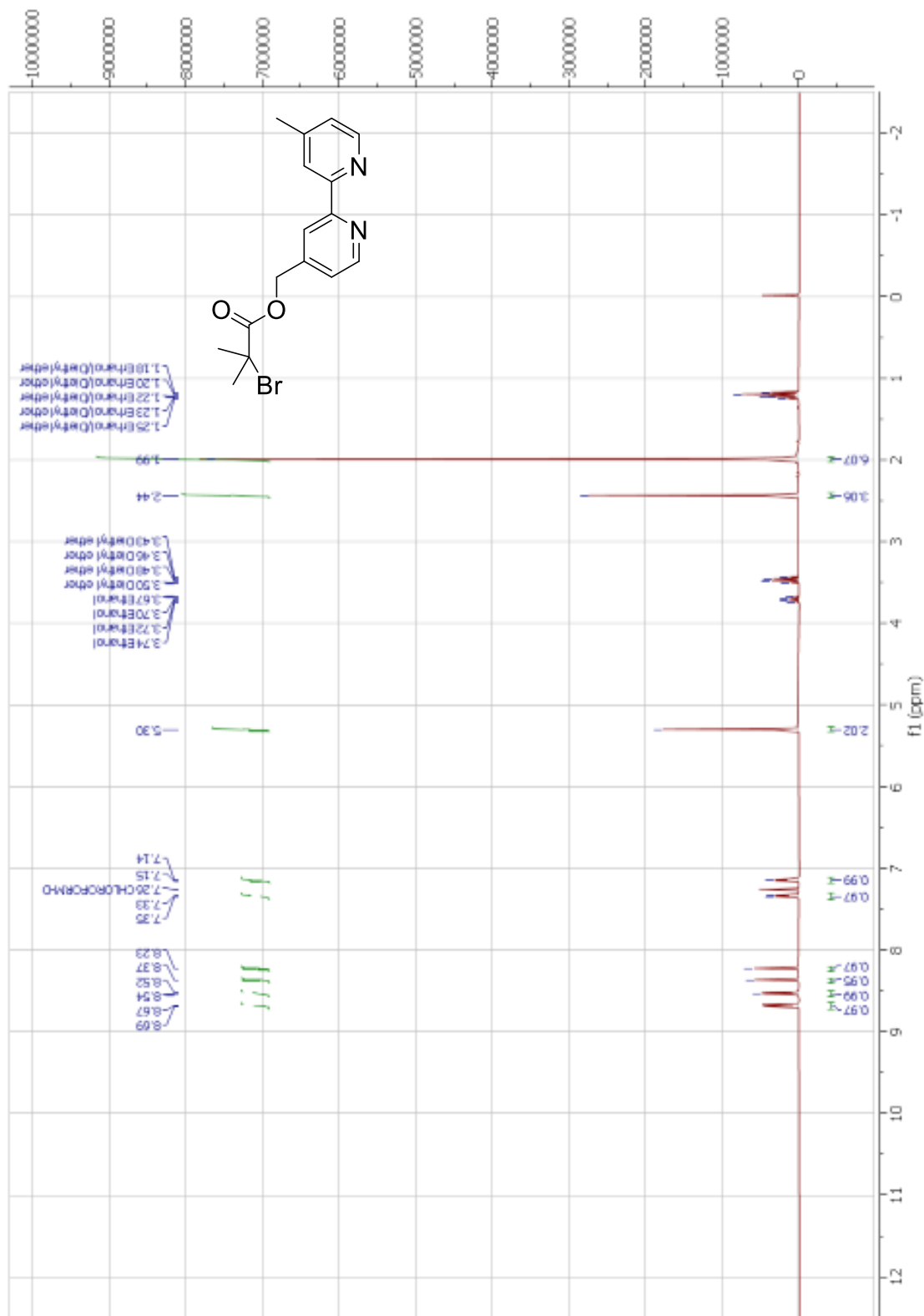
¹H NMR of 3

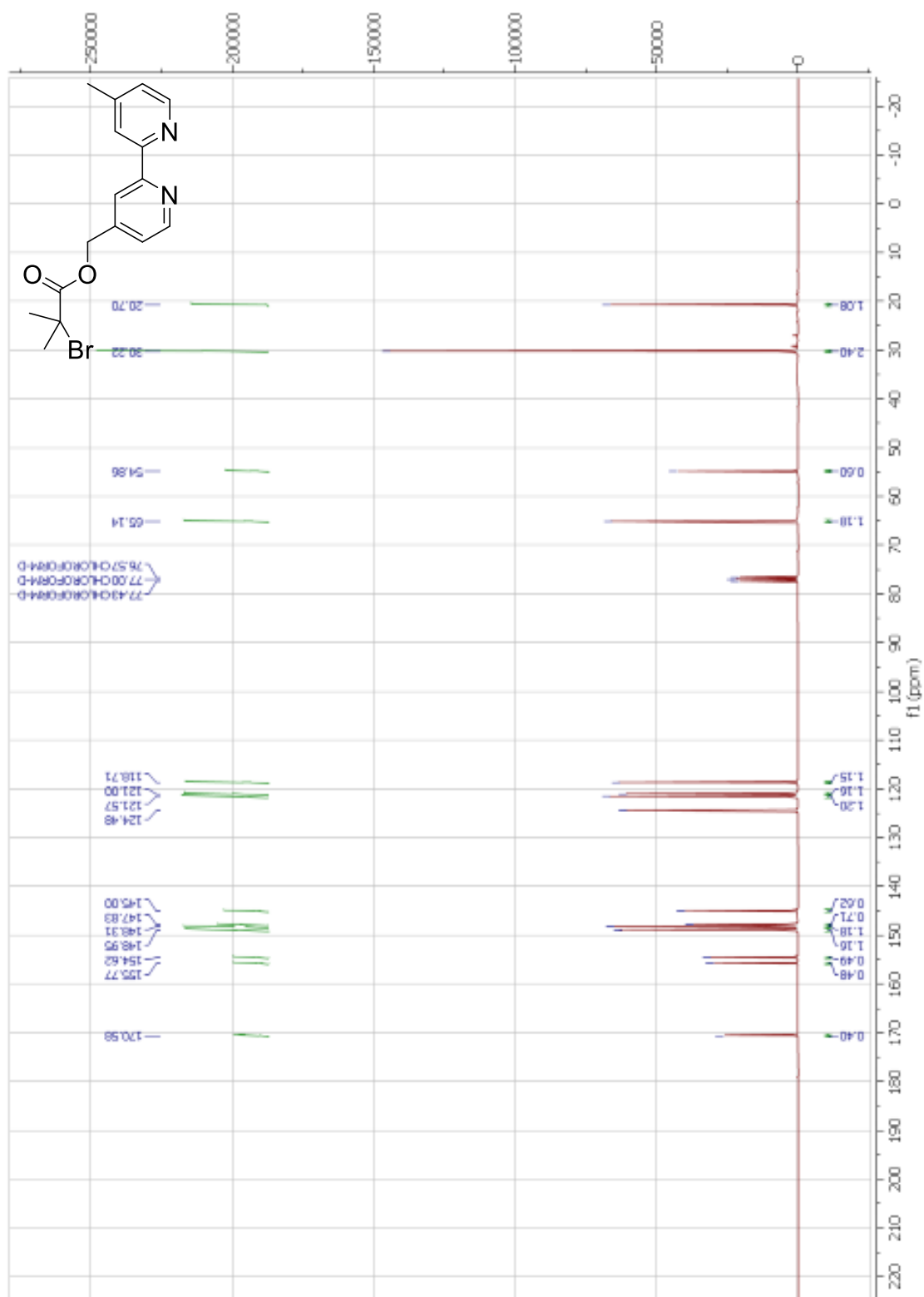
¹H NMR of 4

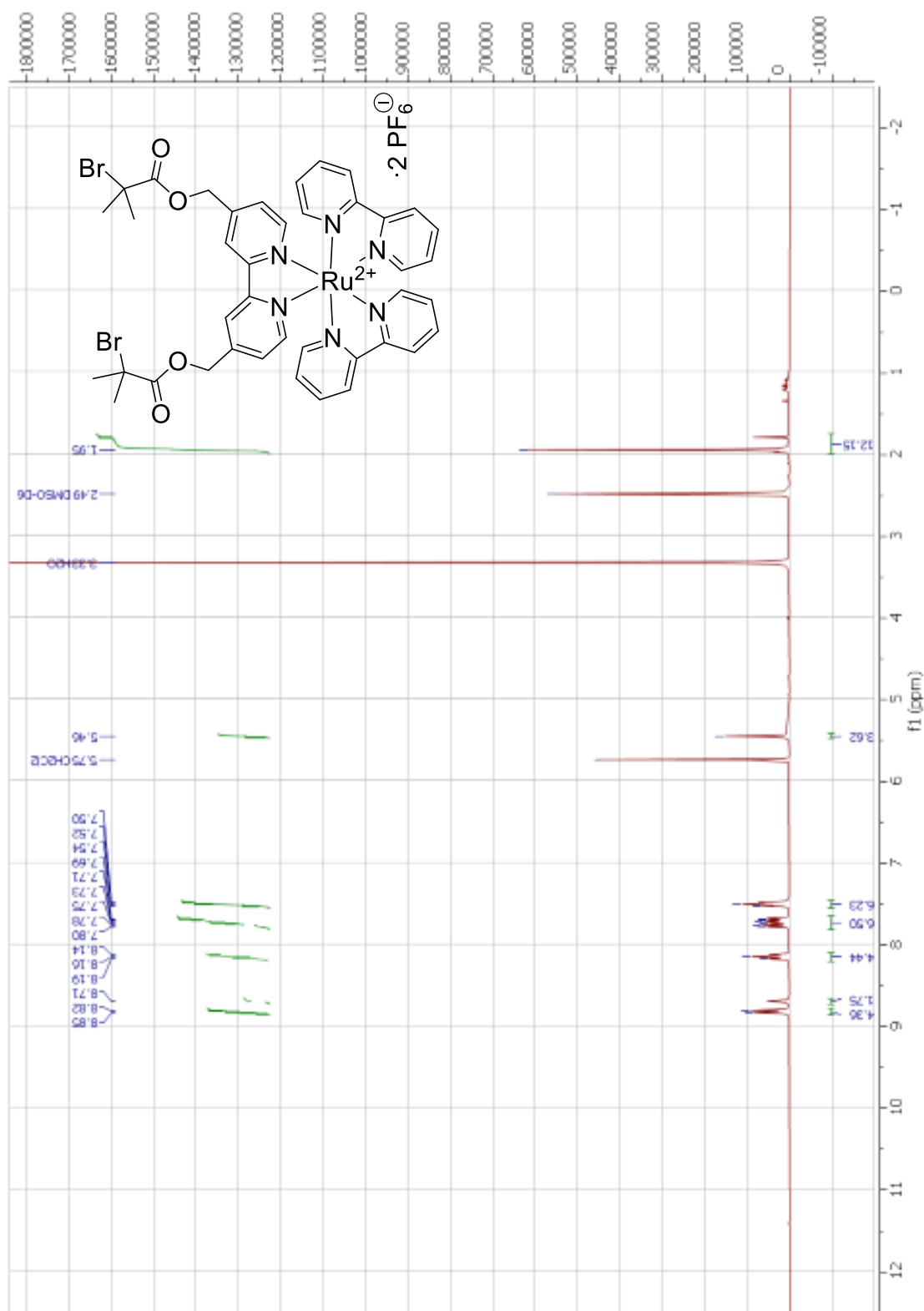
¹H NMR of L1

¹³C NMR of L1

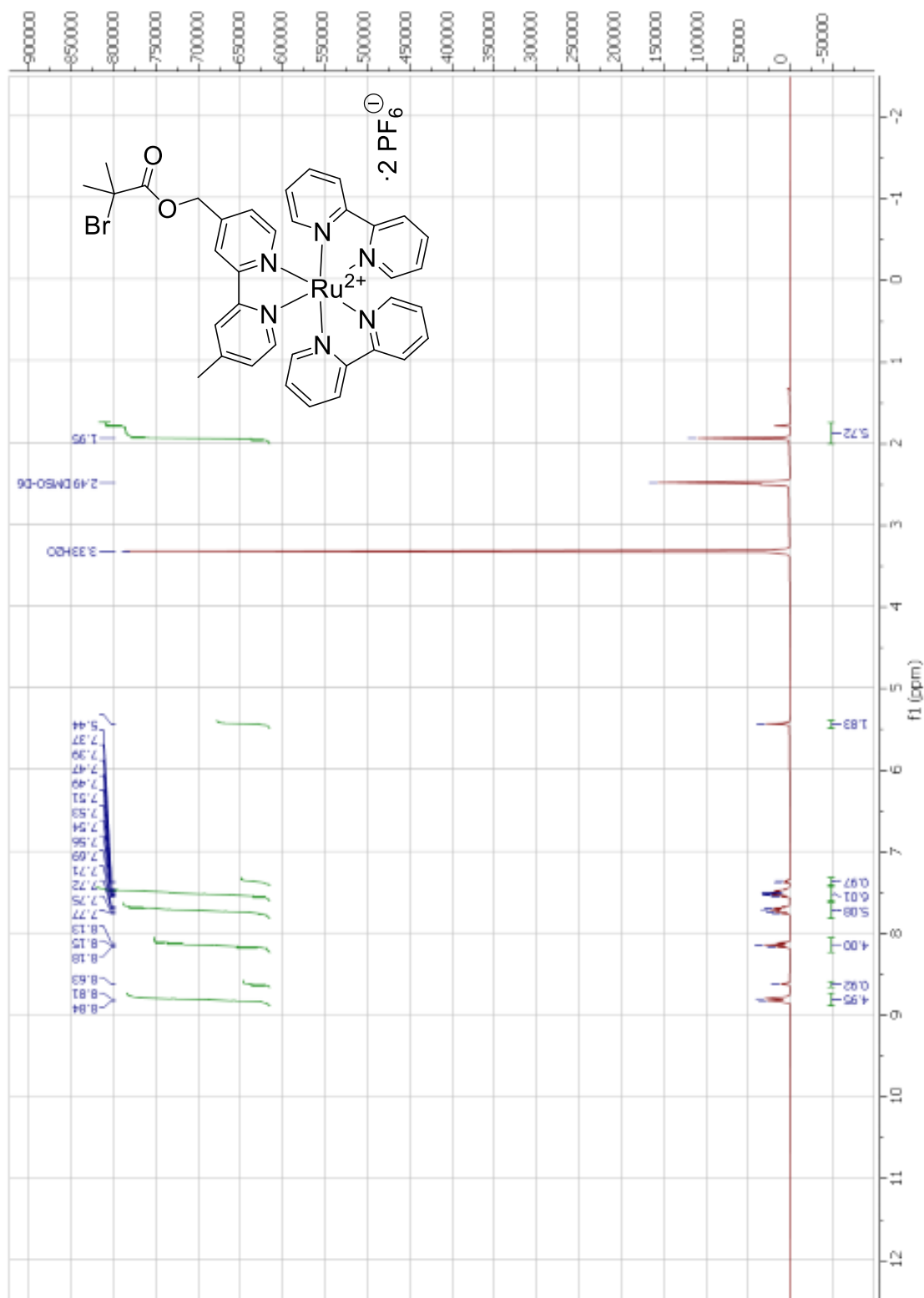
 ^1H NMR of 6

¹H NMR of L2

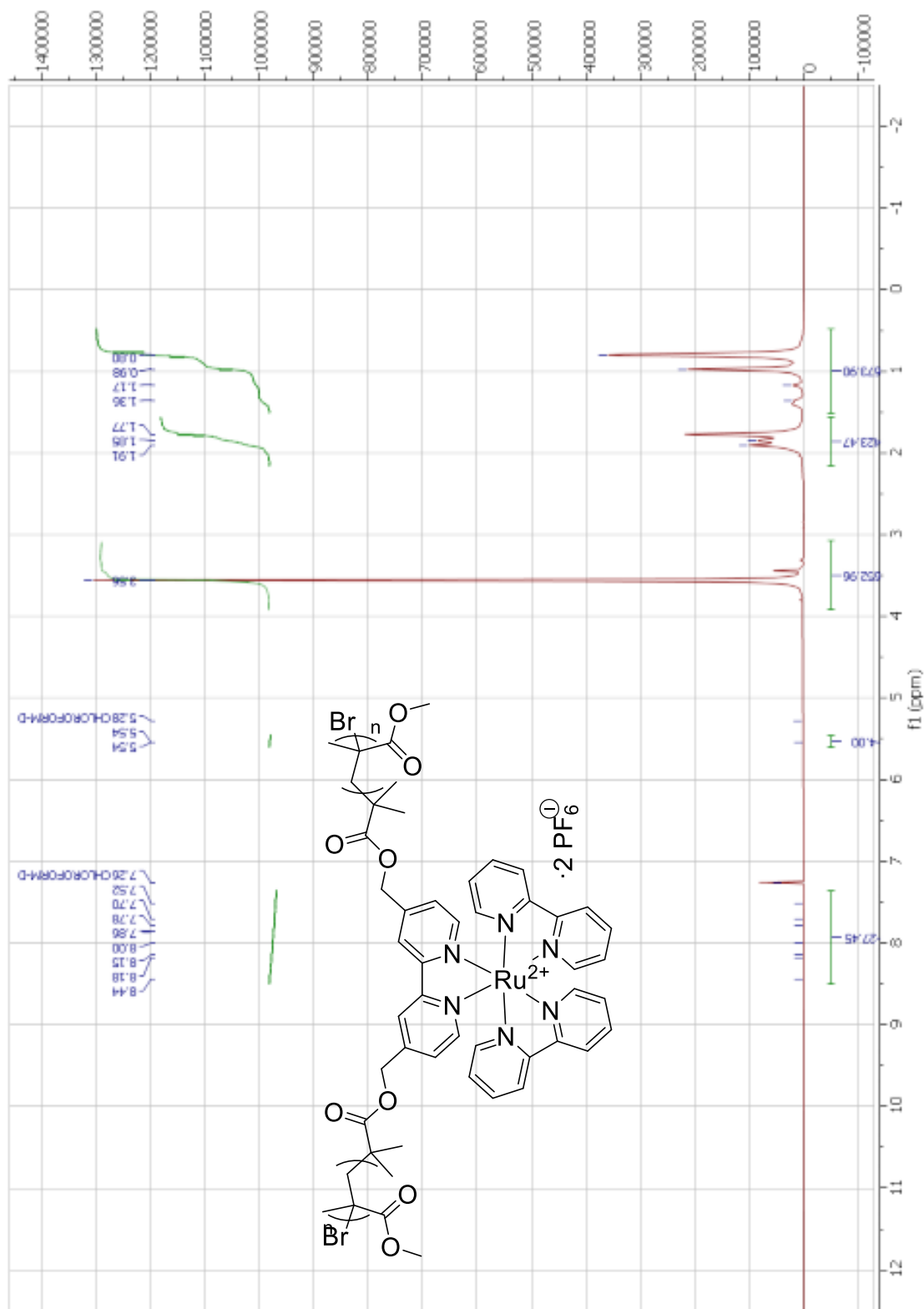
 ^{13}C NMR of L2

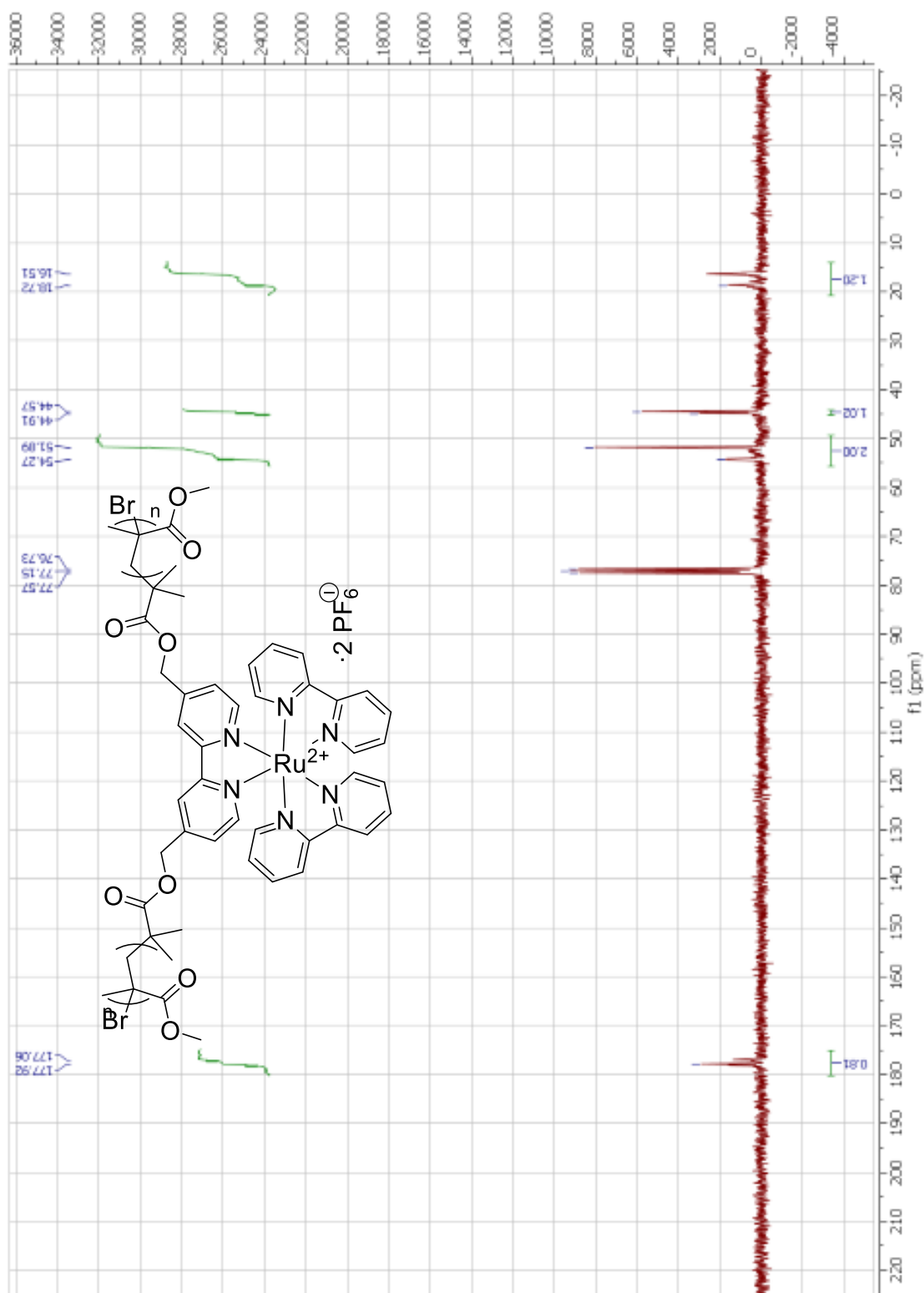


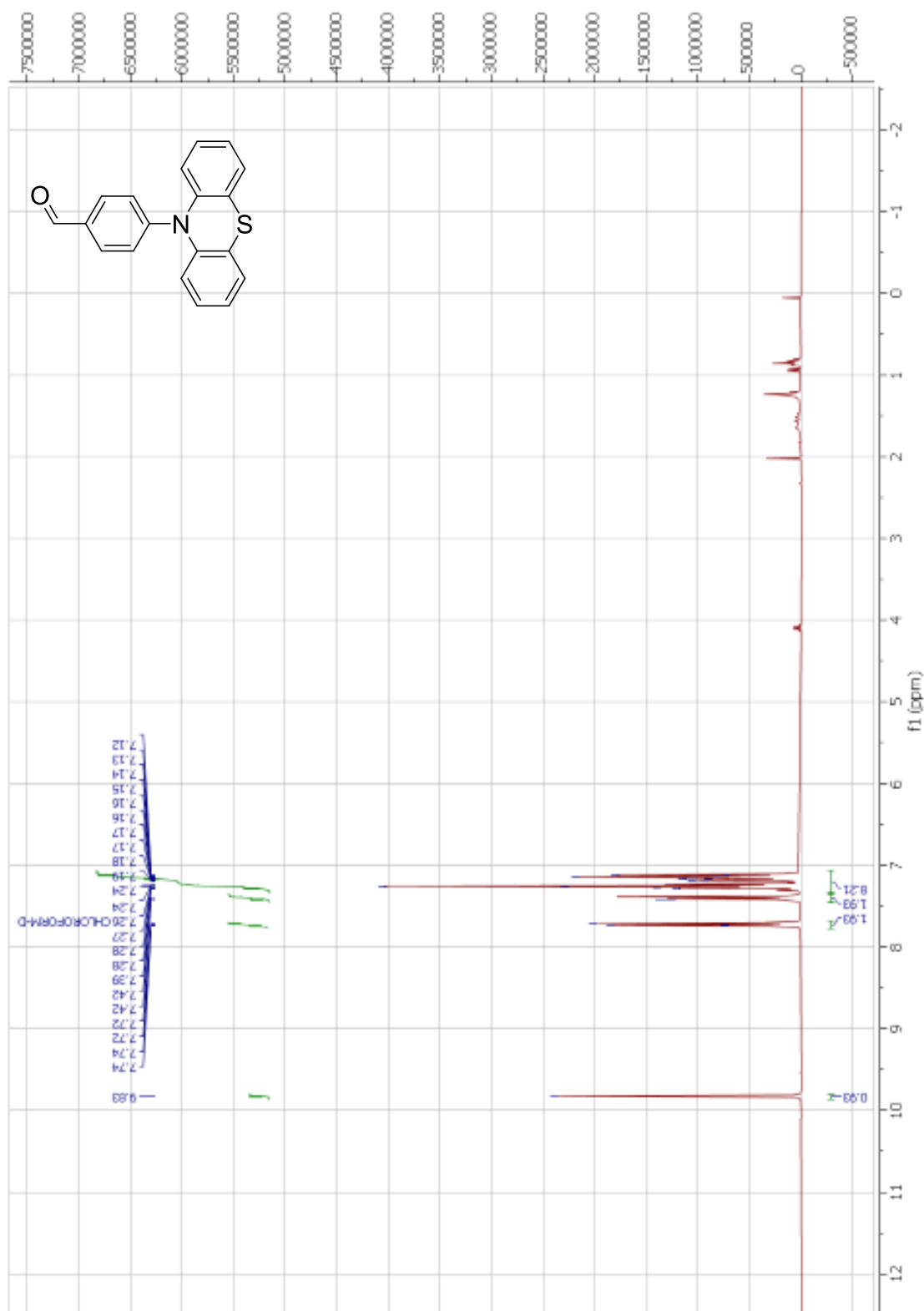
¹H NMR of UPCIS Ru1



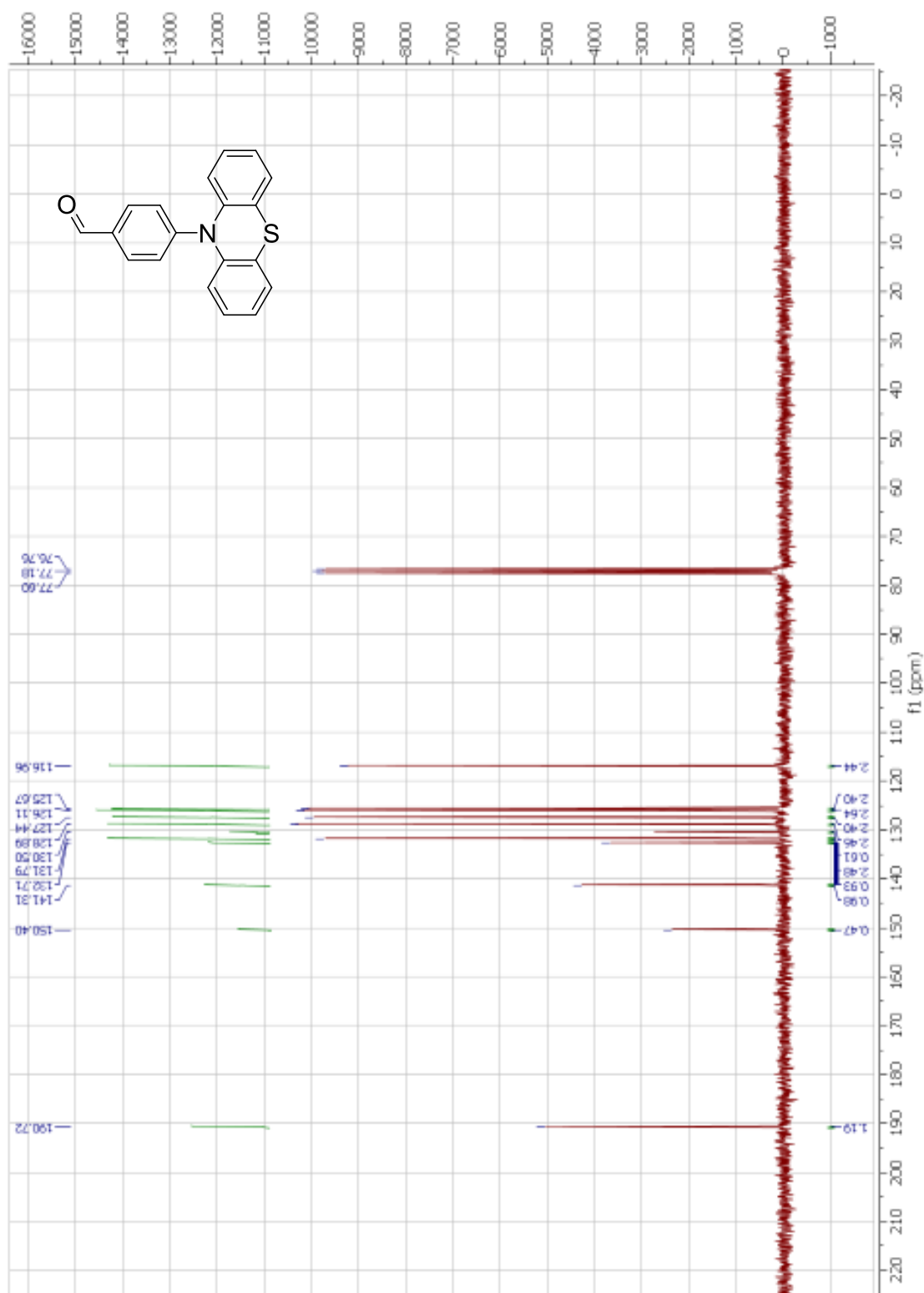
¹H NMR of UPCIS Ru₂

 ^1H NMR of PSC RuPoly1

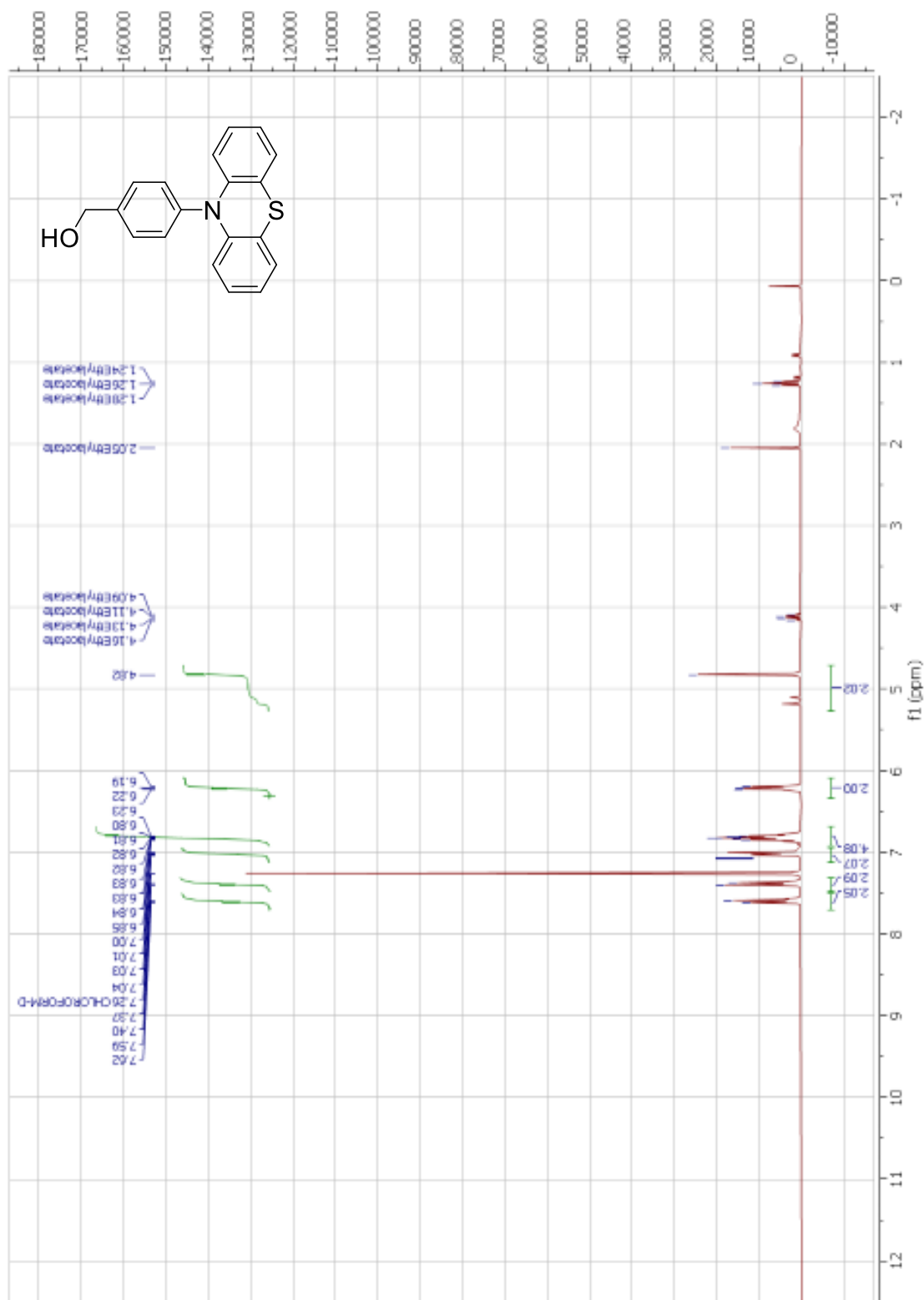
 ^{13}C NMR of PSC RuPoly1



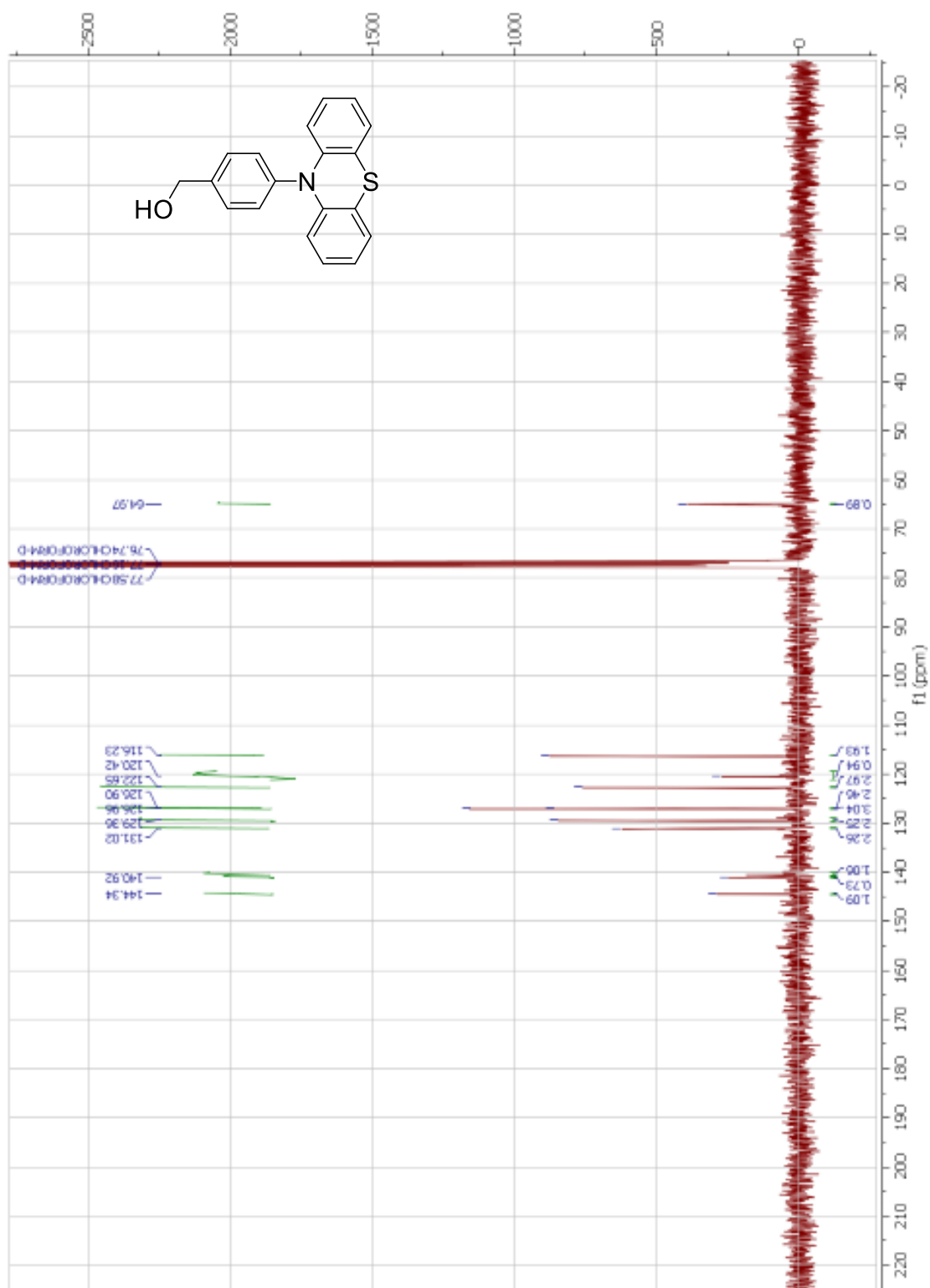
^1H NMR of 4-(10H-phenothiazin-10-yl) benzaldehyde



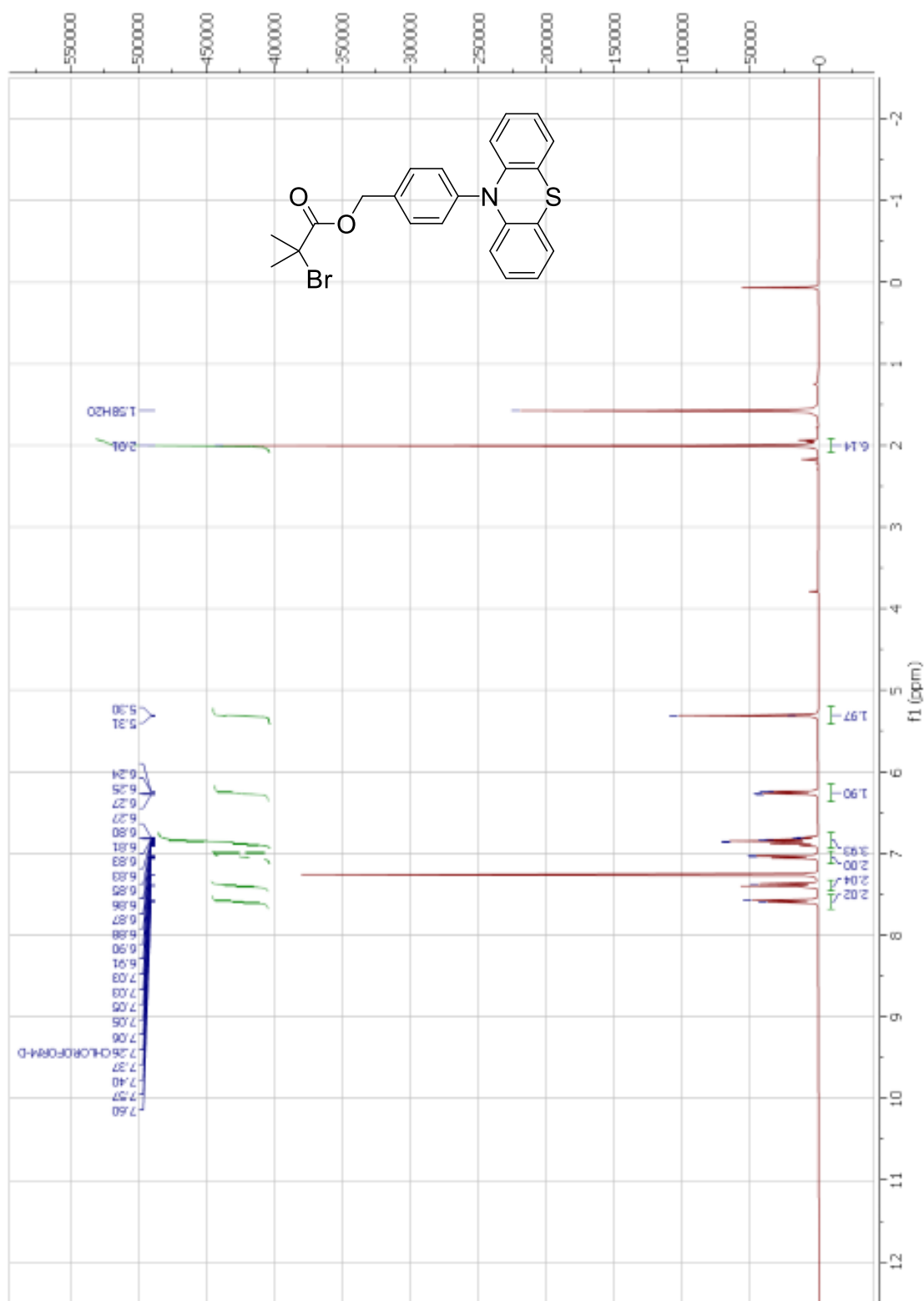
^{13}C NMR of 4-(10H-phenothiazin-10-yl) benzaldehyde

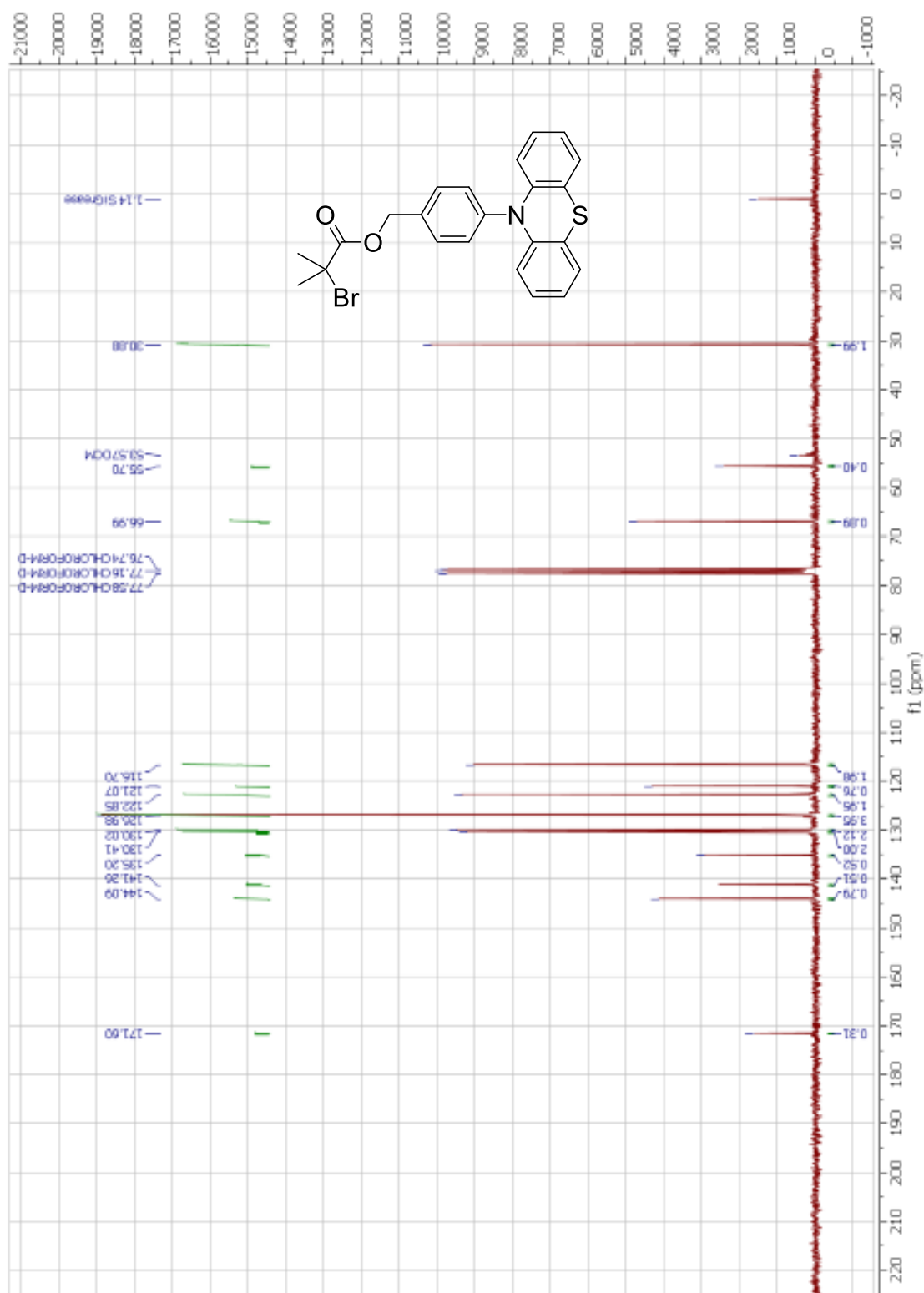


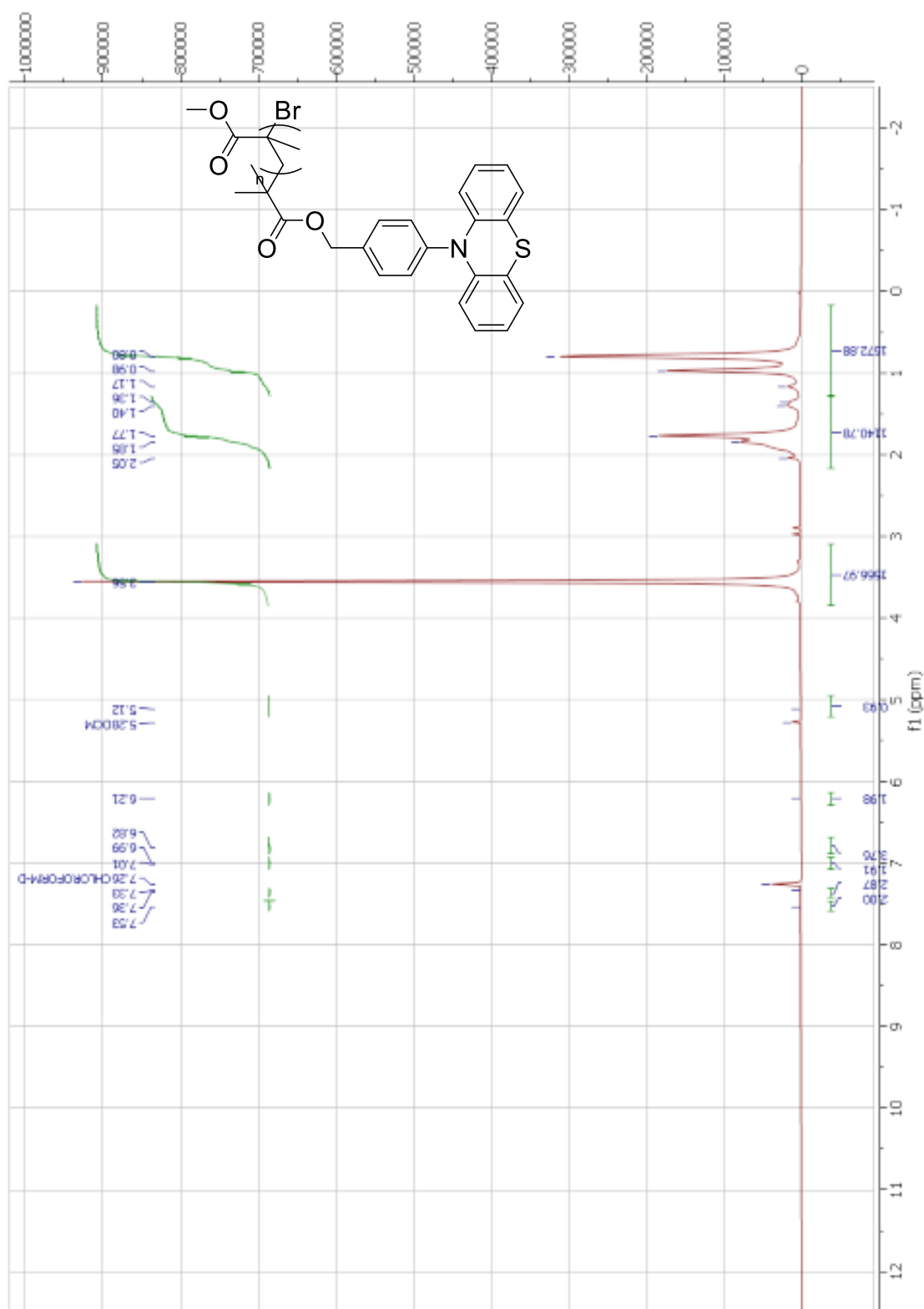
^1H NMR of (4-(10H-phenothiazin-10-yl) phenyl)methanol



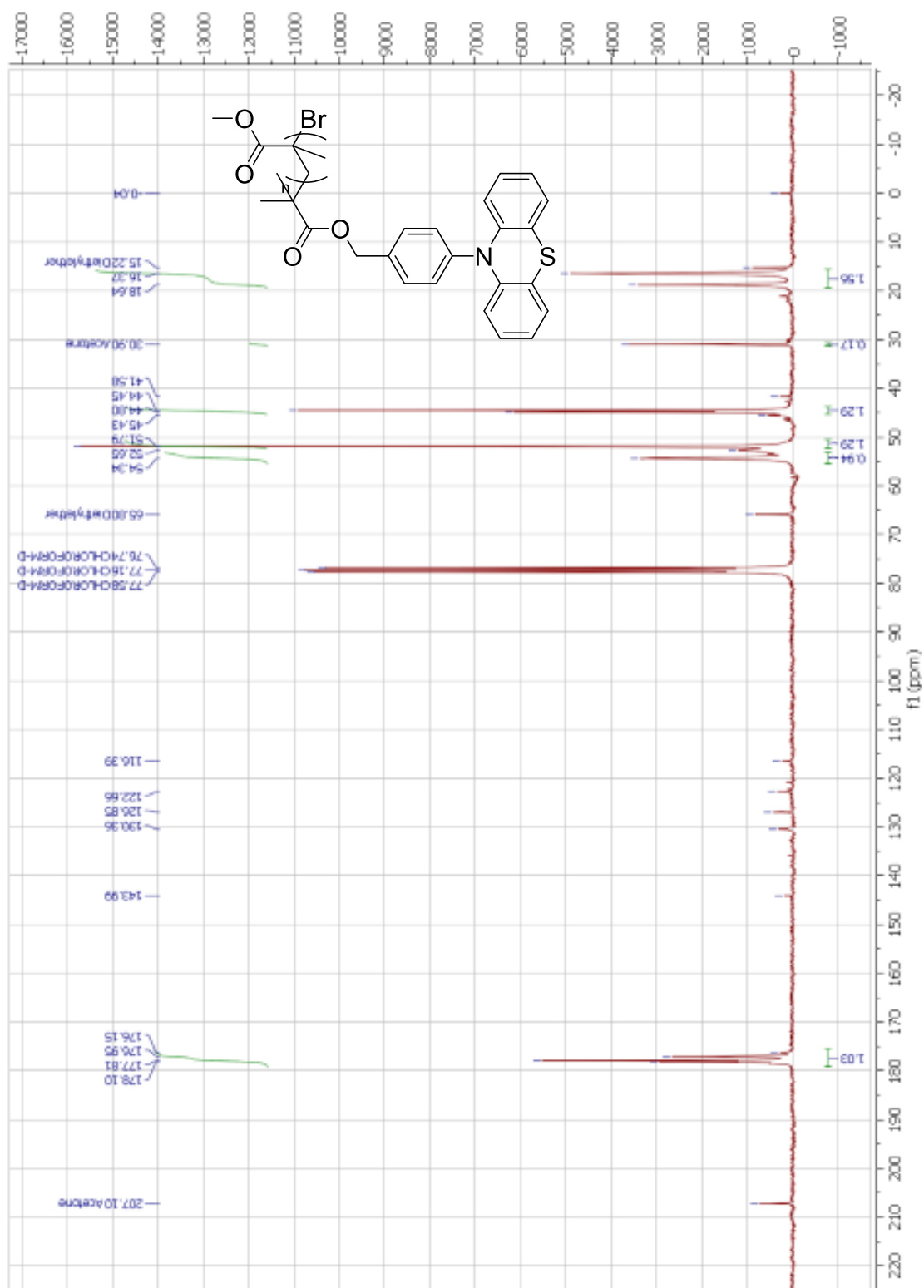
^{13}C NMR of (4-(10H-phenothiazin-10-yl) phenyl)methanol

 ^1H NMR of UPCIS PPH1

 ^{13}C NMR of UPCIS PPH1



¹H NMR of PSC PPHPoly1



¹³C NMR of PPHPoly1

VITA

Matthew A Peavy

Research Chemist

Skillful and dynamic chemist with demonstrated knowledge and experience in the oil and gas and chemical research industries.

— Key Qualifications —

- Proven track record of installing and testing chemical injection equipment on oil and gas wells.
- Adept at identifying and establishing suitable chemical program and ensuring safe and reliable down hole conditions by monitoring workover rigs and production.
- Expertise in recommending solutions for oil and gas wells to extend run time and stimulate natural resource recovery.
- Proficient in Chromatographic Methods, GSC, TLC, GPC-MS Spectroscopic Methods, NMR, IR, UV-Vis, Fluorescence, Distillation, Extraction, Recrystallization, Organic Synthesis, Atom Transfer Polymerization, Weighing, Pipetting, Gaussian 09W, GaussView 5.0, Hansen Solubility Parameters, Sci-Finder, Joel Delta, and ChemDraw 19.0.

Professional Experience

Sam Houston State University - Huntsville, TX

Graduate Research Assistant, 9/2018 to Present

Conduct research and analysis to modify existing photocatalyst through the addition of polymer supports to ease in recovery and reuse without affecting the catalytic activity of the molecule. Catalyst in study currently is tris-bipyridine ruthenium and phenothiazine based. Use organic, inorganic synthesis, TLC, and column chromatography, liquid/ solid and liquid/ liquid extraction techniques. Formulate photo-initiated reactions and optimize reaction conditions. Conduct polymer support addition experiments on photo-catalyst. Develop and execute organic synthesis experiments.

Projects:

- New Polymer-Supported Photo-Catalysts from Unimolecular, Photo-Catalyst Initiator Systems (UPCIS), Graduate Research 2018-2020.
- Asphalt Rheology at the Air/ Water Interface utilizing FTIR, Spring 2018.
- Ultrasonic Effect on Paraffin/ Asphaltene Aggregate Precipitation in Flow, Summer 2017.

Platinum Chemicals LLC - Madisonville, TX

Texas Operations Manager, 2/2014 to 10/2015

Studied surfactant interactions which produce oil, gas, and waters while countering the salinity, and ionic effects of the produced fluids to optimize the well production. Used nitrogen-based corrosion inhibitors to facilitate hydrophobic or hydrophilic interactions. Developed and implemented action plans to increase productivity, client relationship management, and long-term partnership. Validated and followed-up on day-to-day operations such as equipment maintenance, standard operating procedures, safety, and employee morale.

Selected Contributions:

- Coordinated efforts for cross-functional resources, dealers and regional partners to add value to new business initiatives and drive additional revenues with new and existing accounts.
- Oversaw and ensured compliance with operational policies to independent contractors and key customer accounts.

X-Chem LLC– Dew/Bryan, TX

Area Manager, 8/2012 to 2/2014

Integrated analytical and quantitative skills to develop individual business plans, facilitated overall business strategy, and increased market share. Coached the team in daily operations including using proper systems, following procedures, and developing customer service skills. Managed complex and demanding environments, with the ability to balance competing priorities and deliver results. Developed a chemical foam pig for pipeline corrosion and scale treatment.

Selected Contributions:

- Managed state and federal compliance and documentation-maintained company policies and industry knowledge and ensured completion of all customer requirements.
- Maintained excellent staff retention rates, leading to strong experienced teams.

Account Manager, 6/2010 to 8/2012

Oversaw planning and implantation of sales contacts and strategies to enhance organizational values. Researched and recommended suitable chemical programs for oil and gas wells to ensure prolonged run time and stimulate natural resource recovery. Tested and evaluated oil and gas wells to insure appropriate chemical program and interacted with workover rigs to better understand down hole conditions.

- Maintained and nurtured business-to-business relationships to gain loyalty, referrals and repeat business.

Service Technician, 5/2008 to 6/2010

Installed and tested chemical injection equipment on oil and gas wells to ensure correct chemical program and oil quality for salability. Performed field-testing for corrosion, scale, and paraffins.

Additional Experience:

Outside Sales (2007 - 2008), Crawford Electric Supply, Bryan, TX

Outside Sales (2001 - 2007), Elliott Electric Supply, Bryan, TX

Educational Background

Master of Science, Chemistry

Sam Houston State University, Huntsville, TX

Bachelor of Science, Chemistry

Sam Houston State University, Huntsville, TX

Presentations

Poster Presentation: SWRM ACS Regional Meeting, El Paso, TX, 2019
Rational Design and Synthesis of a Photo-redox, Unimolecular Ligand Initiator System for Tandem Catalysis.

Oral Presentation: Peterson Asphalt Conference, Laramie WY, 2018
Asphalt Rheology at the Air Water Interface Utilizing FTIR.

Awards and Scholarships

Graduate Achievement Scholarship, Sam Houston State University, 2019

Graduate School General Scholarship, Sam Houston State University, 2019

Welch Foundation Summer Research Grant, Summer 2017

Professional Memberships

American Chemical Society, 2016-Present

The Society for the Advancement of Material and Process Engineering, 2017 & 2018